



3 4456 0368251 1

# ornl

ORNL/CON-308

**OAK RIDGE  
NATIONAL  
LABORATORY**



## Moisture Effects in Low-Slope Roofs: Drying Rates After Water Addition with Various Vapor Retarders

C. R. Pedersen  
T. W. Petrie  
G. E. Courville  
A. O. Desjarlais  
P. W. Childs  
K. E. Wilkes

OAK RIDGE NATIONAL LABORATORY  
CENTRAL RESEARCH LIBRARY  
CIRCULATION SECTION  
4500N ROOM 175  
**LIBRARY LOAN COPY**  
DO NOT TRANSFER TO ANOTHER PERSON  
If you wish someone else to see this  
report, send in name with report and  
the library will arrange a loan.  
#ON-P1610 175

MANAGED BY  
MARTIN MARIETTA ENERGY SYSTEMS, INC.  
FOR THE UNITED STATES  
DEPARTMENT OF ENERGY

This report has been reproduced directly from the best available copy.

Available to DOE and DOE contractors from the Office of Scientific and Technical Information, P.O. Box 62, Oak Ridge, TN 37831; prices available from (615) 576-8401, FTS 626-8401.

Available to the public from the National Technical Information Service, U.S. Department of Commerce, 5205 Port Royal Rd., Springfield, VA 22161.

This report was prepared as an account of work sponsored by an agency of the United States Government. Neither the United States Government nor any agency thereof, nor any of their employees, makes any warranty, express or implied, or assumes any legal liability or responsibility for the accuracy, completeness, or usefulness of any information, apparatus, product, or process disclosed, or represents that its use would not infringe privately owned rights. Reference herein to any specific commercial product, process, or service by trade name, trademark, manufacturer, or otherwise, does not necessarily constitute or imply its endorsement, recommendation, or favoring by the United States Government or any agency thereof. The views and opinions of authors expressed herein do not necessarily state or reflect those of the United States Government or any agency thereof.

27 254  
200

Energy Division

**MOISTURE EFFECTS IN LOW-SLOPE ROOFS:  
DRYING RATES  
AFTER WATER ADDITION  
WITH VARIOUS VAPOR RETARDERS**

**C. R. Pedersen  
Technical University of Denmark  
(Current affiliation: Danish Building Research Institute)**

**T. W. Petrie  
Marquette University**

**G. E. Courville, A. O. Desjarlais, P. W. Childs, and K. E. Wilkes  
Oak Ridge National Laboratory**

**Part of the  
National Program for  
Building Thermal Envelope Systems and Materials**

October 1992

**Sponsored by  
Office of Buildings and Community Systems**

**Prepared by the  
OAK RIDGE NATIONAL LABORATORY  
Oak Ridge, Tennessee 37831  
managed by  
MARTIN MARIETTA ENERGY SYSTEMS, INC.  
for the  
U.S. DEPARTMENT OF ENERGY  
under contract No. DE-AC05-84OR21400**



3 4456 0368251 1



## TABLE OF CONTENTS

	<u>Page</u>
LIST OF FIGURES .....	v
LIST OF TABLES .....	ix
ACKNOWLEDGMENTS .....	xi
ABSTRACT .....	xiii
EXECUTIVE SUMMARY .....	xv
1. INTRODUCTION .....	1
1.1 OVERVIEW OF THE EXPERIMENT .....	1
2. DETAILED DESCRIPTION OF THE EXPERIMENT .....	5
2.1 THE LARGE SCALE CLIMATE SIMULATOR .....	5
2.2 EXPERIMENTAL SETUP .....	7
2.2.1 DESIGN .....	7
2.2.2 THE WATER-PERMEABLE VAPOR RETARDER .....	14
2.2.3 INSTRUMENTATION .....	16
2.3 EXPERIMENTAL CONDITIONS .....	18
3. MATCH COMPUTER PROGRAM .....	23
4. THERMAL MEASUREMENTS .....	26
4.1 DETERMINATION OF ROOM-DRY R-VALUES .....	26
4.2 HEAT FLUXES DURING ROOM DRY, DYNAMIC RUNS .....	33
4.3 HEAT FLUXES AFTER WATER ADDITION DURING LOW AMPLITUDE TEMPERATURE CYCLES .....	40
4.4 HEAT FLUXES AFTER WATER ADDITION DURING INCREASED AMPLITUDE TEMPERATURE CYCLES .....	48
4.5 SUMMARY OF EFFECTS OF CONDENSATION AND EVAPORATION ON HEAT FLUX TRANSDUCERS .....	57

5.	MOISTURE MEASUREMENTS .....	66
5.1	READINGS FROM MOISTURE PROBES .....	66
5.1.1	PLYWOOD PROBES .....	66
5.1.2	PIN PROBES .....	74
5.2	RESULTS OF GRAVIMETRIC MOISTURE MEASUREMENTS ...	77
5.2.1	MOISTURE CHANGES DURING DRY RUNS .....	78
5.2.2	MOISTURE CHANGES AFTER WATER WAS ADDED .....	78
5.3	PREDICTED DRYING RATES WITH THE VARIOUS VAPOR RETARDER SYSTEMS .....	88
6.	SUMMARY AND CONCLUSIONS .....	101
7.	REFERENCES .....	107

## LIST OF FIGURES

<u>Figure</u>		<u>Page</u>
1	Measured heat fluxes at the top and bottom of a panel of the cold-deck type during a dry and wet dynamic run with identical imposed temperatures. . . . .	xxi
2.1	Schematic of the Large Scale Climate Simulator. . . . .	6
2.2	A diagnostic platform with nine panels for use in the Large Scale Climate Simulator. . . . .	9
2.3	Details of panels 1, 2, 3, and 4 for studying drying rates: cold-deck panels with permeable materials. . . . .	10
2.4	Details of panels 6, 7, 8, and 9 for studying drying rates: warm-deck panels with impermeable materials. . . . .	11
2.5	Design concept of the proprietary water-permeable vapor retarder system. . . . .	15
2.6	Applied temperatures before and after water addition. . . . .	20
4.1	Steady-state, dry R-values for fibrous glass in the cold-deck panels, including control panel 5 (dry throughout test). . . . .	28
4.2	Repeated, steady-state, dry R-values for fibrous glass in the cold-deck panels with solid vapor retarders added to all panels. . . . .	29
4.3	Steady-state, dry R-values for expanded polystyrene in the warm-deck panels. . . . .	30
4.4	Temperatures at the top and bottom of the fibrous glass in panel 5 during dry, dynamic run 6. . . . .	35
4.5	Measured heat fluxes at the top of the fibrous glass with driving temperature difference in panels 1-5 during dry, dynamic run 6. . . . .	36
4.6	Measured heat fluxes at the bottom of the fibrous glass with driving temperature difference in panels 1-5 during dry, dynamic run 6. . . . .	37
4.7	Measured heat fluxes at the top and bottom of panel 2 during dry, dynamic run 6. . . . .	39
4.8	Measured heat fluxes in the middle of the expanded polystyrene with driving temperature difference in panels 6, 7, 8, and 9 during dry, dynamic run 6. . . . .	41

4.9	Measured heat fluxes at the top of the fibrous glass in panels 1–5 during wet, dynamic run 7. . . . .	44
4.10	Measured heat fluxes at the bottom of the fibrous glass in panels 1–5 during wet, dynamic run 7. . . . .	45
4.11	Measured heat fluxes at the top and bottom of panel 2 during dry, dynamic run 6 and wet, dynamic run 7. . . . .	47
4.12	Measured heat fluxes in the middle of the expanded polystyrene in panels 6, 7, 8, and 9 during wet, dynamic run 7. . . . .	49
4.13	Measured heat fluxes at the top of the fibrous glass in panels 1–5 during wet, dynamic run 8 with increased temperatures. . . . .	51
4.14	Measured heat fluxes at the bottom of the fibrous glass in panels 1–5 during wet, dynamic run 8 with increased temperatures. . . . .	52
4.15	Measured heat fluxes at the top and bottom of panel 2 during wet, dynamic run 8 with increased temperatures. . . . .	53
4.16	Measured heat fluxes in the middle of the expanded polystyrene in panels 6, 7, 8, and 9 during wet, dynamic run 8 with increased temperatures. . . . .	55
4.17	Results from MATCH compared to the measured heat fluxes at the top and bottom of the fibrous glass in panel 2 during wet, dynamic run 8 with increased temperature. . . . .	56
4.18	Local effect of condensation and evaporation of moisture on heat flux transducers in permeable materials like fibrous glass. . . . .	59
4.19	Local effect of a non-saturated hygroscopic material on the flow of moisture near heat flux transducers at the top of fibrous glass. . . . .	60
4.20	Local effect of over-hygroscopic moisture content on the flow of moisture near heat flux transducers at the top of fibrous glass. . . . .	63
4.21	Local effect of a vapor retarder on the flow of moisture near heat flux transducers at the bottom of fibrous glass. . . . .	64
5.1	Relative humidity from the plywood probes at the top of cold-deck panels 1–4 during the entire experiment. . . . .	68
5.2	Relative humidity from the plywood probes at the bottom of cold-deck panels 1–4 during the entire experiment. . . . .	69

5.3	Relative humidity from the plywood probes at the top and bottom of panel 2 during the entire experiment. ....	70
5.4	Relative humidity from the plywood probes at the top of warm-deck panels 6–9 during the entire experiment. ....	71
5.5	Relative humidity from the plywood probes at the bottom of warm-deck panels 6–9 during the entire experiment. ....	72
5.6	Uncalibrated response of the pin probes at the top of cold-deck panels 1–4 during the entire experiment. ....	75
5.7	Uncalibrated response of the pin probes at the bottom of cold-deck panels 1–4 during the entire experiment. ....	76
5.8	Uncalibrated response of the pin probes at the top and bottom of cold-deck panel 2 during the entire experiment. ....	79
5.9	Gravimetrically determined moisture content in cold-deck roof panels 1–4 (with significant hygroscopic moisture) after each wet run. ....	84
5.10	Gravimetrically determined moisture content in warm-deck panels 6–9 (with little hygroscopic moisture) after each wet run. ....	85
5.11	Moisture content in the layers of cold-deck panel 1, calculated by MATCH after water was added. ....	91
5.12	Moisture content in the layers of cold-deck panel 2, calculated by MATCH after water was added. ....	92
5.13	Moisture content in the layers of cold-deck panel 3, calculated by MATCH after water was added. ....	93
5.14	Moisture content in the layers of cold-deck panel 4, calculated by MATCH after water was added. ....	94
5.15	Moisture content in the layers of warm-deck panel 6, calculated by MATCH after water was added. ....	95
5.16	Moisture content in the layers of warm-deck panel 7, calculated by MATCH after water was added. ....	96
5.17	Moisture content in the layers of warm-deck panel 8, calculated by MATCH after water was added. ....	97
5.18	Moisture content in the layers of warm-deck panel 9, calculated by MATCH after water was added. ....	98



## LIST OF TABLES

<u>Table</u>		<u>Page</u>
2.1	Moisture content of various materials at 60% RH and 20°C (68°F). . . . .	19
2.2	Temperatures in the guard and climate chambers during dry, steady-state runs. .	21
4.1	Apparent thermal conductivities of the insulation in each panel. . . . .	32
5.1	Distribution of deliberately added moisture (g/m <sup>2</sup> ) in the roof test panels. . . . .	81



## ACKNOWLEDGMENTS

The authors wish to acknowledge the Technical University of Denmark for providing support for Carsten Rode\* during a six-month stay at Oak Ridge National Laboratory (ORNL), and Marquette University for providing partial support for Tom Petrie during his one-year sabbatical spent at ORNL. Guest assignments at the ORNL Building Envelope Research Center have a significant impact on the quality and diversity of research at the center, and are vital to maintaining the center as a worldwide leading institution for the promotion of improved understanding and performance of roof systems.

\*Carsten Rode has changed his name from Carsten Rode Pedersen. References to this work and other prior work in the literature will continue to be found under Pedersen.



## ABSTRACT

Tests have been conducted in the Large Scale Climate Simulator (LSCS) of the U.S. Department of Energy (DOE) Building Envelope Research Center at the Oak Ridge National Laboratory (ORNL) to investigate downward drying rates of various unvented, low-slope roof systems. A secondary objective was to study heat flow patterns so as to understand how to control latent heat effects on impermeable heat flux transducers. Nine test sections were tested simultaneously. Five sections had a plywood deck above fibrous-glass insulation and were examples of cold-deck systems. These five sections had various vapor retarder systems on a gypsum board ceiling below the insulation. The other four sections had a lightweight insulating concrete deck below expanded polystyrene insulation and the same vapor retarder systems, and were examples of warm-deck systems. The cold-deck systems had materials that were relatively permeable to water vapor, while the materials in the warm-deck systems were less permeable. All test sections were topped by an impermeable roofing membrane.

Four different vapor retarder systems were used below the two kinds of insulation to make up eight of the test sections. One system was a solid sheet of polyethylene, another was polyethylene deliberately punched with holes, the third was a water-permeable vapor retarder, and the fourth was no vapor retarder at all. The holes in the polyethylene simulated an imperfectly applied solid film. The water-permeable vapor retarder is designed to be able to dry out initially wet roofs by providing a path for liquid water to escape downward through it but retard vapor flow upward. Water was added to sheets of blotting paper over the insulation in these eight test sections after determining their dry steady-state and dynamic thermal characteristics. The ninth test section was of the cold-deck type with a solid polyethylene vapor retarder, but it remained room-dry throughout.

The test sections were instrumented with thermocouples between all layers and with small heat flux transducers at the bottom and top of the fibrous-glass insulation and in the middle of the expanded polystyrene insulation. Two different kinds of moisture probes were used to qualitatively monitor the movement of the moisture. Weighing about half the volume of the materials in the test sections before and after water was added and after each wet run gave a quantitative but inaccurate, as it turned out, measure of the changing moisture content.

The heat flux measurements showed that heat conduction dominates the system using impermeable insulation materials, with only a slight increase due to increased thermal conductivity of wet expanded polystyrene. There was significant transfer of latent heat in the test sections with permeable insulation, causing the peak heat fluxes to increase by as much as a factor of two. With temperatures imposed that are typical of summer days, latent heat transfer associated with condensation and evaporation of moisture in the test sections was measured to be as important as the heat transfer by conduction. This was found to be consistent with results from Moisture and Temperature Calculations for Constructions of Hygroscopic Materials (MATCH), a computer model of moisture movement and heat transfer, including latent effects. The MATCH results also suggested that impermeable heat flux transducers next to non-saturated hygroscopic materials respond mostly to conduction, while the response of ones near saturated materials such as vapor retarders estimates the total heat flow.

Weighing the specimens yielded the rates of drying of each test section and of the components in it. The sections without a vapor retarder dried out rapidly, losing all the added water and some hygroscopic moisture that was present initially. Of the sections with a vapor retarder, the ones with the water-permeable vapor retarder were able to dry out all or most of the added water within a few weeks. Some water was able to escape when the vapor retarder consisted of a layer of polyethylene with punched holes. The solid polyethylene vapor retarder showed little or no drying when measured to the accuracy with which changes in water content could be determined in these tests. The water-permeable vapor retarder and the polyethylene with holes verify that downward drying is possible using the high temperatures imposed on roofs in summer. How to achieve this potential when reroofing over wet materials requires more study.

## EXECUTIVE SUMMARY

Moisture in roof systems has been a long-standing concern for several reasons. Leaks into interior spaces are always unacceptable, and dimensional instability, corrosion, and material disintegration can lead to early failure. In addition, wet insulation will perform below thermal performance levels specified during design. A more recent issue relates to the increased investment in roof insulation during the past ten to fifteen years. The membranes on these roofs are aging, leaks are developing, and replacement is required. The choices are to reroof over the old roof, preserve only part of the old roof, or tear off and replace everything. Basic questions about reroofing include whether or not recovered wet insulation dries and, if so, how rapidly in suitable environments? Also, are systems available to design rapid downward drying potential into new roofs? A program of research has been initiated at the U.S. Department of Energy (DOE) Building Envelope Research Center at the Oak Ridge National Laboratory (ORNL) to study proposed answers to these and related questions.

The primary objective of the experiment described in this report was to determine if it is possible, without ventilation of the roof cavity but through the use of certain kinds of vapor retarders, to dry out low-slope roofs that contain excessive amounts of water. The drying was driven by high temperatures above the roof and achieved by a diffusive transport of moisture downward. Control over the experimental conditions and the kinds of vapor retarders showed when and to what extent downward drying is possible.

The impact of the presence of moisture on heat transfer rates in the insulation was also studied. This experiment follows a preliminary test in which water was trapped in low-slope roofs with various insulations. The effect of diurnal moisture migration on thermal performance was evident in the results. Lessons learned in that test led to the secondary objectives for this test: to understand the mechanism for latent heat effects on impermeable heat flux transducers, and to make it possible to account for the effects in the design of experiments with moist, permeable materials. One way to account for the effects is to locate heat flux transducers so that some respond only to the conducted heat while others respond to the total heat flux.

Suitable thermal driving forces for downward drying are normally obtained in the summer period when roof surface temperatures are sufficiently high to drive the moisture towards the bottom. Rather than test roofs outdoors during summer conditions, better control over these conditions is possible in the Large Scale Climate Simulator (LSCS) of the Building Envelope Research Center. A controlled amount of water can be added and typical roof surface temperatures can be programmed and repeated for several consecutive days without any interruptions by conditions which are adverse for drying.

Two types of roof systems were investigated. The first, an example of a cold-deck system, contained fibrous-glass insulation, which is especially permeable to water vapor, mounted under a plywood deck. This insulation permits as much moisture as the thermal driving forces allow to migrate down in the daytime when exterior temperatures are elevated. The other type, an example of a warm-deck system, was insulated with expanded polystyrene, which is less permeable than fibrous glass, and had a lightweight concrete deck toward the interior. The terms cold deck and warm deck are commonly used in the European roofing industry to refer to systems with insulation below and above the deck, respectively. Diurnal effects are minimized due to the impermeable insulation; moisture migration is not influenced much by the daily peaks in temperature. Moisture moves only in the average direction of the vapor pressure gradients over a period of time.

Water was added to four test sections of each roof type, three with three different vapor retarders and one with no vapor retarder at all. The different vapor retarders were a solid sheet of polyethylene, a sheet with holes punched in a well-defined pattern, and a water-permeable vapor retarder. The polyethylene with holes simulated a solid polyethylene vapor retarder with poor overlap of separate sheets, or badly sealed penetrations. The water-permeable vapor retarder was a novel design which would allow initially wet roofs to dry out, but at the same time prevent vapor intrusion from below. It consisted of a layer of synthetic fabric with strips of polyethylene on each side and exposed fabric between them. The top and bottom strips were staggered so that the membrane had a good vapor resistance and worked well as a vapor retarder. When moisture condenses on the membrane, which occurred in this experiment when the moisture was driven down in the construction by a hot roof surface, it

flows through the membrane by capillary action. The effect is to dry out the roof. The roof test panels with a solid polyethylene vapor retarder and without a vapor retarder served to define the limiting behavior of the test panels with respect to drying. A ninth panel of the cold-deck type with a solid polyethylene vapor retarder was used as a control; no water was added to it. All nine panels were tested simultaneously by constructing them into the 3.7 by 3.7 m (12 by 12 ft) test area available in a diagnostic platform for the LSCS.

The resulting 1.1 by 1.1 m (43 by 43 in.) square test sections used common roofing materials assembled in layers on top of a support frame. Temperatures were measured by thermocouples at most interfaces between layers. Heat fluxes were measured at the top and bottom of the fibrous-glass insulation in the cold-deck panels, and in the middle between the expanded polystyrene boards in the warm-deck panels. The heat flux transducers are thin, impermeable devices with embedded thermopiles, calibrated while situated in locations and materials similar to their test configurations.

Two different kinds of moisture probes were used to give qualitative data on the movement of moisture in the roofs. An electrical capacitance pin probe responded quickly to increases in the moisture content of the material into which it was embedded. However, its response was not calibrated for the kinds of materials or temperature variations encountered in this experiment. The other type of probe was based on the electrical resistance of plywood and gave a calibrated measure of relative humidity, but took several days to respond to changes in the moisture content of its environment.

A more quantitative measure was desired of the total amount and distribution of moisture in the eight panels to which water was added during the experiment. Most of the insulation from the guard area around the central core of each section was weighed at the start of the experiment. It was removed and weighed again before and after water was added, and shortly after the end of each subsequent run, until the end of the experiment. A small disk was removed from each of the four plywood decks and weighed to yield information about the whole deck from which it came. Sheets of blotting paper were placed at the top of all sections and over the solid polyethylene in the two sections where it was used. Blotting paper was a convenient means to distribute added water and to collect condensed water for

weighing. The pieces of the insulation in the central area held the instrumentation, that was connected by lead wires to the data acquisition system. This insulation could not be removed easily or weighed accurately with the instrumentation in place.

A series of nine test runs was scheduled in order to achieve the goals of the experiment, with special focus on providing realistic conditions for downward drying. No water was added to any of the panels in the initial runs. All the materials did, however, contain hygroscopic moisture because they were stored in the laboratory, at approximately 60% RH, before the assembly of the roof panels. Relative to most insulation materials, plywood's hygroscopic moisture content is particularly large.

During the first five runs, before water was added, the apparent thermal conductivities and their reciprocals, the apparent R-values, of the materials in the roof panels were determined as functions of temperature. The temperatures in the climate chamber above and the guard chamber below the specimens were held steady at various levels. The imposed thermal driving forces were downward at first, then upward. The results from the cold-deck panels appeared unreliable when the resulting heat flux was downward. The hygroscopic moisture in the plywood, when it was driven down through the insulation, seemed sufficient to disturb the heat flux measurements. Using the results from the runs with upward thermal driving forces gave reasonable values for the apparent thermal conductivities and their temperature variation. Repetitions of the runs with upward thermal driving forces were performed after the panels had gone through the whole experiment. Polyethylene sheets were inserted in the bottom of all the cold-deck panels to prevent any upward flow of moisture. The apparent thermal conductivities for all the panels were then even more consistent with each other. The primary purpose for obtaining the "dry" thermal conductivities was to use them as references for the results from the dynamic dry and wet runs that followed the original steady dry runs.

The dynamic dry run comprised a series of diurnal cycles of the roof surface temperatures before water was added to the panels. This run was primarily a reference for a run with identical temperature variation after the addition of water. It was discovered, however, that the hygroscopic moisture from the plywood in the cold-deck roofs with fibrous-glass insulation

influenced the heat flow readings. Heat flux transducers were located at the bottom of the fibrous glass, immediately over the vapor retarder if one was present, and at the top of the insulation, immediately under the plywood deck. Heat flux peaks were largest at the bottom even though the temperature variations were imposed from the top of the roof. It is concluded that moisture driven out of the plywood condensed and evaporated on the bottom transducer and caused the increased measured heat fluxes there. The location of the top transducer was also next to plywood and blotting paper, in anticipation of adding water later. These very hygroscopic materials seemed to prevent similar effects on this transducer.

The warm-deck roofs were insulated with expanded polystyrene, which is considerably less permeable to the flow of water vapor than fibrous glass. Based on experience from a preliminary experiment under similar conditions, these roof panels had only one heat flux transducer, which was located in the middle of the insulation. This location in impermeable insulation resulted in no apparent latent heat effects in the response of the transducers in these panels before or after water was added. The only effect of moisture in expanded polystyrene insulation was a small increase in heat flows, which may be explained by a slightly higher apparent thermal conductivity of this insulation when moisture accumulated in it.

The bottom heat flux transducers in the cold-deck panels were surrounded by much condensate shortly after the addition of water, and they responded significantly to moisture effects. Meanwhile, the top transducers read approximately the same as they did during the dry runs because of the hygroscopic materials next to them. To illustrate the difference, Fig. 1 shows heat fluxes at the bottom and top of one of the cold-deck panels. The diurnally varying temperatures imposed on the panels were the same for the wet and dry runs shown in Fig. 1. Enough time elapsed in the wet run so that each transducer showed the same response pattern from day to day, and the top fluxes were shifted relative to the bottom so that the peaks coincided in time. The top transducer was next to hygroscopic plywood and blotting paper. Water was added at the top of the panel five days before the beginning of the results shown for the wet run in Fig. 1. The added water had no apparent effect on the top transducer. The bottom transducer was next to a sheet of polyethylene with holes, but the relatively few holes were not sufficient to prevent condensation on or around the transducer in the wet case. The response of the wet transducer on the bottom was 80%

larger for the daytime peaks (negative numbers) and 125% larger for the nighttime peaks (positive numbers) compared to that of both top ones and the dry bottom one, and was probably due to condensation and subsequent evaporation.

Moisture and Temperature Calculations for Constructions of Hygroscopic Materials, (MATCH), a numerical model for the combined heat and moisture transfer that takes the latent heat effects into account, was used to predict the total of latent and sensible heat flows. The total was approximately what was indicated by the bottom transducer in the wet case. Consistent with the results from MATCH, the top transducer seemed to respond to only the sensible (conducted) heat. The latent heat component of the total heat transfer when moisture is moving in the roof construction can be approximated by comparing the top and the bottom heat fluxes. In this way, it is found to be as large as the sensible heat; that is, the total heat flux doubles due to the effects of moisture.

The gravimetric technique for determining the moisture content in the panels was subject to major uncertainties. The most important was that it was impossible to pick up all the condensed moisture from interior surfaces in the panels, so small amounts of drying were not accurately detected. Thus, even the two panels, one of each type, that had a solid sheet of polyethylene as the vapor retarder appeared to have lost about a fourth of the water that was added, but most likely did not lose any. The two panels having polyethylene vapor retarders with holes seemed to lose about half the added water, but most likely lost only about a fourth.

The water-permeable vapor retarder in the permeable cold-deck panel allowed all the added water to escape within three weeks, while the cold-deck panel using polyethylene with holes showed that 45% of the added water escaped. In the warm-deck panel insulated with expanded polystyrene, approximately 60% of the added water appeared to have dried out through the water-permeable vapor retarder compared to 50% for the polyethylene with holes. Thus, the drying effect with a water-permeable vapor retarder is at least as good as when the polyethylene has holes punched in it. Drying with the water-permeable vapor retarder is better, however, when the insulation is permeable and non-hygroscopic, providing optimal conditions for condensate to gather on this vapor retarder and wick through the synthetic fabric which forms its core.

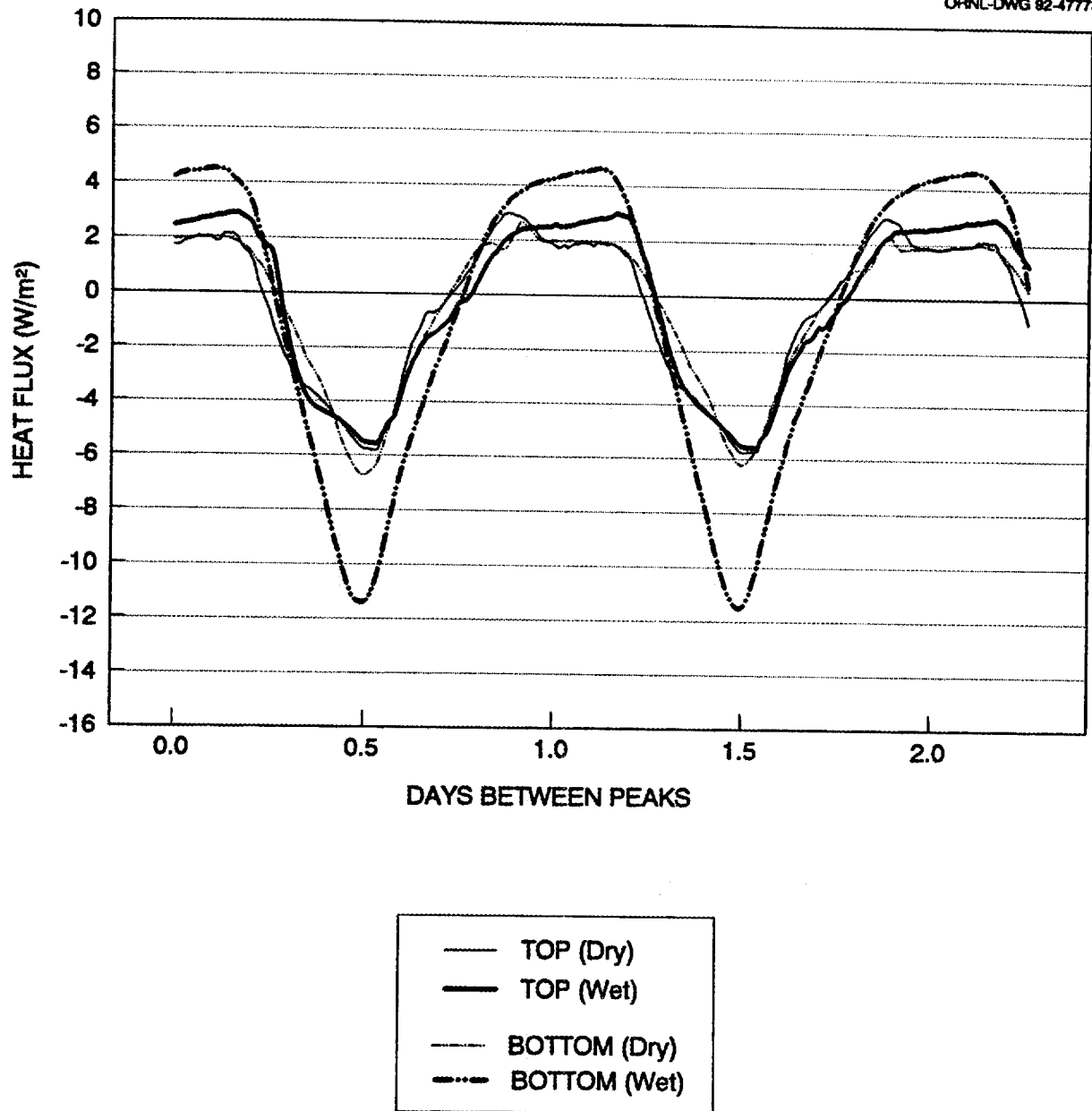


**Fig. 1. Heat fluxes measured at the top and bottom of a panel of the cold-deck type during dry and wet dynamic runs with identical imposed temperatures.**

A fourth pair of panels used no vapor retarder at all. In the cold-deck panel, all the water added, as well as a substantial amount of the hygroscopic moisture from the plywood, escaped within the three weeks of the wet tests. All the added water in the warm-deck panel also dried out. Thus, both the water-permeable vapor retarder and the polyethylene with holes do present enough resistance to prevent complete drying in the time allowed in this experiment.

The experiment showed that downward drying without venting is possible using the heat imposed on the roof on summer days. Drying requires that vapor retarder systems be installed that allow some moisture to migrate through them. However, some climates still require roofs to have a good vapor retarder in order to minimize the accumulation of moisture from upward migration during cold periods. The water-permeable vapor retarder appears to meet both criteria when building new roofs. How the principles the water-permeable vapor retarder embodies should be implemented when reroofing over wet roofs so as to obtain drying in the summer and avoid rewetting in the winter is still unclear and further study is recommended.

## 1. INTRODUCTION

Moisture in roof systems has been a long-standing issue for the roofing industry for a number of reasons. Leaks into interior spaces are always unacceptable. Dimensional instability, corrosion, and material disintegration can lead to early failure, and wet insulation will perform below thermal performance levels specified during design. A more recent concern relates to the increased investment in roof insulation during the past ten to fifteen years. The membranes on these roofs are aging, leaks are developing, and repair or replacement is required. The choices are to reroof over the entire old roof, preserve only the undamaged part of the old roof, or tear off and replace everything. Basic questions about reroofing include whether or not recovered wet insulation dries and, if so, how rapidly? Also, are systems available to design rapid downward drying potential into new roofs? A program of research has been initiated at the U.S. Department of Energy (DOE) Building Envelope Research Center at the Oak Ridge National Laboratory (ORNL) to study proposed answers to these and related questions.

This report deals with a study of the effect of moisture in low-slope roofs. It is an investigation of drying rates and thermal performance while downward drying occurs under summer conditions without roof venting. Various means were allowed for retention or escape of moisture downward into the space below the test sections. This experiment used measurement and predictive techniques and procedures developed especially for it, and the purpose of this report is to document these techniques and procedures in detail. The techniques and procedures sought to measure and predict moisture movement and heat transfer simultaneously. A numerical model for combined heat and mass transfer, Moisture and Temperature Calculations for Constructions of Hygroscopic Materials (MATCH), which was essential for understanding the heat flux measurements, is included in the techniques.

### 1.1 OVERVIEW OF THE EXPERIMENT

An important objective of this study was to determine if it is possible to dry roofs that contain excessive amounts of water without ventilation of the roof cavity, but through use of certain kinds of vapor retarders. The drying is driven by high temperatures above the roof

and is achieved by a diffusive transport of moisture downward. Control over the experimental conditions and the kinds of vapor retarders showed when and to what extent downward drying is possible, which will be of interest in the decision to reroof over wet materials.

Suitable thermal driving forces for downward drying are normally obtained in the summer period when roof surface temperatures are sufficiently high to drive the moisture toward the bottom of the roof system. Rather than test roofs outdoors during summer conditions, better control over these conditions is possible in the Large Scale Climate Simulator (LSCS) of the DOE Building Envelope Research Center at ORNL. Typical roof surface temperatures can be programmed and repeated for several consecutive days without any interruptions by conditions that are adverse for drying.

We investigated two roof types. As an example of a cold-deck system, the first contained, under a plywood deck, a fibrous-glass insulation that was especially permeable to water vapor. Its density was slightly less than that usually used in low-slope roofs, allowing as much moisture as the thermal driving forces permitted to migrate down in the daytime when the exterior surface temperature was elevated. The other type, an example of a warm-deck system, had a lightweight concrete deck toward the interior and was insulated with expanded polystyrene, which was much less permeable than the fibrous glass. In the warm-deck system, moisture migration was not influenced much by the daily peaks in temperature but proceeded downward in response to the average direction of the vapor pressure gradient during the experiment. The terms cold deck and warm deck are commonly used in the European roofing industry to refer to systems with insulation below and above the deck, respectively.

There were four versions of each roof type, three with three different vapor retarders, and one with no vapor retarder at all. The different vapor retarders were a solid sheet of polyethylene, a sheet with holes punched in a well-defined pattern, and a water-permeable vapor retarder. The latter was a novel vapor retarder that would allow initially wet roofs to dry out, but at the same time, retard vapor intrusion from below much better than no vapor retarder. The roof test panels with a solid polyethylene vapor retarder and without a vapor retarder defined the limiting behavior of the test panels.

Quantifying the impact of the presence of moisture on heat transfer rates in the insulation was another important objective of this moisture test. A preliminary experiment with similar materials and conditions showed that the latent heat effect on overall heat transfer through a roof with fibrous-glass insulation is quite important. The transfer of latent heat affects the energy flow to or from the space below such a roof, as well as the apparent heat fluxes measured by calibrated heat flux transducers used to monitor heat flow locally in the roof. Transducer readings became difficult to interpret, however, because the transducer is made of an impermeable material. In the preliminary experiment, transducers were embedded in the middle of permeable insulation and responded to the moisture flow to an unknown degree, measuring the conduction heat transfer and some of the latent heat.

The conclusion from the preliminary experiment was that, for permeable materials, the amount of latent heat effects which appear in the transducer response depends on the relative distance of the transducer from a condensate layer (where total latent effects should be seen) and a non-saturated hygroscopic layer (where only sensible effects should be seen). To test this hypothesis in the cold-deck panels for this experiment, transducers were located at the interfaces between the fibrous-glass insulation and its neighboring materials. When the neighboring material was impermeable (such as a vapor retarder), we hoped that the full latent heat effect would be registered by the transducer, because all the moisture that had migrated through the fibrous glass condensed at this location. When the neighboring material was plywood or some other hygroscopic material at non-saturated conditions, its ability to adsorb moisture should have caused the transducer to behave more like it does when placed in an impermeable medium. For the relatively impermeable expanded polystyrene in the warm-deck panels, heat flux transducers were located only in the middle of the insulation. Experience from the preliminary experiment suggested that no latent effects were expected due to the limited mobility of moisture in this material.



## 2. DETAILED DESCRIPTION OF THE EXPERIMENT

This section describes the apparatus, including the moisture probes used in the experiment, and provides the construction details of the roof test specimens, as well as the time schedule for the major activities during the experiment.

### 2.1 THE LARGE SCALE CLIMATE SIMULATOR

We conducted the experiment in the Large Scale Climate Simulator (LSCS) in the Building Envelope Research Center. The LSCS is a unique facility for controlled testing of whole roof systems under steady-state and dynamic conditions. It consists of three separate chambers where the environment can be controlled and monitored (Fig. 2.1). The roof specimen being tested is placed between a climate chamber above and a guard chamber (containing the optional metering chamber) below. The climate chamber imposes outdoor or environmental conditions, while the guard and metering chambers maintain indoor conditions. The specimen may be as large as 3.7 by 3.7 m (12 by 12 ft), of which the central 2.4 by 2.4 m (8 by 8 ft) covers the metering chamber when it is in place. We used only the climate and guard chambers in this test. The specimen is mounted on a diagnostic platform that can be lifted in and out of the chamber, thereby allowing pre- and post-test work to be done on the specimen outside the LSCS. Subdivision of the platform into smaller areas allows more than one specimen to be tested at the same time, but prevents the use of the metering chamber for tests in the guarded hot box mode. Detailed technical description of the LSCS is provided by Huntley (1989).

Temperatures in the climate chamber may be varied between -40 and 66°C (-40 and 150°F) and between 7 and 66°C (45 and 150°F) in the two lower chambers. The temperatures may be programmed to any desired scheme, from steady levels to rapid cycles. Furthermore, the dew point can be controlled in the climate and the guard chambers, and solar heating may be simulated in the climate chamber by using infrared heating lamps. The ability to vary temperatures in the climate chamber above the test sections according to a

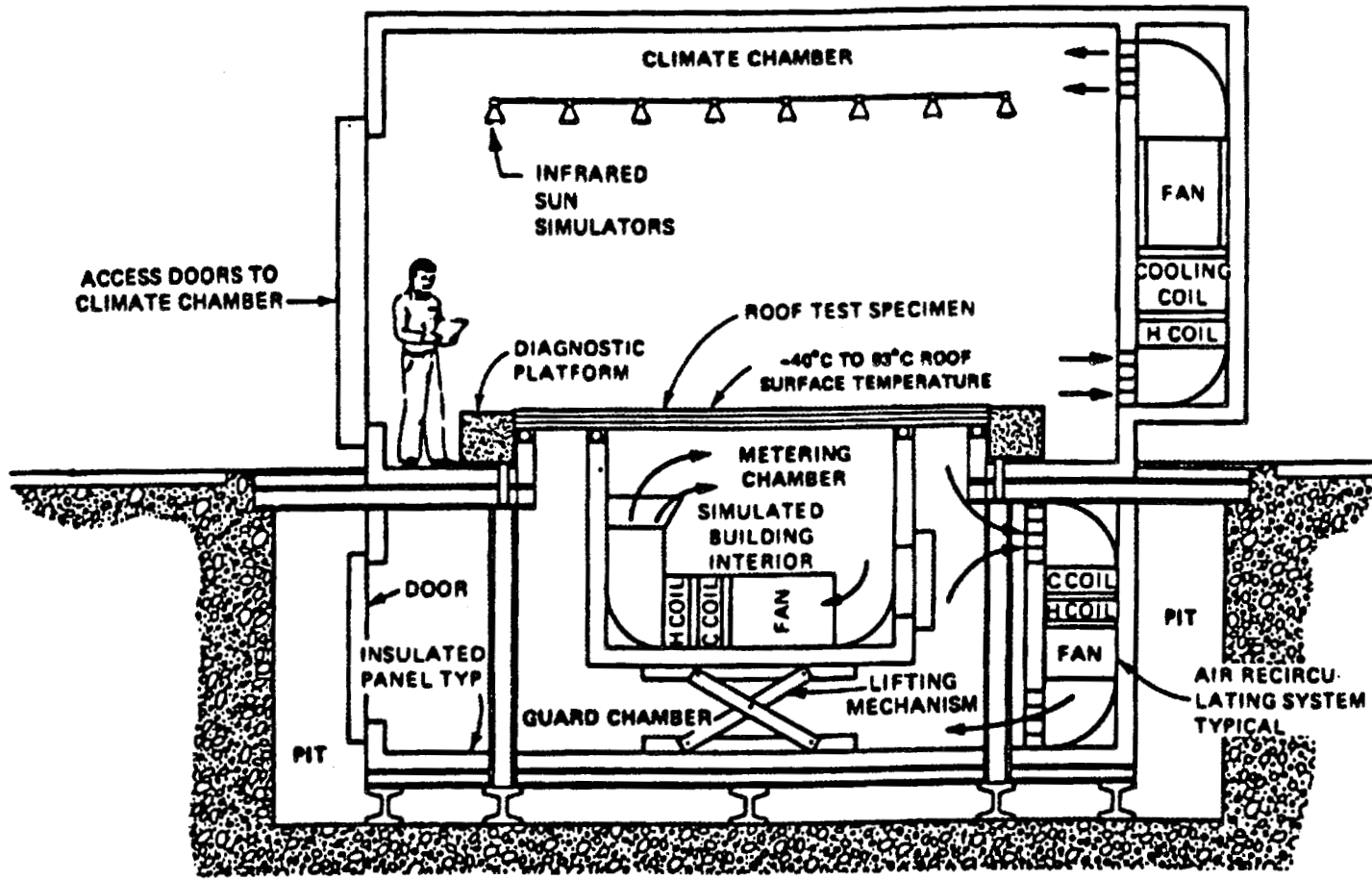


Fig. 2.1. Schematic of the Large Scale Climate Simulator.

programmed scheme conducive to drying is of special interest for this experiment. Because of this capability, there were no interruptions due to conditions adverse to drying. Because moisture movement is a relatively slow process, such interruptions could extend greatly the time needed to get meaningful results and mask the results by hysteresis effects.

## 2.2 EXPERIMENTAL SETUP

### 2.2.1 Design

The diagnostic platform for this experiment was divided by a wooden gridwork into nine equal areas for roof test panels, as Fig. 2.2 shows. Each of these areas had inside dimensions of 1.09 by 1.09 m (43 by 43 in.). The wood framing that formed the walls of each test panel was made from 3.8 by 16.5 cm (1.5 by 6.5 in.) wood joists insulated on the side with 2.5 cm (1 in.) of extruded polystyrene. To improve the vapor tightness of this framing system, we sealed the wood by applying a liquid sealant, and sealed all edges with silicone caulking.

Each panel is supplied with lifting brackets so it can be assembled individually before being lifted into the grid on the diagnostic platform. As stated in the overview of the experiment, the roof test panels have either a cold or warm deck. The cold-deck system, with a wooden deck on top of the insulation, is typical for roofs being manufactured in Europe. The warm-deck system has lightweight insulating concrete. Steel deck constructions will be studied during the next phase of the project. Their potential for downward drying would depend on the frequency and size of openings in them.

The cold-deck roof constructions comprise, from top to bottom: (see Fig. 2.3 for details)

- Ethylene propylene diene monomer (EPDM) membrane (white, 1.1 mm, 45 mil, reinforced) plus a layer of polyethylene,
- 12.7 mm (0.5-in.) plywood,
- 114 mm (4.5-in.) medium density fibrous glass ( $52 \text{ kg/m}^3$ ,  $3.3 \text{ lb/ft}^3$ , unfaced),
- Vapor retarder (if present), and
- 12.7 mm (0.5-in.) gypsum board.

The warm-deck roof constructions comprise, from top to bottom: (see Fig. 2.4 for details)

- EPDM membrane (black, 1.1 mm, 45 mil) with added layer of polyethylene,
- 51 mm (2 in.) expanded polystyrene ( $14 \text{ kg/m}^3$ ,  $0.88 \text{ lb/ft}^3$ ),
- Vapor retarder (if present), and
- Lightweight concrete ( $470 \text{ kg/m}^3$ ,  $29 \text{ lb/ft}^3$ ), about 108 mm (4.25-in.) thick, cast in-situ.

The color of the EPDM had no significant effect on these experiments. The difference in color merely allowed easy identification of the cold- and warm-deck types when viewed from above. Each roof type was repeated in four sections, with four different vapor retarder systems. One had a regular solid sheet of polyethylene (0.15 mm, 6 mil) as vapor retarder, and another had the same kind of polyethylene with holes of 5.5 mm (0.22 in.) diameter in a rectangular pattern, 273 mm (10.75 in.) apart (approximately 13 holes per square meter). The holes were to simulate, in a regular way, the gaps in a solid vapor retarder which occur in practice when separate sheets are not overlapped tightly or penetrations through the vapor retarder are not sealed. The third test panel of each type had a water-permeable vapor retarder, which is described in Sect. 2.2.2. The fourth panel had no vapor retarder. We added water to these eight panels after tests to determine non-wetted thermal performance and moisture content. A ninth panel was constructed identically to the cold-deck panel using a solid sheet of polyethylene as vapor retarder, except that it had no sheets of blotting paper at the top and bottom. No water was added to this panel in the experiment, because it served as a control.

Unless the bottom of a panel was a permeable material, there could be no downward drying of the test panel during the experiment. In the cold-deck panels this was ensured by making the bottom of the panels out of a piece of sheet aluminum, 3 mm- (0.12 in.-) thick, with a 0.97 m (38 in.) square cut out of the center. The remaining perimeter of this metal plate supported the materials when they were mounted in the panel. The warm-deck panels had a metal lattice that allowed downward drying and provided additional support for the panels.

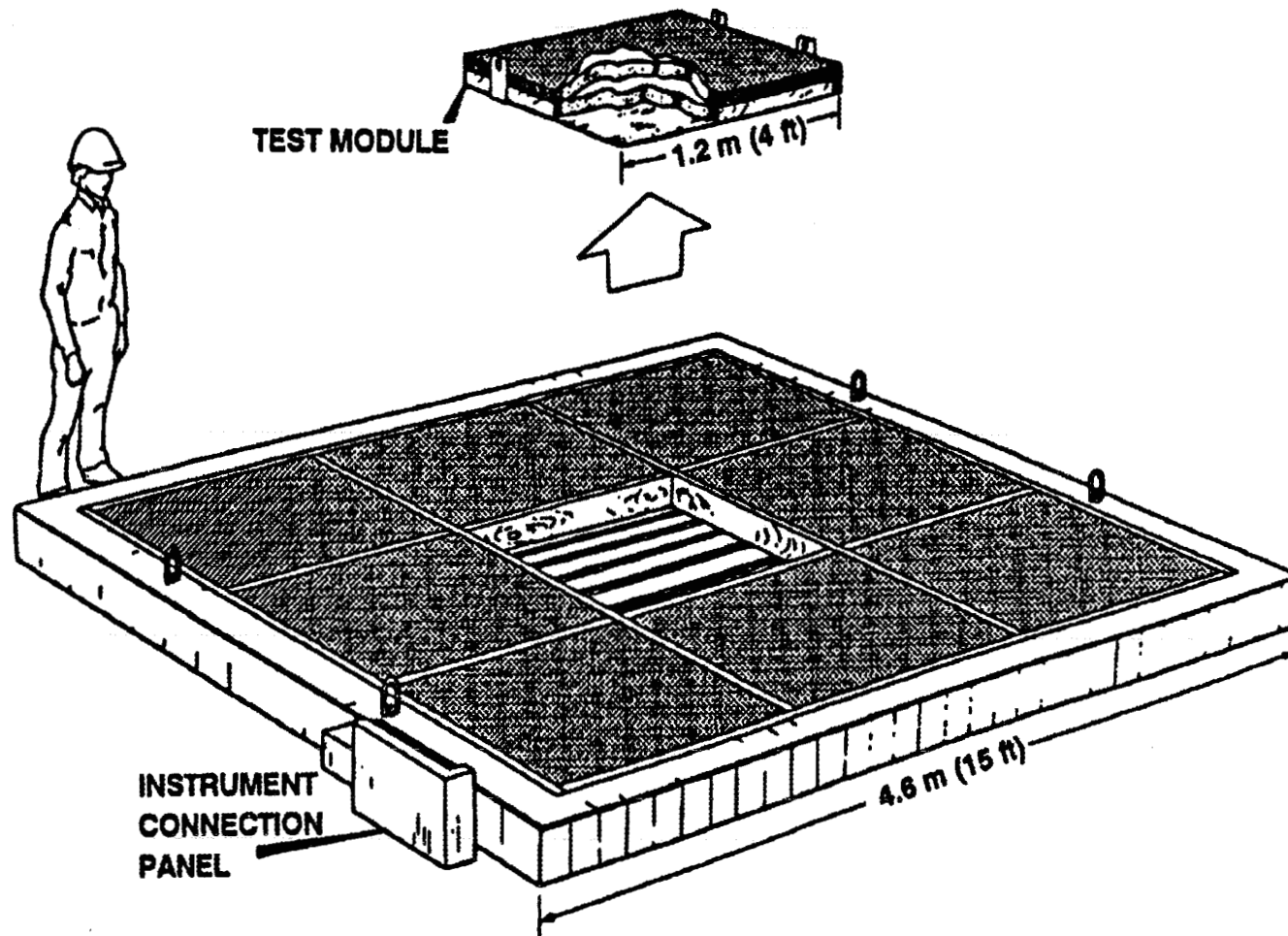


**Fig. 2.2. A diagnostic platform with nine panels for use in the Large Scale Climate Simulator.**

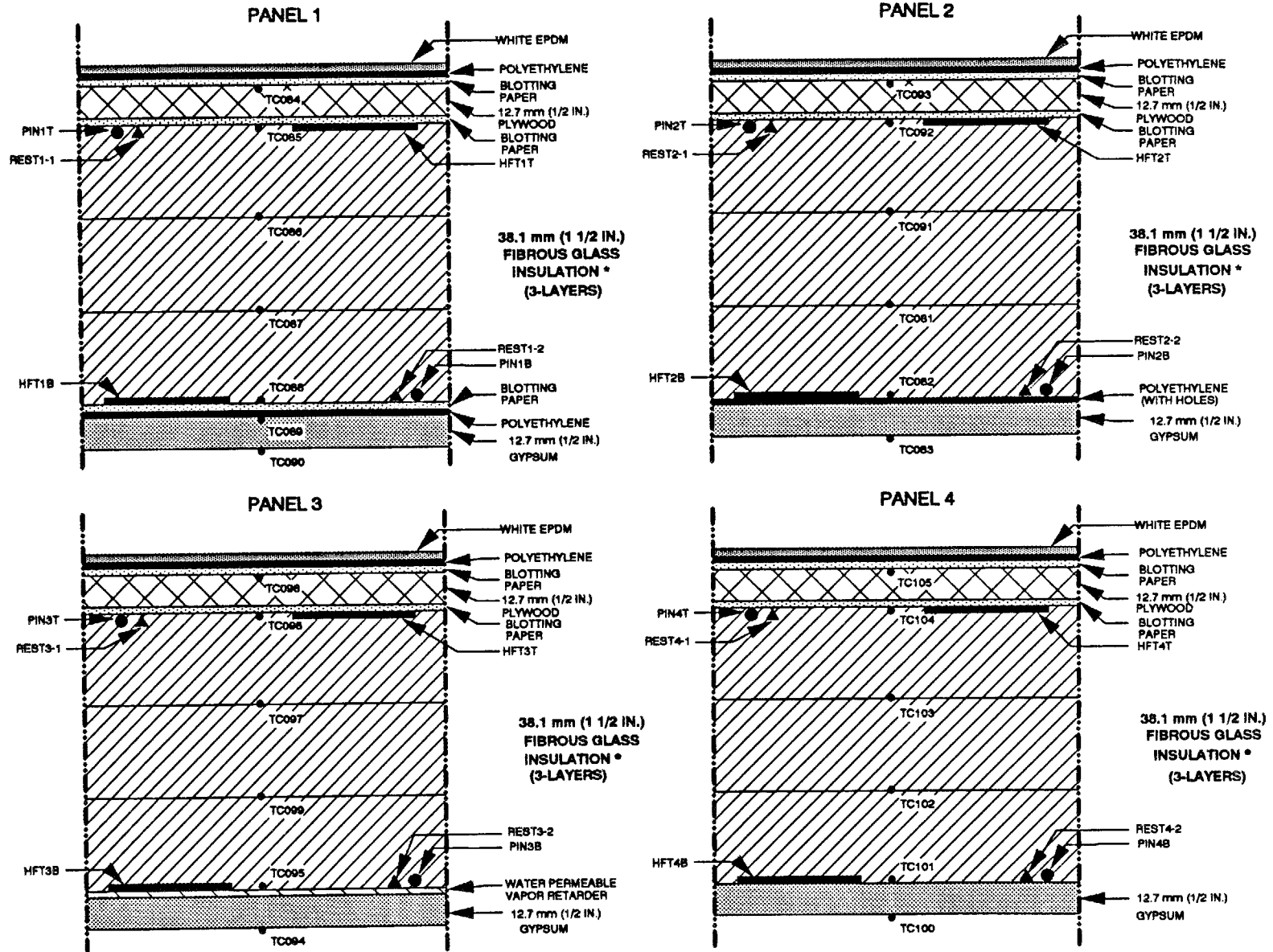


**Fig. 2.3. Details of panels 1, 2, 3, and 4 for studying drying rates: cold-deck panels with permeable insulation\* materials.**  
 Legend: PIN = PIN Moisture Probe; REST = Resistance Moisture Probe; TC = Thermocouple; HFT = Heat Flux Transducer

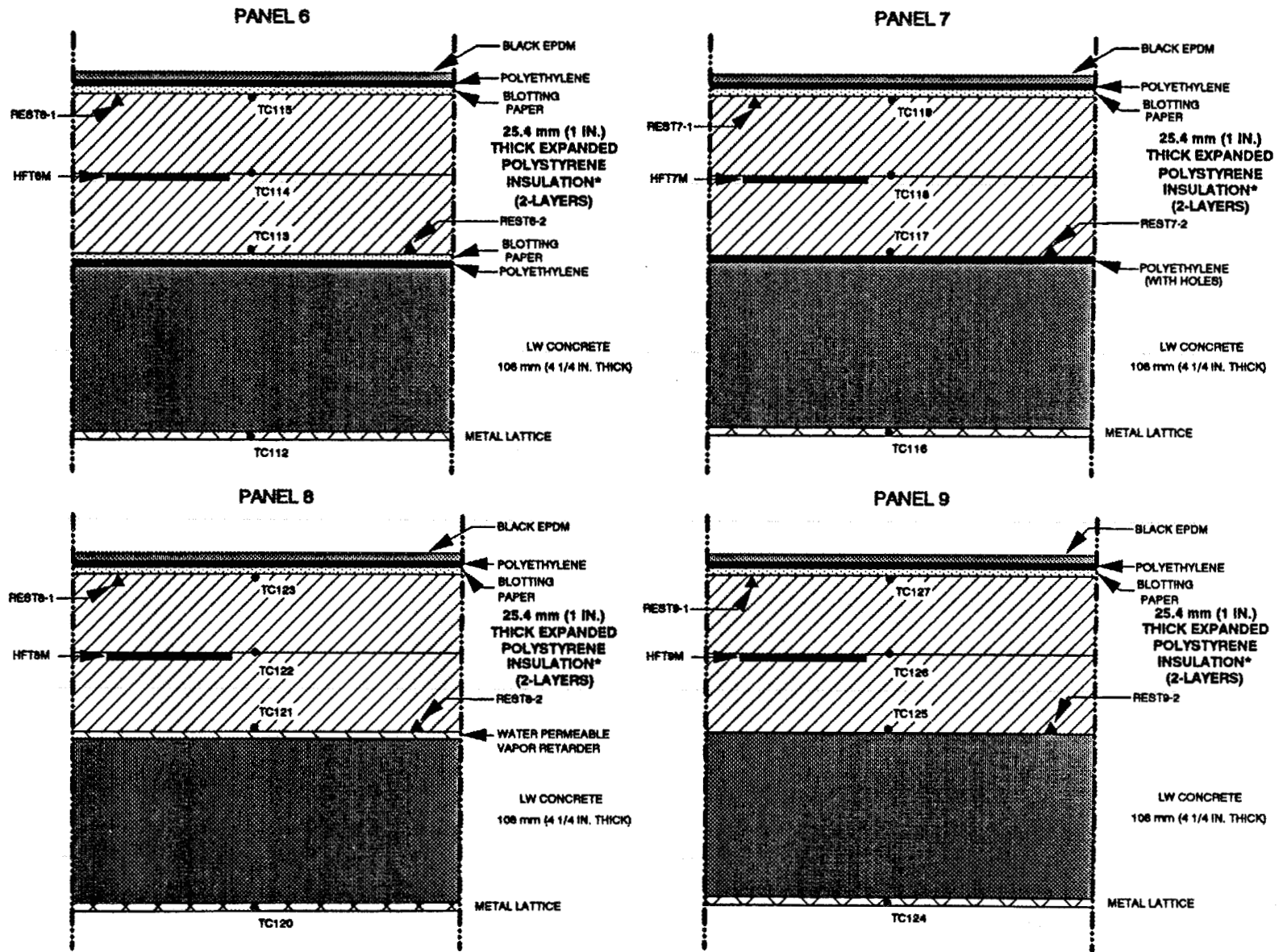


**Fig. 2.4. Details of panels 6, 7, 8, and 9 for studying drying rates: warm-deck panels with impermeable insulation\* materials.**  
 Legend: PIN = PIN Moisture Probe; REST = Resistance Moisture Probe; TC = Thermocouple; HFT = Heat Flux Transducer

To provide access to specimens inside the panels during the experiment, we attached roofing membranes so that they could be lifted easily from the panels. Removal of the membrane was done by releasing screws holding 2.5 cm- (1 in.-) wide metal strips around the perimeter of the panels, which in turn kept the roof membrane in place. We sealed the membrane to the frame with a bead of silicone caulking between the membrane and the wood joists.

To permit removal for weighing of as much as possible of the materials in each section, we cut the insulation in each section into a center square piece approximately 61 by 61 cm (2 by 2 ft), which was surrounded by approximately 24 cm- (9.5 in.-) wide guard pieces of the same material. Experience from prior studies and estimates of edge effects assured us that one-dimensional movement of heat and moisture would occur in the central area where the instruments were located. Two or three layers of insulation were present in each panel, allowing the materials to be cut into slightly different sizes in each layer. This prevented the occurrence of vertical cracks all the way from the top to the bottom of a section. Because the center pieces held the thermal and moisture instrumentation, lead wires from them to the data acquisition system prevented their easy removal from the test sections. We weighed only the guard pieces, under the assumption that lateral distribution of water in liquid and vapor forms was uniform. If so, the moisture content of the guard pieces was to the total moisture content in the system as their area was to the total area.

For this experiment, any water added or originally in the test panels could escape only from the bottom of the sections. To allay any concern that moisture would diffuse through the EPDM membranes at high temperature, we added a sheet of 0.15 mm (6 mil) polyethylene directly below the EPDM in all panels.

We added sheets of blotting paper ( $440 \text{ g/m}^2$ ,  $0.09 \text{ lb/ft}^2$ ) at certain material interfaces in order to ensure even lateral distribution of the water when it was added. They also helped to measure the amount of moisture that condensed at these interior surfaces of the panels. The places where blotting paper was added included the top of the expanded polystyrene in the warm-deck panels, and on each side of the plywood in the cold-deck panels. The panels

with solid polyethylene as the vapor retarder were given a sheet of blotting paper between the insulation and the polyethylene to absorb the moisture condensed there. We did not add blotting paper at this location in the panels with the water-permeable vapor retarder or the polyethylene with holes. This avoided artificial enhancement of the lateral moisture transport over these vapor retarders, possibly to locations which would change the performance of the system. As mentioned above, the control panel did not have any blotting paper.

The lightweight insulating concrete in the warm-deck panels was cast in-situ with the panels as molds and vermiculite as aggregate. The casting took place approximately 50 days before the final assembly of the panels and the beginning of the tests. Ten days after the concrete was cast, we moved the panels to a conditioning chamber at 32°C (90°F). The temperature in the chamber was raised to 47°C (116°F) after another 10 days. The dew point in the chamber was the same as in the ambient laboratory air, that is, around 15°C (50°F). After 10 days at the elevated temperature, we removed the panels from the chamber and stored them in an air-conditioned environment at 26°C (78°F) and a relative humidity of about 60% (dew point temperature of 17°C or 63°F).

Moisture probes made from small pieces of plywood were cast into the top, middle, and bottom of the concrete to monitor the level of moisture content during the conditioning. Two fasteners, approximately 2.5 cm (1 in.) apart, were screwed into each piece of plywood, a wire was attached to each screw, and the connections sealed with epoxy. The electrical resistance between the pair of screws on each piece of plywood responds to the level of moisture content at its location. Initially, when the moisture content of the plywood is above fiber saturation, the resistance is quite low. Later, when the moisture level goes into the hygroscopic region, this simple moisture probe signals a decrease in moisture content by a measurable increase in resistance.

Although the concrete became surface dry after a few days in the laboratory air, the center moisture probe did not signal hygroscopic levels of moisture content in the concrete

until after the temperature was raised during conditioning. We took the panels out of the chamber when the resistance of all moisture probes corresponded to 50% RH if the probes were in air. The lead wires to these probes were disconnected before assembling the rest of the roof panel.

### **2.2.2 The Water-Permeable Vapor Retarder**

The water-permeable vapor retarder is a proprietary vapor retarder developed at the Technical University of Denmark (Korsgaard, 1985). Its properties are such that diffusion of water vapor into a roof from the inside air is hindered by a relatively high vapor resistance. Any excessive liquid inside the roof cavity from the construction period or from minor leaks will not be trapped inside the cavity, because liquid moisture can be transported through the water-permeable vapor retarder. This is possible when condensation takes place during summer in the interface between the insulation and the vapor retarder.

Figure 2.5 shows a cross section of the water-permeable vapor retarder to illustrate its design concept. It consists of a layer of synthetic fabric with good capability to support capillary suction. On each side of the fabric are strips of polyethylene film. These strips are staggered so that they overlap each other by 5 to 6 centimeters (2 to 3 inches). Thus, the fabric is exposed on the top and the bottom side of the vapor retarder at different lateral locations, not allowing a direct permeable path for vapor diffusion, yet permitting liquid to wick through the fabric from an exposed place on top to another on the bottom of the layer.

Figure 2.5 also shows the major paths of moisture transport through this vapor retarder. Diffusion of water vapor through the membrane must take place through the thin layer of fabric and one or two layers of polyethylene, or the vapor must proceed along the long narrow path through the fabric from opening to opening. The path of least water-vapor resistance of the system is along the fabric, yielding a permeance which is less than that of a solid polyethylene film but significantly more than that of a single thin layer of fabric. Liquid water, however, is rapidly transported through the membrane. When it condenses on

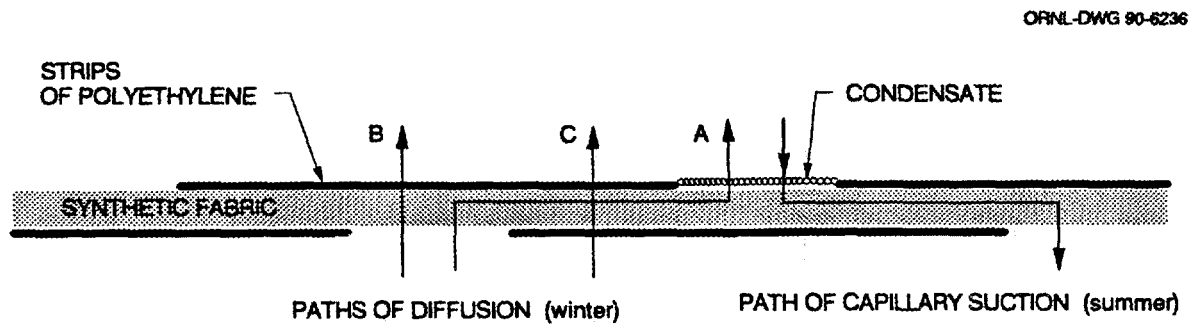


**Fig. 2.5. Design concept of the proprietary water-permeable vapor retarder system.**

the part of the membrane where the fabric is exposed at the top, capillary action transports it to the part of the membrane where the fabric is exposed at the bottom. The water may evaporate or pass through to the ceiling material on which the water-permeable vapor retarder lies.

### 2.2.3 Instrumentation

Detailed cross sections of cold-deck roof test panels 1–4 are shown above in Fig. 2.3. Fig. 2.4 shows the warm-deck panels 6–9. Panel 5, which remained dry except for hygroscopic moisture throughout the experiment, is not shown. It is identical to panel 1 but does not contain moisture probes or sheets of blotting paper.

Temperatures were measured by thermocouples at most interfaces between layers. In the cold-deck roofs shown in Fig. 2.3, these locations were on each side of the plywood deck, between the insulation boards, on top of the vapor retarder, and on the bottom of the gypsum ceiling. In the warm-deck panels shown in Fig. 2.4, temperatures were measured at the top, middle, and bottom of the expanded polystyrene, and at the metal lattice at the bottom of the concrete. The outside surface temperature of the membrane was also measured for the panels, as were the dry-bulb and dew point temperatures in the chamber above the roof panels (the climate chamber) and in the chamber below (the guard chamber).

We measured heat fluxes at the top and bottom of the fibrous-glass insulation in the cold-deck panels, and in the middle between the expanded polystyrene boards in the warm-deck panels. The heat flux transducers were of a thermopile type with outside dimensions of approximately  $2.5 \times 51 \times 51$  mm ( $0.094 \times 2 \times 2$  in.). The transducers were calibrated while situated in locations and materials similar to their test configurations. We calibrated the transducers next to plywood and gypsum at  $13^\circ\text{C}$  ( $55^\circ\text{F}$ ) and  $34^\circ\text{C}$  ( $93^\circ\text{F}$ ), respectively; we calibrated the ones in expanded polystyrene at  $23^\circ\text{C}$  ( $74^\circ\text{F}$ ). Calibration of 2 of the 14 transducers at different temperatures showed that the sensitivity decreased by  $0.15\%/^\circ\text{C}$  ( $0.085\%/^\circ\text{F}$ ). The data analysis used a constant value for the sensitivity at the respective

calibration temperatures, which approximated the mean temperatures at the location of the transducers in the experiment. To avoid effects of moisture migration during the transducer calibration, the plywood of the cold-deck assembly was held against the cold plate in the heat flow meter apparatus used for the calibrations.

We used two different kinds of moisture probes in the experiment. The electrical capacitance pin probe consists of two, parallel, 3.3 cm- (1.31 in.-) long rows of metal pins, 8 mm (0.33 in) apart, that were inserted 2.5 cm (1 in.) into the test material. The pins are mounted in a plexiglas socket with wires connected to each row of pins. The electrical capacitance between the two rows increases with moisture content in the material. We inserted pin probes into the top and bottom of the insulation of the four cold-deck panels to which water was added. The probe is produced on a prototype basis at ORNL and has been described previously by Motakef (1989) and Courville (1987).

The other type of probe used in the experiment was a plywood, electrical resistance probe. It consists of a 50 mm (2 in.) disc of 12.7 mm (0.5 in.) plywood with two electrodes nailed into it. The electrical resistance between the electrodes was calibrated to give the moisture content in the plywood. The moisture content may be interpreted as the relative humidity of the probe environment, using the sorption isotherm for the plywood. The calibration data for these probes were supplied by the manufacturer and accounts for temperature effects. Due to the size of the probe, it responds slowly to changes in the environment. Readings were not required every 10 minutes as with the automated data acquisition system of the LSCS, which was provided to follow dynamic effects with the other sensors. Therefore, we took readings manually twice per day with an ohmmeter that suited the probes' high resistances, on the order of megohms, and compiled temperature data from the thermocouple built into each probe. We installed the plywood probes in the top and bottom of the insulation of all the cold-deck panels to which water was added.

As a more quantitative measure of the total amount of moisture in the panels, we removed specimens of the materials in the roof assemblies shortly after the end of each wet run in the test sequence. Four disks, approximately 10 cm (4 in.) in diameter, were removed from each of the plywood decks, along with the sheets of blotting paper and most of the

insulation from the guard area. As mentioned above, the pieces of the insulation in the central area held instrumentation that was connected by lead wires to the data acquisition system, and they could not be removed easily or weighed accurately with these instruments in place.

### 2.3 EXPERIMENTAL CONDITIONS

We scheduled a series of test runs in order to achieve the goals of the experiment, with special focus on providing realistic conditions for downward drying. Figure 2.6 shows schematically the temperatures that were held in the upper (climate) and lower (guard) chambers during the course of the whole experiment. No water was added to any of the panels in the first six runs. All the materials did, however, contain hygroscopic moisture, because they were stored in the laboratory at approximately 60% RH before the assembly of the roof panels. Relative to most insulation materials, plywood's hygroscopic moisture content is particularly large. Table 2.1 provides moisture content at 60% RH and 20°C (68°F) of materials typical of those used in this study.

The first five runs were steady-state tests carried out in order to determine the thermal resistance of the individual materials as a function of temperature. The climate chamber was warmer than the guard chamber in the first two runs; that is, heat flow was downward. Because most of the hygroscopic moisture inside the roof cavity was located in the plywood in the cold-deck panels, it was driven out slowly and condensed on the vapor retarder during these two runs. Heat flux measurements were disturbed somewhat when this happened. In the next three runs the guard chamber was kept warmer than the climate chamber. This provided reliable values of dry resistance at three different average temperatures. After imposition of the desired climate chamber temperature, steady-state conditions were obtained within 4 days in run 3 (in order for the condensed water to evaporate and migrate back to the plywood) and within 2 days in runs 4 and 5. Table 2.2 lists the exact temperatures in the chambers during the steady-state runs.

**Table 2.1. Moisture Content of Various Materials at 60% RH and 20° C (68° F)**

Material	Water to dry mass ratio (%)	
	Desorption	Adsorption
Expanded polystyrene	4.2	3.8
Fibrous glass (18 kg/m <sup>3</sup> )	1.6	1.3
Filter paper	6.0	6.0
Gypsum board (24° C, 57.5% RH)*	1.5	1.0
Lightweight concrete (640 kg/m <sup>3</sup> )	5.8	3.7
Pine (510 kg/m <sup>3</sup> )	14	11
Plywood (600 kg/m <sup>3</sup> )	14	11.5
Rockwool (42 kg/m <sup>3</sup> )	0.6	0.55
Rubber	.65	.65

(Hansen, 1986; \*Richards, 1992)

Another dry run, run 6, followed the steady-state tests, and lasted for three consecutive days. The guard chamber temperature was kept constant at 23.9°C (75°F), while the temperature in the climate chamber varied in diurnal cycles between 15.6 and 43.3°C (60 and 110°F). The cycles were not perfectly sinusoidal; the desired shape was determined by observing real roof membrane temperatures on a cloudy summer day and stretching the profile to the desired level.

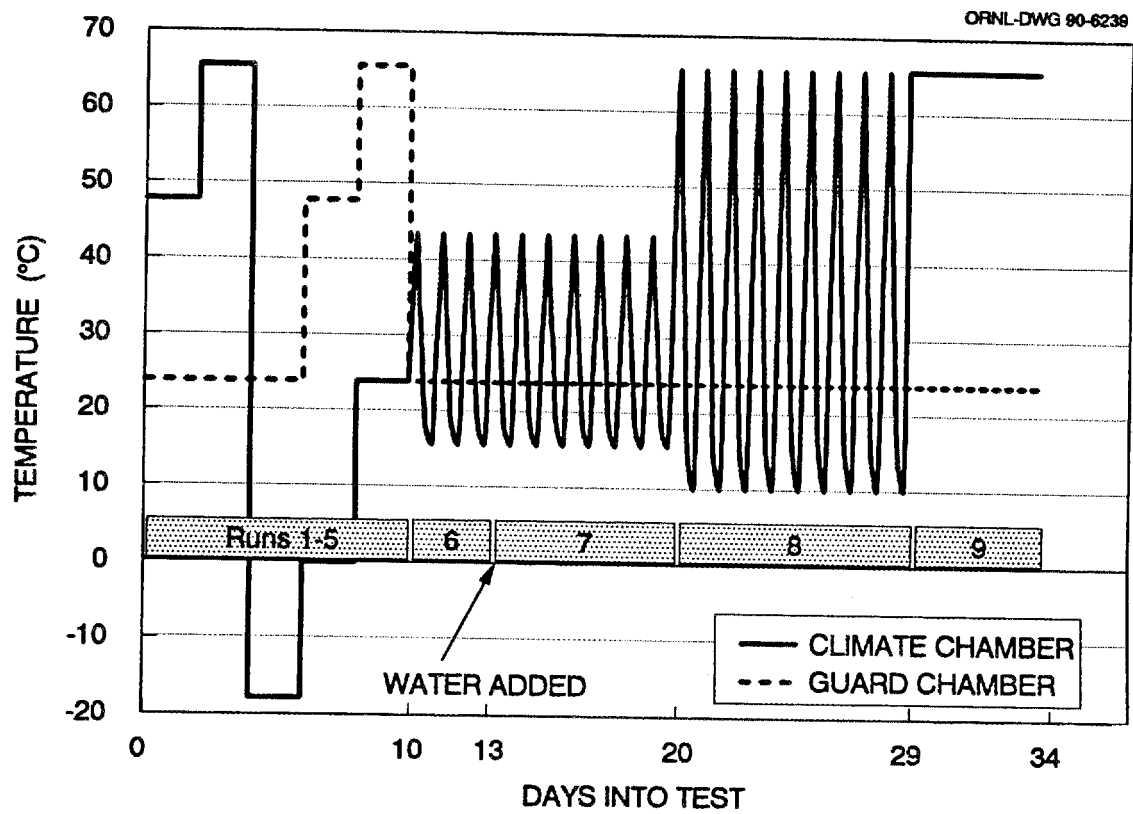


**Fig. 2.6. Applied temperatures before and after water addition.**

Between runs 6 and 7, water amounting to  $1 \text{ kg/m}^2$  ( $0.205 \text{ lb/ft}^2$ ) was added at the top of panels 1–4 and 6–9. The temperatures imposed in run 7 were identical to those in run 6, and run 7 lasted for a week. We increased the amplitude of temperatures in the climate chamber in run 8 to get a variation between 10 and  $65.6^\circ\text{C}$  ( $50$  and  $150^\circ\text{F}$ ) typical of a sunny summer day. Run 8 lasted for nine days. Finally, climate chamber temperatures were held steady at  $65.6^\circ\text{C}$  ( $150^\circ\text{F}$ ) for five days to comprise run 9.

After run 9, we moved the diagnostic platform holding the nine panels for this test out of the LSCS and stored it in the Building Envelope Research Center. Well after the end of run 9, panels 1–4 were disassembled and a solid polyethylene vapor retarder was added just below the insulation in them, even if they already had a vapor retarder system. The panels were then reassembled and the platform was reinserted in the LSCS for repeats of the conditions of runs 3, 4, and 5, which were steady-state runs with upward-directed thermal driving forces. Just as in the original runs 3, 4, and 5, we held conditions long enough to obtain several hours of steady-state performance. Unlike the original runs, steady-state was achieved in less than a day for each set of conditions. This was evidence that the panels were indeed dry. The purpose of these runs was to check the dry thermal performance of the permeable-fibrous glass insulation in a situation where any moisture, even hygroscopic moisture, was prevented from moving.

**Table 2.2. Temperatures in the Guard and Climate chambers during dry, steady-state runs**

Run No.	Climate Chamber		Guard Chamber	
	$^\circ\text{C}$	$^\circ\text{F}$	$^\circ\text{C}$	$^\circ\text{F}$
1	47.8	118	23.9	75
2	65.6	150	23.9	75
3	-17.8	0	23.9	75
4	0	32	47.8	118
5	23.9	75	65.6	150



### 3. MATCH COMPUTER PROGRAM

The one-dimensional model known as MATCH was used throughout this experiment to interpret the measured heat fluxes and distributions of temperature and moisture. The main features of MATCH are

- one-dimensional, finite difference model,
- transient moisture and temperature calculations,
- moisture transport by vapor diffusion and liquid flow by capillary suction,
- moisture impacts included in thermal properties and enthalpy release/uptake by phase conversions,
- advanced description of moisture retention curves expressed as a function of moisture content including treatment of hysteresis,
- environmental conditions constant or from a file containing experimental or test meteorological data,
- library of material properties attached to model,
- user friendly preprocessor,
- program runs on a personal computer, and
- applies to roofs as well as other building constructions.

Detailed description of MATCH is available in Pedersen (1990). How MATCH predicts the thermal behavior of test specimens during the migration of moisture and its predictive capability regarding moisture flow and distribution are the capabilities that have relevance for this experiment. The presence of moisture enhances the conduction of heat in insulation, because the higher thermal conductivity of water increases the conductivity of moist insulation. Moreover, there is an appreciable latent contribution to heat transfer when moisture evaporates or sublimates at one location, diffuses through part of the construction, and condenses or freezes at another place. This phenomenon carries a large amount of enthalpy directly from the evaporation or sublimation plane to the condensation plane. MATCH is able to account for both the enhanced conduction and the latent heat transfer in one-dimensional, homogeneous layers of roofing materials.

To account for the effect of moisture requires knowing where the moisture is and how it migrates. Transient moisture transport by vapor diffusion is described by Fick's law and the local accumulation of moisture by the sorption curves for the materials. At the water concentrations possible in this study, we did not expect transport of moisture in the liquid phase by capillary suction to make an important contribution to the total moisture transport. Parameters used in MATCH to describe moisture transport phenomena were not measured for the actual materials used but have been chosen from values in the literature for similar materials. Results from the moisture probes and the weighings provide reference points and trends to ensure that these choices have been made properly.

#### 4. THERMAL MEASUREMENTS

Section 4.1 reports on the determination of the dry R-values of the materials from the early, steady-state runs and repeated runs with upward thermal driving forces. These values are used in subsequent sections to interpret results from transient phenomena after the addition of water. A dry, dynamic run, described in Sect. 4.2, is also included for comparison to results after the addition of water. Results for the wet, dynamic runs are presented in Sects. 4.3 and 4.4. Section 4.5 summarizes the effects of moisture on the heat flux transducers embedded in permeable materials and shows detailed schematics of the mechanisms involved. These results demonstrate that sensible and combined sensible-latent heat fluxes can be measured simultaneously by properly locating the heat flux transducers.

##### 4.1 DETERMINATION OF ROOM-DRY R-VALUES

As Fig. 2.6 shows, the initial runs in this experiment consisted of several periods where the guard and climate chamber temperatures were kept steady at various levels. Steady-state occurs when the heat fluxes in the panels become constant in time. We added no water; however, we expected hygroscopic moisture to be present in some of the materials, especially in the plywood, because we stored the materials in the laboratory at about 60% RH before the assembly of the panels.

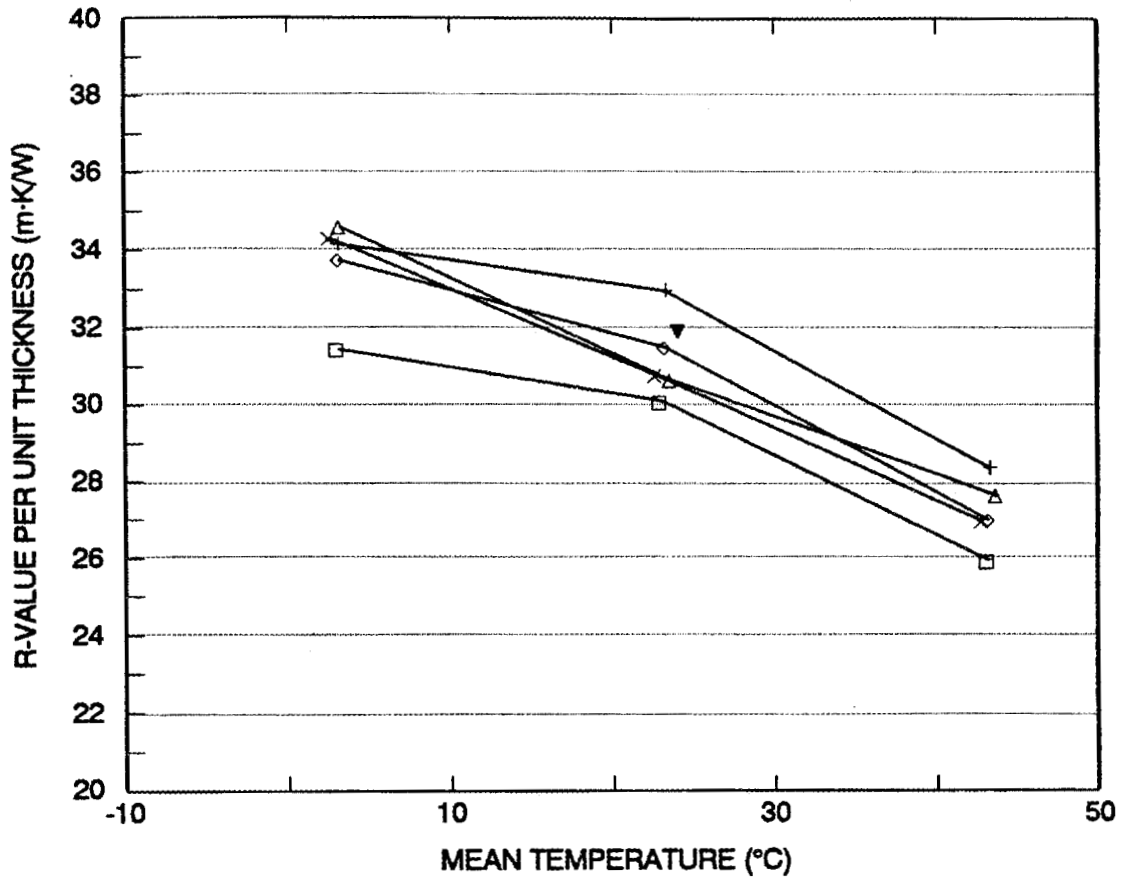
We judged the time to reach steady-state by observing how the heat fluxes changed with time. We maintained steady-state conditions for at least four hours in accordance with ASTM C 236 procedures (ASTM, 1987), which we followed as closely as possible. We used values of temperature differences across the insulation,  $\Delta T$ , and heat fluxes,  $q$ , at 10-minute intervals from the last four hours in the calculation of R-values,  $R$ , according to the averaging technique:

$$R = \frac{\sum \Delta T_i}{\sum q_i} \quad (1)$$

The heat fluxes we used in Eq. (1) were either the readings from the single heat flux transducers in the warm-deck constructions, or the average of the two heat flux transducer readings in the cold-deck constructions. The heat flux transducers indicated that hygroscopic moisture was moving in the cold-deck roofs, especially in runs 1 and 2. The response from the bottom transducer was often about 15% higher than that from the top, although the temperatures were steady.

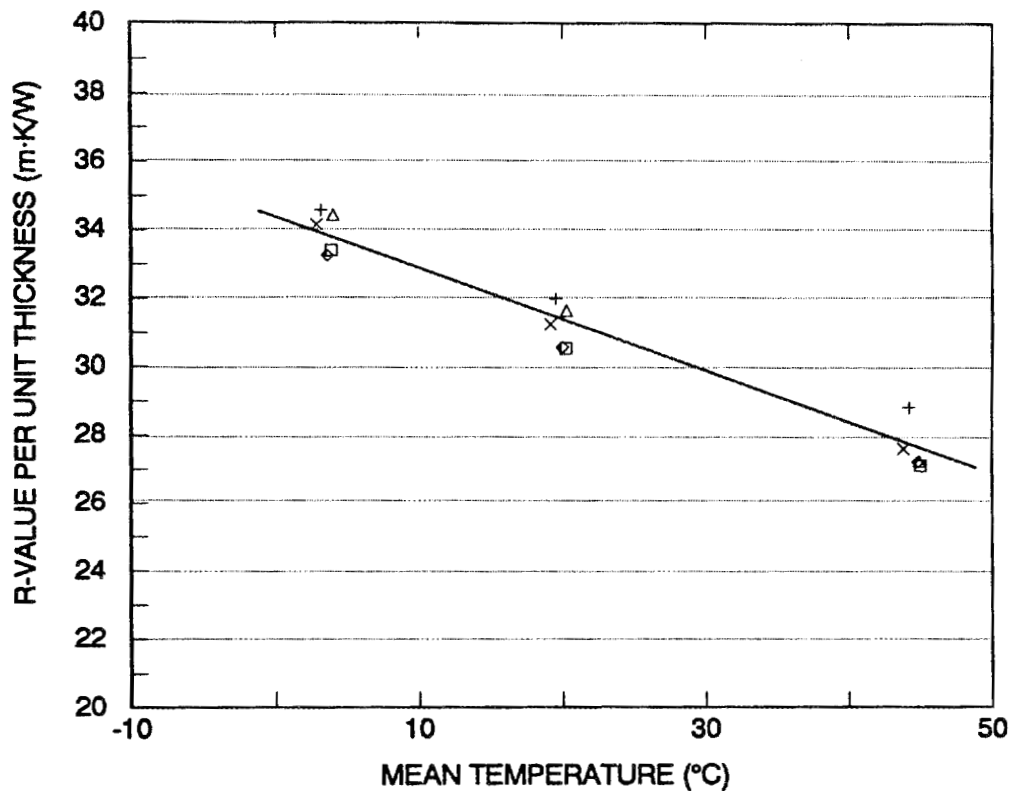
We performed calculations according to Eq. (1) for the total thickness of insulation in each section, and we plotted the R-values from these calculations per unit thickness versus the mean temperatures at which they were measured. Multiplying the R-values per meter thickness (in the SI units of  $\text{m}\cdot\text{K}/\text{W}$ ) by 0.144 converts them into R-values per inch [in the USCS units of  $\text{h}\cdot\text{ft}^2\cdot^\circ\text{F}/(\text{Btu}\cdot\text{in.})$ ]. Figures 4.1 and 4.2 show results for the fibrous-glass panels, and Fig. 4.3 depicts the R-values for the expanded polystyrene. Only results from the steady-state runs with upward thermal driving forces (runs 3, 4, and 5) are shown. The heat flux results from the first two runs, when the moisture was migrating downward out of the plywood, are not likely to characterize dry insulation in the cold-deck roofs.

The lines on Figs. 4.1 and 4.3 connect three data points for each panel and show the R-value per unit thickness for the insulation in each panel. The ORNL Metals and Ceramics (M&C) Division used specimens of the same insulation materials during the calibration of the heat flux transducers. From the calibration test it was possible to determine the overall thermal resistance of the insulation in which the transducers were calibrated. The symbols labeled M&C ORNL in Figs. 4.1 and 4.3 show these values, which agree with the data from the LSCS. Data from ASHRAE (1989) for the unit resistances of fibrous glass and expanded polystyrene lie several percent below and above the data in Figs. 4.1 and 4.3, respectively. We judged the actual materials used in the experiment to be different enough from the ASHRAE materials to cause these discrepancies.



- PANEL 1 - POLYETHYLENE (Water added later)
- + PANEL 2 - POLYETHYLENE WITH HOLES
- ◇ PANEL 3 - WATER-PERMEABLE VAPOR RETARDER
- △ PANEL 4 - NO VAPOR RETARDER
- × PANEL 5 - POLYETHYLENE (Dry throughout)
- ▼ M & C - ORNL

**Fig. 4.1. Steady-state, dry R-values for fibrous glass in the cold-deck panels, including control panel 5 (dry throughout test).**



- PANEL 1 - POLYETHYLENE (Water added later)
- + PANEL 2 - POLYETHYLENE WITH HOLES
- ◇ PANEL 3 - WATER-PERMEABLE VAPOR RETARDER
- △ PANEL 4 - NO VAPOR RETARDER
- × PANEL 5 - POLYETHYLENE (Dry throughout)

**Fig. 4.2. Repeated, steady-state, dry R-values for fibrous glass in the cold-deck panels with solid vapor retarders added to all panels.**

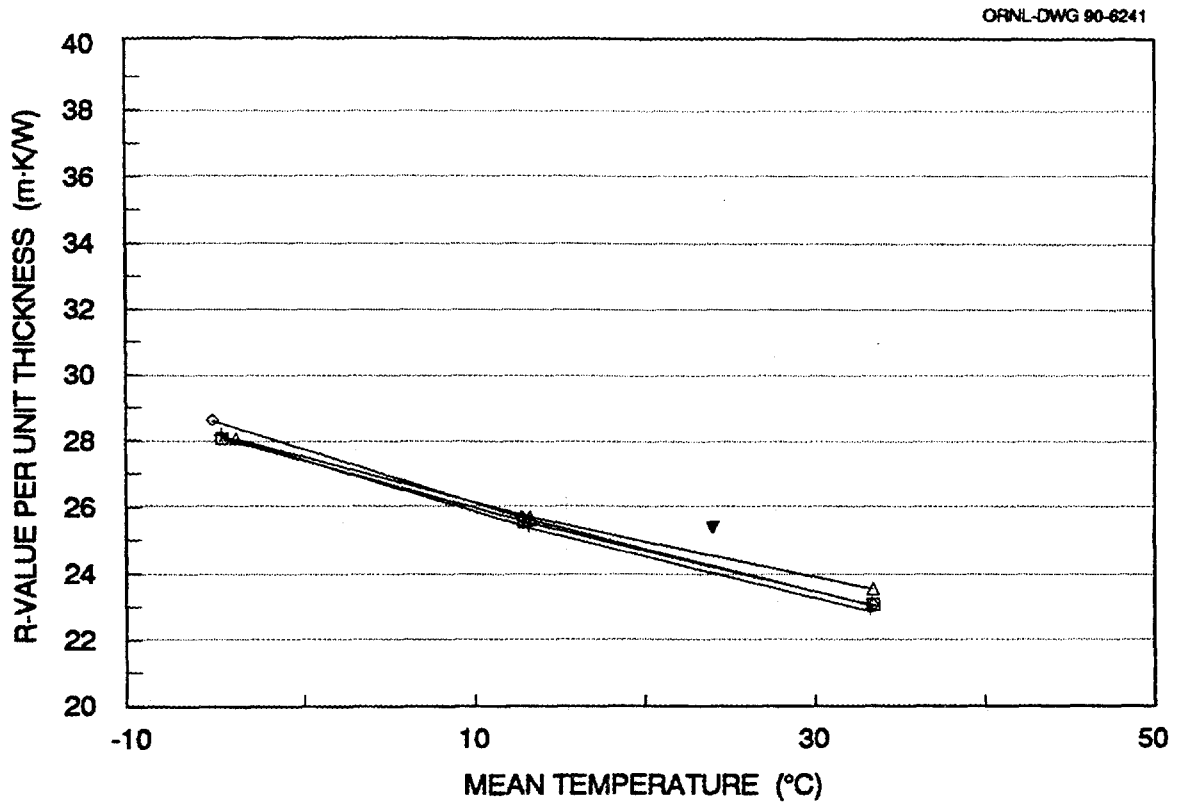


**Fig. 4.3. Steady-state, dry R-values for expanded polystyrene in the warm-deck panels.**

Figure 4.1 shows a value for panel 1 at a low temperature (run 3) that is below the envelope created by the other data on the figure, except for one value, which is high and came from panel 2 at mid-temperature (run 4). All the data for a high temperature (run 5) seem consistent. The likely cause of the two values outside of the envelope was occasional problems with data acquisition from the heat flux transducers in these early runs. These difficulties were solved before the dynamic runs and the repeated steady-state runs.

Figure 4.2 shows the results from runs repeating the conditions of runs 3, 4, and 5 after the whole experiment had been completed. Before obtaining these data, panels 1–4 were disassembled and solid sheets of polyethylene were inserted directly under the insulation and the bottom transducer to ensure that any moisture that could possibly be left at the bottom of these panels could not flow upward. Figure 4.2 exhibits consistency and little scatter about a common curve fit for the data from all five panels. The scatter about the best fit line is of the order of  $\pm 3\%$ , which is the reproducibility observed in duplicate calibrations of three of the ten heat flux transducers used in these panels. Three heat flux transducers had duplicate calibrations, because one transducer had been previously calibrated facing the same material (plywood or gypsum) as it did in this experiment. The procedure used by the ORNL M&C Division allows four transducers to be calibrated simultaneously and, therefore, ten transducers requires three runs. We performed two additional duplicate calibrations to check our reproducibility.

Figure 4.3 compares the measured results for the temperature variation of the thermal resistance of the expanded polystyrene used in the test, and shows that the measurements from all four panels agree with each other. The apparent R-value obtained during the heat flux transducer calibration lies about the same distance above the LSCS data for expanded polystyrene as is did for fibrous glass in Fig. 4.1.

In order to perform simulations with MATCH, thermal conductivities of the materials were needed. Table 4.1 lists thermal conductivities as a function of temperature, which we produced for the insulation in each panel by regression analysis of the data in Figs. 4.1, 4.2, and 4.3. To convert thermal conductivities in units of  $W/(m\cdot K)$  to units of

Btu·in/(h·ft<sup>2</sup>·°F), divide by 0.144. If the low value at low temperature for panel 1 in Fig. 4.1 is neglected, panel 1 has  $k_1 = 0.0271 + 2.7 \cdot 10^{-4} \cdot T$ , where  $k$  and  $T$  have the units of W/(m·K) and (°C), respectively. The temperature variation of apparent thermal conductivity for panel 1 then seems too steep. If the high value at mid-temperature for panel 2 in Fig. 4.1 is neglected, then panel 2 has  $k_2 = 0.0288 + 1.5 \cdot 10^{-4} \cdot T$ , where  $k$  and  $T$  have the units of W/(m·K) and (°C), respectively. The apparent thermal conductivity of panel 2 is not affected significantly. For all practical purposes, all the fibrous-glass curve fits are the same, as are all the expanded polystyrene curve fits. But, for consistency, the results from Figs. 4.1 and 4.3 for individual panels are used later in MATCH.

Table 4.1. Apparent thermal conductivities of the insulation in each panel

Fibrous glass	
Panel 1 (with polyethylene)	$k_1 [W/(m \cdot K)] = 0.0307 + 1.7 \cdot 10^{-4} \cdot T (^{\circ}C)$
Panel 2 (with polyethylene with holes)	$k_2 = 0.0281 + 1.5 \cdot 10^{-4} \cdot T$
Panel 3 (with water-permeable vapor retarder)	$k_3 = 0.0289 + 1.8 \cdot 10^{-4} \cdot T$
Panel 4 (without vapor retarder)	$k_4 = 0.0285 + 1.7 \cdot 10^{-4} \cdot T$
Panel 5 (dry control with polyethylene)	$k_5 = 0.0285 + 2.0 \cdot 10^{-4} \cdot T$
All cold-deck panels (repeat runs)	$k_{FG} = 0.0290 + 1.6 \cdot 10^{-4} \cdot T$
Expanded polystyrene	
Panel 6 (with polyethylene)	$k_6 = 0.0366 + 2.0 \cdot 10^{-4} \cdot T$
Panel 7 (with polyethylene with holes)	$k_7 = 0.0365 + 2.2 \cdot 10^{-4} \cdot T$
Panel 8 (with water-permeable vapor retarder)	$k_8 = 0.0361 + 2.2 \cdot 10^{-4} \cdot T$
Panel 9 (without vapor retarder)	$k_9 = 0.0364 + 1.8 \cdot 10^{-4} \cdot T$

We determined the apparent thermal conductivity of the aerated concrete used in the warm-deck panels from the measurements as well. Because the concrete was cast in-situ, its actual thickness varied from panel to panel. Using an average value for the thickness in all four panels, the average thermal conductivity in runs 3, 4, and 5 was 0.092 W/(m·K). We measured the temperature differences across the concrete directly, and the value of heat flux was taken from the response of the transducer in the middle of the impermeable expanded polystyrene. In steady-state without local latent effects of moisture, heat flux was uniform throughout a test section.

## 4.2 HEAT FLUXES DURING ROOM-DRY, DYNAMIC RUNS

We varied the temperatures in the upper climate chamber in diurnal cycles in run 6 before the addition of water to eight of the roof panels. The purpose was to observe the heat fluxes at the top and bottom of the fibrous-glass insulation and in the middle of the expanded polystyrene and compare the results with those obtained for identical boundary conditions after the addition of water.

Section 4.1 mentioned that it seemed that hygroscopic moisture moved in the cold-deck panels and affected their heat flux transducers in runs 1 and 2 with downward thermal driving forces. Runs 3, 4, and 5 with upward thermal driving forces did not show similar effects. In this section, the heat fluxes measured in run 6, with diurnal temperature variations causing both downward and upward thermal driving forces, will be shown and discussed to provide additional evidence for the observations in runs 1 through 5. The sign convention is that positive heat fluxes indicate upward heat flow; that is, heat lost from the building through the roof. Dividing heat fluxes in  $\text{W/m}^2$  by 3.15 yields values in  $\text{Btu}/(\text{h}\cdot\text{ft}^2)$ . Upward thermal driving forces cause upward heat fluxes, but if distance increases in the upward direction, upward heat fluxes are caused by negative temperature gradients.

Figure 4.4 shows the temperatures measured directly under the membrane and on the underside of the gypsum board in panel 5, the control panel of the permeable cold-deck type. These data are typical of the imposed temperatures for all the cold-deck panels. The shape of the temperature curve for the roof surface is not perfectly sinusoidal; it has a large peak in the daytime, while the temperature varies little in the nighttime. This mirrors actual diurnal roof surface temperature variations observed in summer.

Figure 4.5 shows the measured heat fluxes at the top of the five panels with fibrous-glass insulation and a hygroscopic plywood deck. The difference between the bottom and the top temperatures in Fig. 4.4 is also plotted in Fig. 4.5. We calculated the difference as bottom minus top in order to have the same sign as the heat fluxes. All the transducers

were between the insulation and the blotting paper or plywood. The heat fluxes are practically identical to one another, but their shape is slightly distorted relative to that of the temperature difference. The nighttime (upward) heat flux already reaches its maximum value before the half-day marks (which correspond roughly to midnight of a daily cycle), while the temperatures peak well after these marks. The heat fluxes remain at a plateau for most of the night. The temperature differences fall sharply after reaching their maximum values. Note that the peak heat fluxes here at the top are approximately  $-5.5 \text{ W/m}^2$  for day and  $2.5 \text{ W/m}^2$  for night. If moisture causes slight effects, they are the same for each panel.

Figure 4.6 shows the measured heat fluxes at the bottom of the panels with fibrous-glass insulation. The transducers were on top of the vapor retarder when one was present, except in panel 1 where there was a layer of blotting paper between the transducer and the polyethylene sheet. The curves from panels 1 and 4 are well behaved. Their shape follows that of the imposed temperatures, which are again shown as in Fig. 4.5. The peak heat fluxes were approximately  $-4.2 \text{ W/m}^2$  for day and  $2.0 \text{ W/m}^2$  for night, slightly less than the peak values measured at the top. This would be expected, because the temperature variations were imposed at the top.

However, the heat fluxes at the bottom of the other three panels, depicted in Fig. 4.6, are not so well behaved. Their return to positive values was more rapid at the end of the daytime hours than for panels 1 and 4. The nighttime heat fluxes peaked at about  $2.0 \text{ W/m}^2$ , as in panels 1 and 4, but deviated from a smooth curve. At the beginning of daytime, the slope of the downward heat flux was steeper than the slope in panels 1 and 4. The daytime heat flux peaks were approximately  $-6 \text{ W/m}^2$ , compared to  $-5.5 \text{ W/m}^2$  at the top. It is significant that the magnitude of these peak values was larger than it was for the transducers at the top despite the temperature variations being imposed at the top.

The heat flux transducer data from the bottom of panels 1 and 5 differ from each other, as Fig. 4.6 exhibits. All the cold-deck panels had heat flux transducers in depressions routed out of the top and bottom of the fibrous-glass insulation. Although both panel 1 and panel 5 had a solid polyethylene vapor retarder, there was a significant

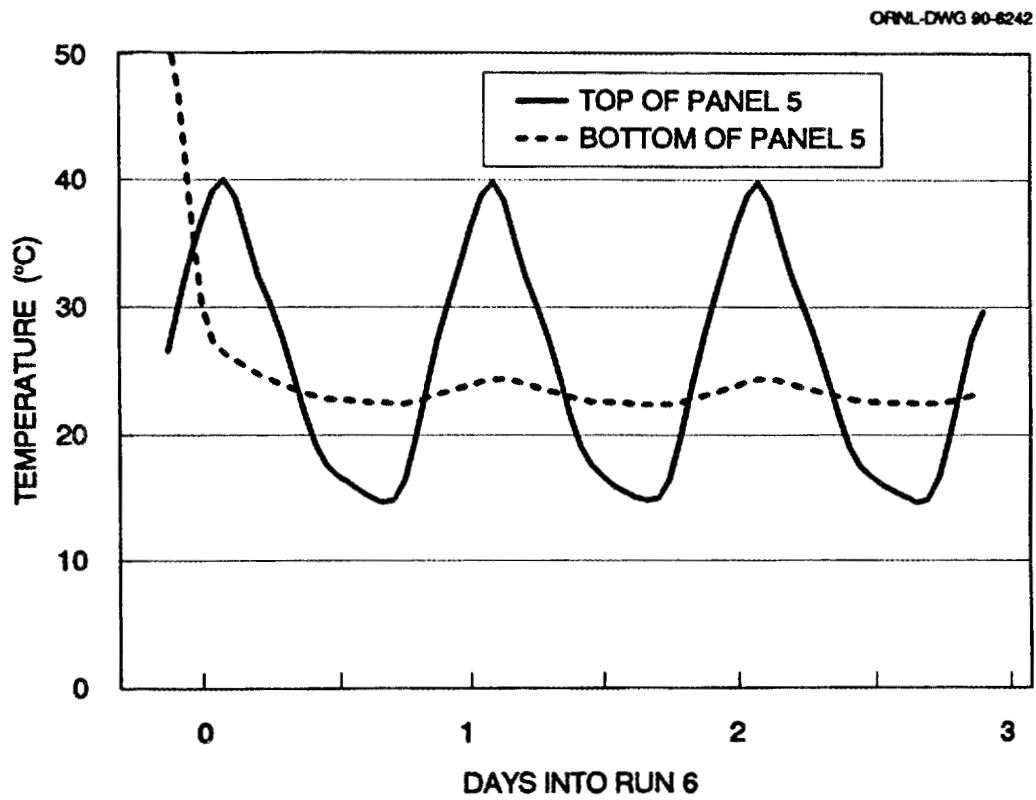


**Fig. 4.4. Temperatures at the top and bottom of the fibrous glass in panel 5 during dry, dynamic run 6.**

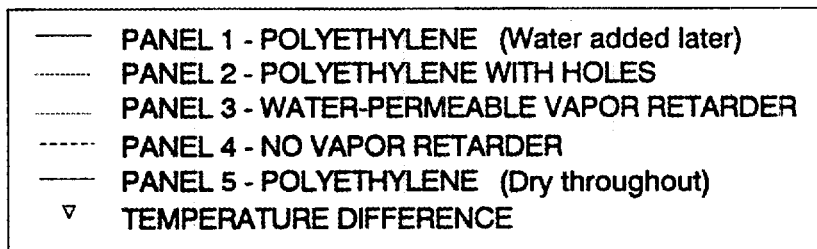
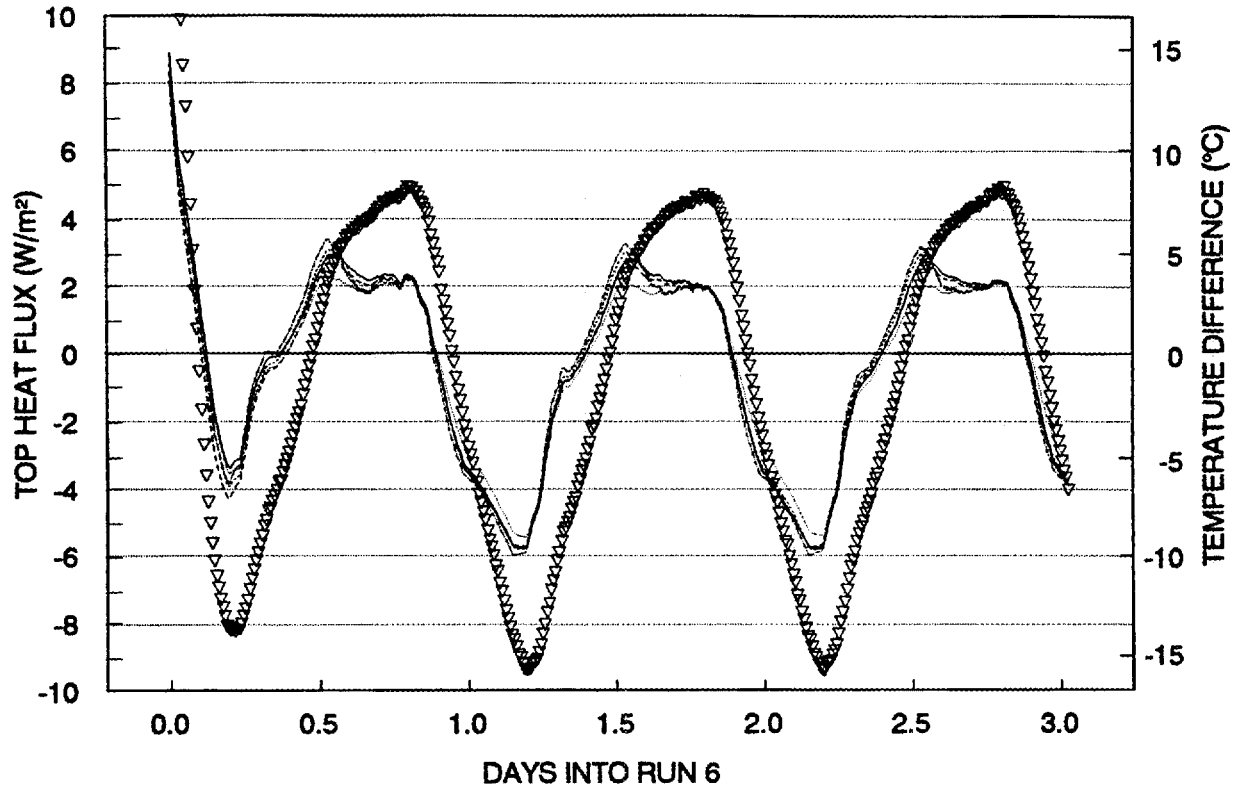


**Fig. 4.5. Measured heat fluxes at the top of the fibrous glass with driving temperature difference in panels 1-5 during dry, dynamic run 6.**

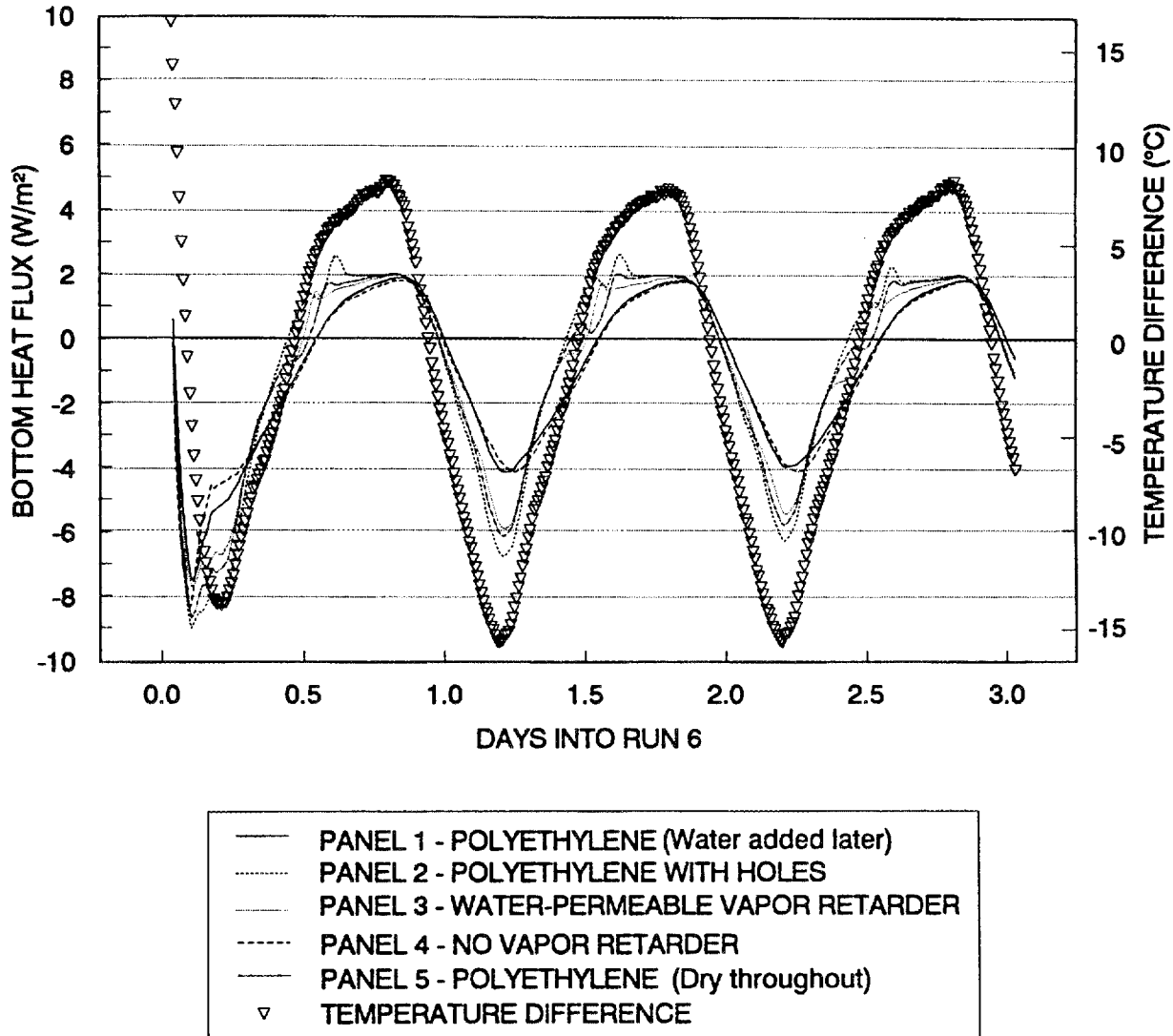


**Fig. 4.6. Measured heat fluxes at the bottom of the fibrous glass with driving temperature difference in panels 1-5 during dry, dynamic run 6.**

difference between them even before water was added to panel 1 — the sheet of blotting paper between the insulation and the polyethylene in panel 1. The blotting paper was not present in panel 5. On the other hand, the bottom heat flux readings were the same for panels 1 and 4. Panel 4 had neither a vapor retarder nor blotting paper; the bottom heat flux transducer faced gypsum board. See Fig. 2.3 to recall details of the constructions.

To emphasize the difference between the top and bottom heat fluxes in each panel, Fig. 4.7 focuses on the panel with the largest daytime heat fluxes, panel 2, which has a polyethylene vapor retarder with holes. As expected, the time lag between top and bottom heat fluxes appears. However, the negative heat flux values have a larger peak at the bottom than at the top, although the difference becomes smaller as the run progresses. Taking this observation as the first evidence, we hypothesize that moisture migrating in the panels can condense on or evaporate from the heat flux transducers when there is no hygroscopic material next to the transducer. If the transducer is located directly on top of a vapor retarder, moisture flowing down during the daytime will condense on the vapor retarder as well as on the transducer. At night this moisture will evaporate from the top of the transducer, affecting it until evaporation is complete. Because the impermeable transducer has a relatively high thermal conductivity, it takes only a small temperature difference across its surfaces to cause large apparent heat fluxes. If phenomena such as condensation and evaporation change the temperature of one surface a small amount relative to the value for sensible heat flow only, significant changes and irregularities in apparent heat flux can also occur.

On the other hand, if the transducer is in contact with a hygroscopic material, the moisture can evaporate from the transducer as fast as it condenses or, effectively bypass the transducer and be absorbed in the hygroscopic layer. For instance, in panel 1, despite the presence of a vapor retarder, the blotting paper was able to absorb some moisture at hygroscopic vapor pressures (less than saturation). This effect should become less pronounced after the addition of water. The blotting paper is then wetter and the vapor pressure near it comes closer to saturation. In panel 4 without a vapor retarder,

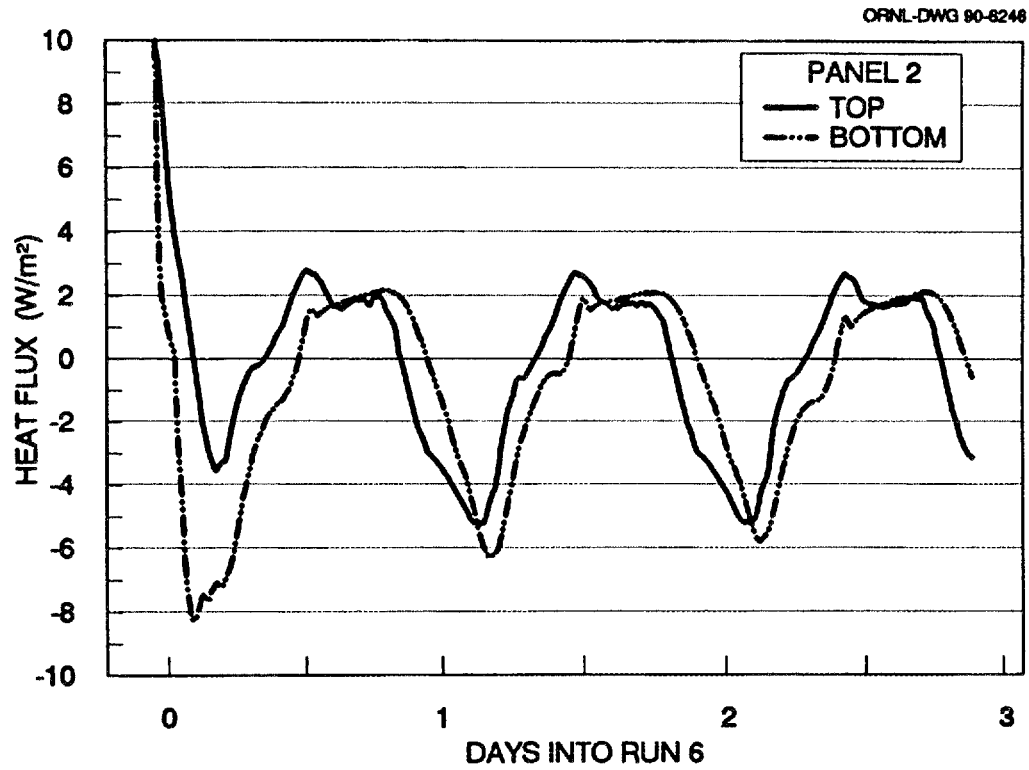


**Fig. 4.7. Measured heat fluxes at the top and bottom of panel 2 during dry, dynamic run 6.**

hygroscopic moisture could also bypass the transducer by entering the underlying gypsum. Gypsum will rapidly transport moisture through to the guard chamber, because gypsum is a highly permeable material.

Figure 4.8 shows the heat fluxes measured in the middle of panels 6–9 with expanded polystyrene insulation and warm, lightweight concrete decks. The heat fluxes have a shape that corresponds to that of the imposed temperature difference across the panels. The temperature difference is about the same as it is in Figs. 4.5 and 4.6 for the cold-deck panels, but the total R-value of the warm-deck panels is significantly less than that of the cold-deck panels, so more heat flows. There is almost perfect agreement among the four heat flux curves; apparently there were no moisture effects to cause any significant differences. There was no wood used to construct these panels, which means no large source of hygroscopic moisture. Expanded polystyrene is far less permeable to vapor diffusion than fibrous glass. Therefore, the amounts of moisture that could potentially move in diurnal cycles are much smaller.

#### **4.3 HEAT FLUXES AFTER WATER ADDITION DURING LOW AMPLITUDE TEMPERATURE CYCLES**

After we added water amounting to  $1 \text{ kg/m}^2$  of panel cross sectional area (0.87% of the fibrous glass volume; 1.7% of the expanded polystyrene volume) to the top of all panels except panel 5, the temperature cycles imposed in run 6 were repeated. This run, designated run 7, lasted for seven days. Heat flux results shown in this section compare directly to those in Figs. 4.5–4.8. We changed the scale of the ordinate in the graphs to accommodate the larger negative heat flux values that were obtained after water was added. Figs. 4.5–4.8 show heat fluxes for panel 5, although we added no water to this panel. Panel 5 heat flows help determine if problems with control of conditions or data acquisition masqueraded as moisture effects.

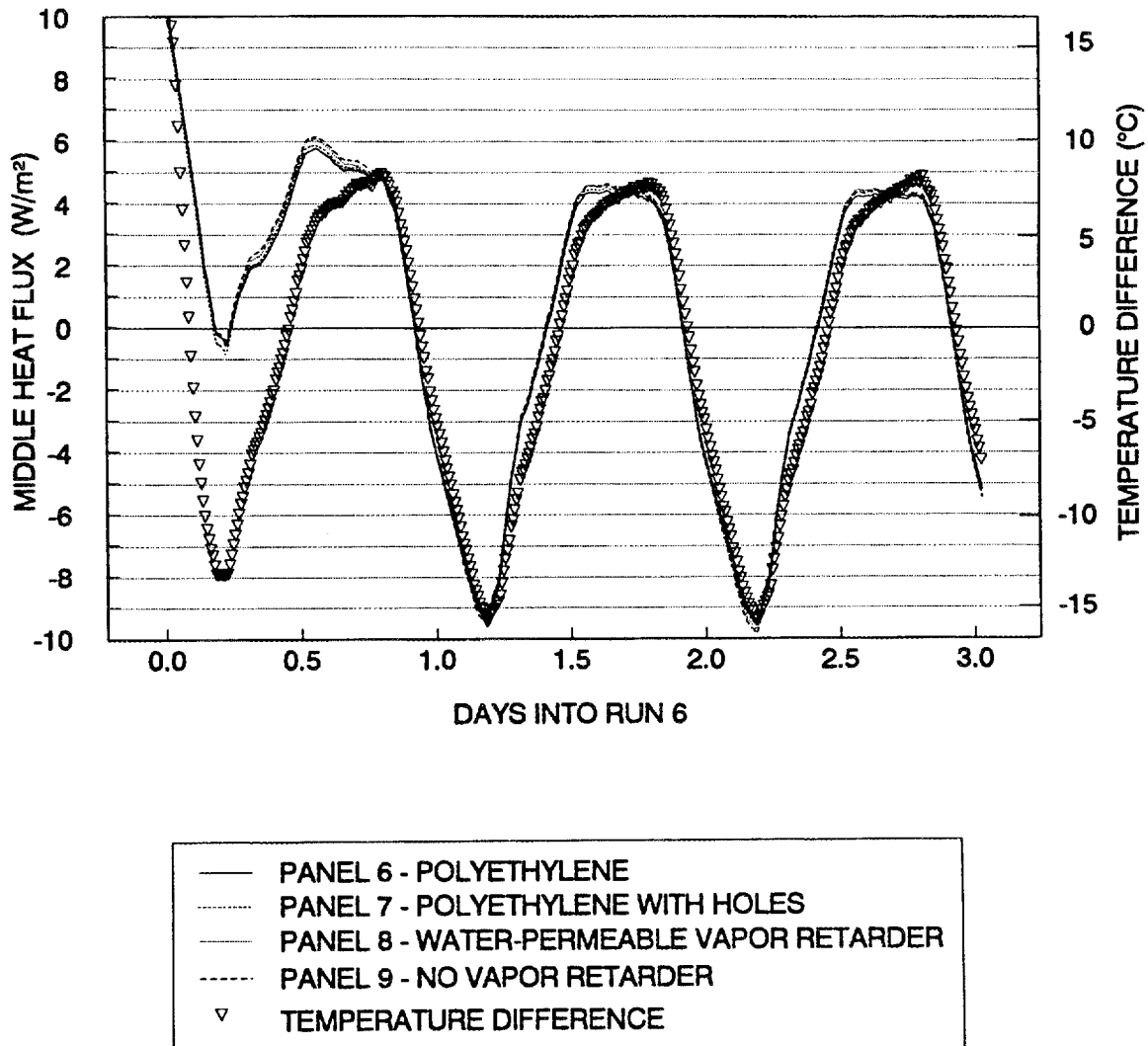


**Fig. 4.8. Measured heat fluxes in the middle of the expanded polystyrene with driving temperature difference in panels 6,7, 8, and 9 during dry, dynamic run 6.**

To put into perspective the amount of water added to all panels except panel 5, recall Table 2.1, which shows that plywood has a hygroscopic water content between 11.5 and 14% of dry weight. The plywood in panels 1-5 weighed about  $6 \text{ kg/m}^2$  of panel area. The hygroscopic moisture in the plywood at the start of the experiment was, therefore, about  $0.69\text{--}0.84 \text{ kg/m}^2$ . Plywood seldom dries to below 6% hygroscopic water by weight ( $0.36 \text{ kg/m}^2$  for this experiment). The  $0.4 \text{ kg/m}^2$  or so of hygroscopic moisture able to dry out of the plywood is a significant fraction of the water added, and its effects are likely to be seen, along with the effects from the water added deliberately.

However, the water added is significantly more than the hygroscopic moisture, especially if some hygroscopic moisture escaped during the dry runs. The dominant transport mechanism and resulting location of the moisture should be the following: all the water was added to the blotting paper under the membrane. During diurnal cycles some of it will be driven down through the insulation in the daytime, and, in a relatively closed system, up again at night. The potential for downward transport should be larger than it is for upward transport, because saturation vapor pressures increase rapidly with increasing temperature, and the imposed daytime temperature differences are greater than the nighttime values. If the permeability of the insulation permits it, the moisture should collect predominantly at the bottom of the roof panels within a few days. In the cold-deck panels, the moisture still present at the top will soak into the plywood. Moisture content in the blotting paper at the top will decrease to hygroscopic levels. In the cold-deck panel without a vapor retarder at the bottom, the moisture that moves down in the day will migrate into the guard chamber. There is little potential for upward moisture flow in the night because of the small temperature differences.

Figure 4.9 corresponds to Fig. 4.5, showing the measured heat fluxes at the top of the fibrous glass in the cold-deck panels, although Fig. 4.9 shows only the first five days of this run. Heat fluxes for the last two days of the run were practically identical to those on the last day shown in the graph. We will present the heat fluxes for the last two days of the run for panel 2 later to emphasize the difference between results in this run and run 6.

Positive and negative heat fluxes increased during the first two or three days after water was added to panels 1, 2, and 3 with some sort of vapor retarder. After a few days the heat fluxes in panels 1, 2, and 3 settled to approximately the same values that they showed when they were dry. Panel 4 without a vapor retarder had the same heat flux readings as in the preceding dry run, and panel 5 behaved as it did in run 6.

Fig. 4.10 shows the bottom heat fluxes in panels 1-5 for comparison to Fig. 4.6. When wet, panels 1, 2, and 3 with vapor retarders have considerably larger peaks of apparent heat fluxes in both directions than does panel 4 without a vapor retarder. These peaks are also more than twice what they were when the same panels were room-dry, as panel 5 still is. Note that the heat flux in panel 1 with a solid polyethylene vapor retarder and blotting paper was around 20% less than in panels 2 and 3, which used no blotting paper but employed vapor retarders that allowed water to escape. The blotting paper in panel 1 was under the transducer between the insulation and the vapor retarder. Heat flux in panel 4 without a vapor retarder appeared to be unaffected by the moisture after the first day. It then had the lowest heat flux peaks of all the panels, including panel 5 which had hygroscopic levels of moisture trapped in it.

Figures 4.9 and 4.10 provide more convincing evidence for the hypothesis we introduced in Sect. 4.2 to explain the results of run 6. We theorize that when the transducer contacts a hygroscopic material or has a path with low vapor resistance to the air in the guard chamber below the test sections, the moisture can bypass the transducer. This will happen as long as the moisture content in the material beyond the transducer does not exceed hygroscopic levels. Otherwise, the moisture will condense in and on the material as well as on the transducer. In the case of moisture bypass, the transducer indicates only conducted heat. When moisture condenses, both conducted and latent heat are indicated.

We believe that condensation takes place on the transducers at the top of the fibrous glass during the first few nights when the moisture comes from below and the blotting paper is still wet. There is no potential for driving the moisture around the transducers; the blotting paper is already saturated. This condensed moisture evaporates the next day.

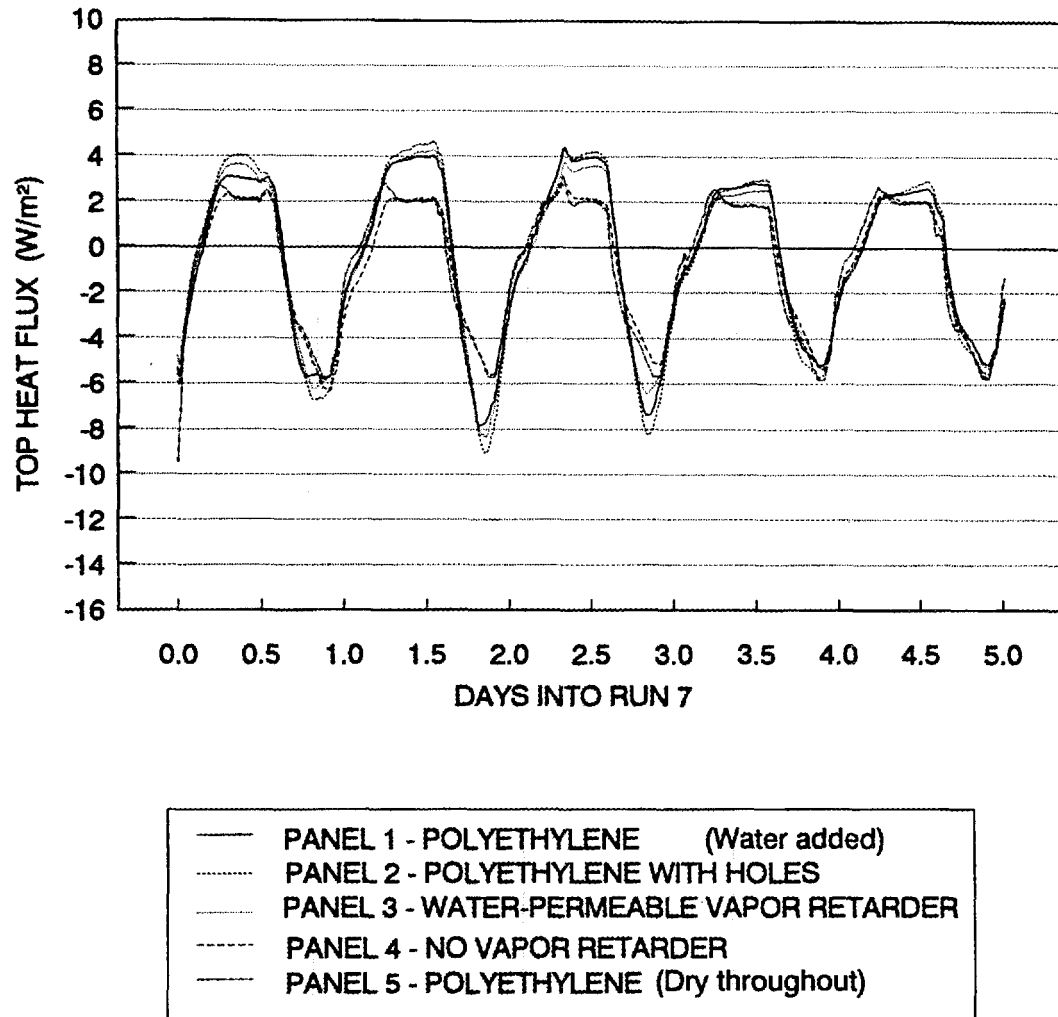


**Fig. 4.9. Measured heat fluxes at the top of the fibrous glass in panels 1-5 during wet, dynamic run 7.**

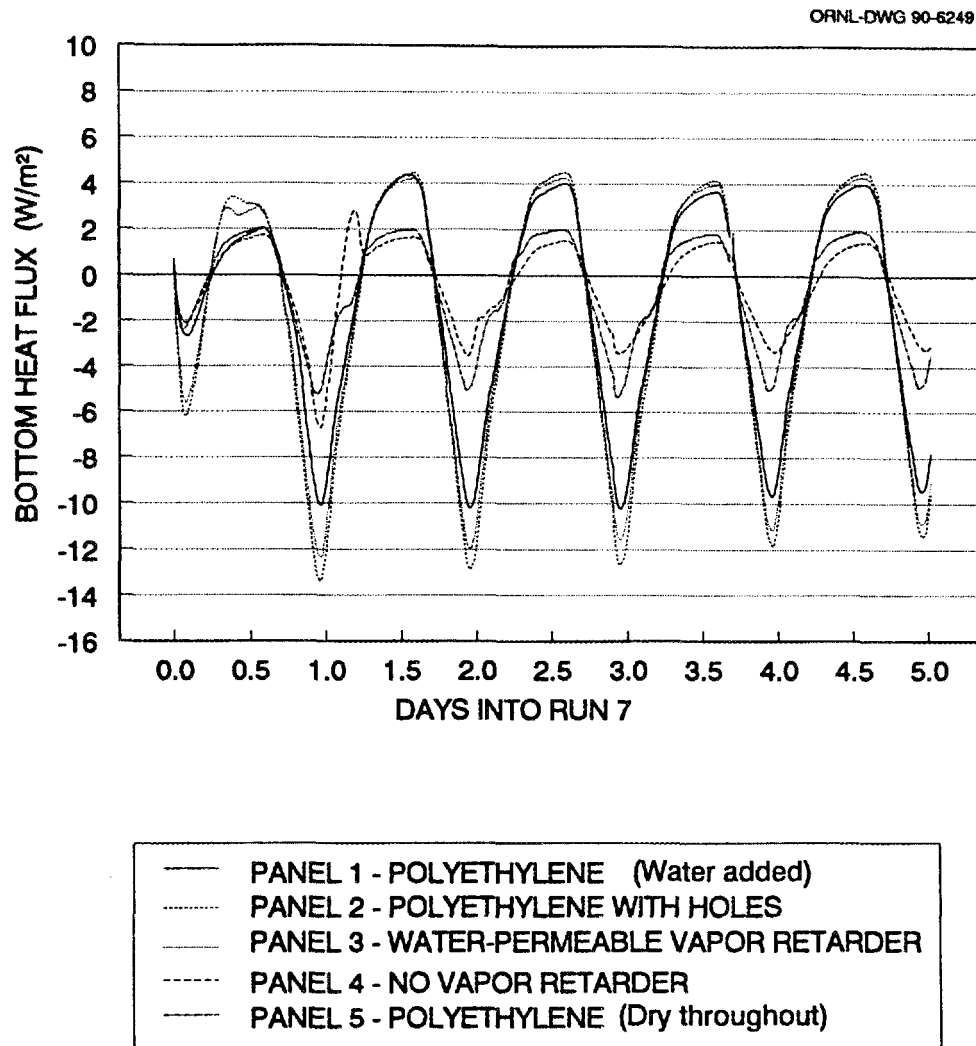


**Fig. 4.10. Measured heat fluxes at the bottom of the fibrous glass in panels 1-5 during wet, dynamic run 7.**

The blotting paper becomes dry after a few days; bypassing may take place, and measured heat fluxes become smaller. In panel 4 without a vapor retarder, there is no condensation at night on the top transducer because there is practically no upward moisture transport, whereas the top of panel 5 has relatively dry, hygroscopic plywood.

We theorize that condensation also takes place on the transducers at the bottom of the panels with vapor retarders, even panel 5, which contained only hygroscopic moisture. The exception is panel 1 with a solid vapor retarder, because it had blotting paper on top of the vapor retarder. This paper was dry the first day. However, on the following days, even when the blotting paper had more than hygroscopic moisture content, readings of the heat flux transducer were slightly smaller than what corresponds to full condensation. The small moisture effects seen at first at the bottom of panel 4 without a vapor retarder may be caused by condensation of moisture in the interface between the gypsum and the insulation. Such condensation may take place in the first days of the run when the intensity of the moisture flux from the top is highest and the gypsum cannot pass it all through to the chamber below.

Figure 4.11 shows the heat fluxes at the top and bottom of panel 2, which uses polyethylene with holes as its vapor retarder. The dry results are from Fig. 4.7 for run 6. The curves have been shifted so peaks coincide. Data from the last three days of run 7 when the situation was steady periodic comprise the wet results. The added moisture had no apparent effect on the top transducer in the last days of run 7. Its response was the same as it was in the last two days of the dry run 6. The bottom transducer, however, gave readings at the end of run 7 that were repeatedly more than 80% larger during the day and 125% larger during the night than in run 6 when it was affected by hygroscopic moisture alone.

Figure 4.12 shows the results after water was added to the warm-deck panels with expanded polystyrene insulation. The curves are practically identical to those in Fig. 4.8, obtained before the addition of water. The only difference is that the daytime amplitude slowly increased. This could indicate that the expanded polystyrene continued to absorb a little moisture, increasing its apparent thermal conductivity and causing increased

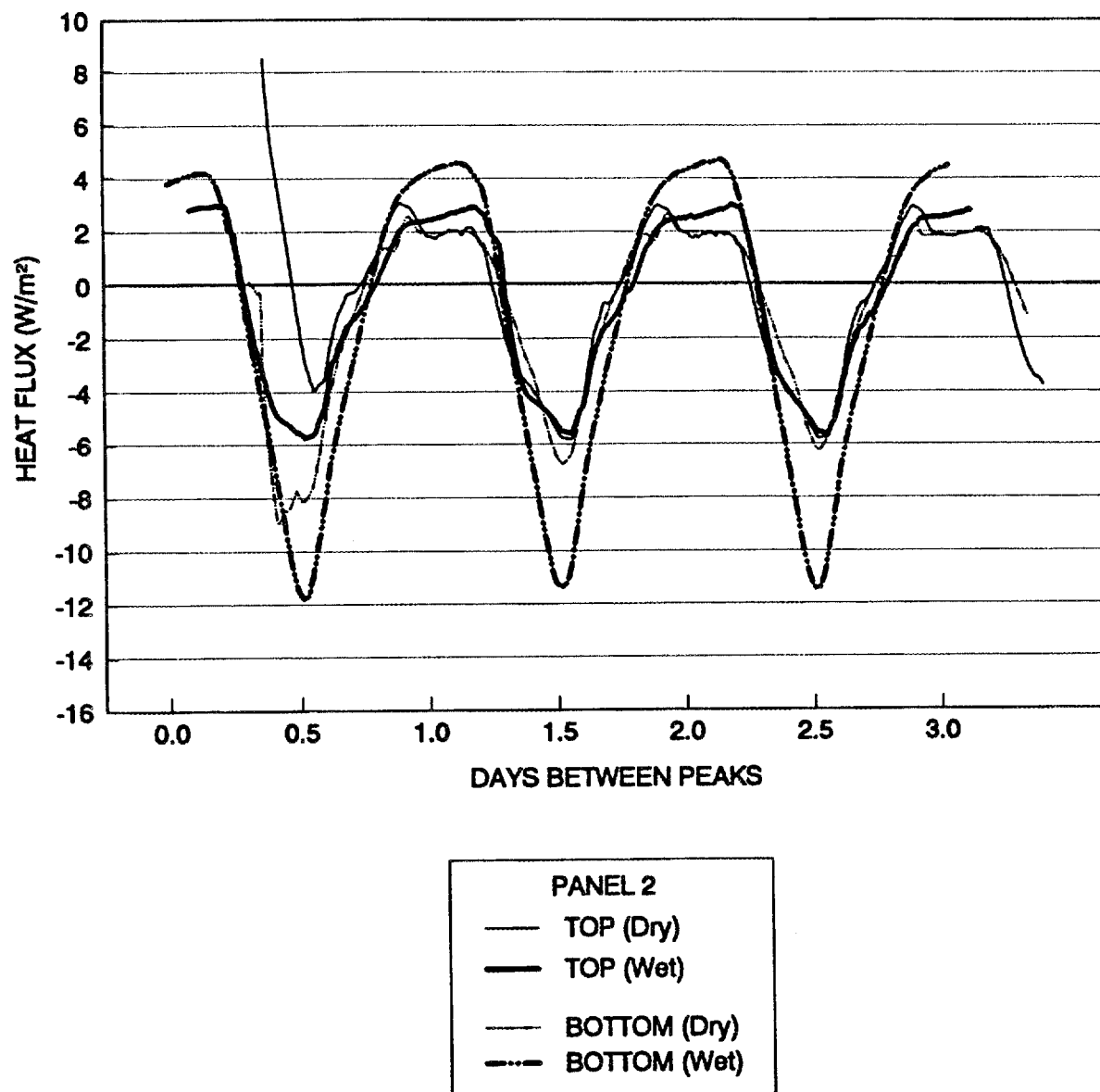


**Fig. 4.11.** Measured heat fluxes at the top and bottom of panel 2 during dry, dynamic run 6 and wet, dynamic run 7.

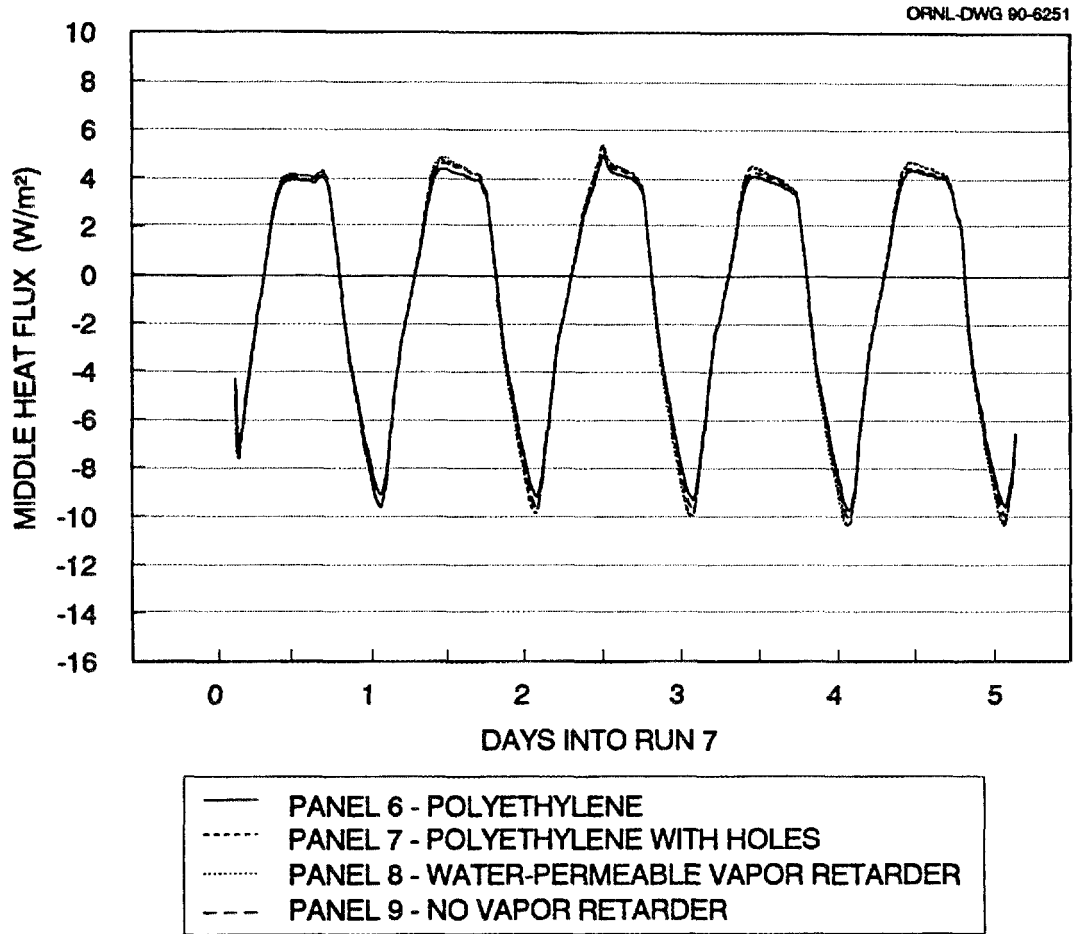
conduction heat flows. Figure 4.12 shows no pronounced deviations from smooth curves. Such deviations would have been expected if there were latent heat effects on the transducers embedded in the middle of the insulation, as we noted for transducers in the middle of fibrous-glass insulation in a preliminary experiment prior to this series of tests. The major lesson learned from the preliminary experiment was that the response of heat flux transducers embedded in fibrous glass was too complicated to interpret. Hence, we selected locations at the top and bottom of the fibrous glass for panels 1-5. Figure 4.12 shows that single transducers embedded in the middle of the insulation are adequate for monitoring heat fluxes in the impermeable polystyrene.

#### **4.4 HEAT FLUXES AFTER WATER ADDITION DURING INCREASED AMPLITUDE TEMPERATURE CYCLES**

In run 8, we increased the amplitude of the temperature cycles in the climate chamber. The new maximum and minimum temperatures were 66°C (150°F) and 10°C (50°F), respectively. Thus, the temperature difference imposed from the top of the roof system was doubled. These temperatures are comparable to those encountered on a dark roof membrane on sunny summer days. Run 8 lasted for approximately nine days.

Section 5 provides details about the amount and movement of the moisture during this and the previous run. The main trend we noticed in run 8 was that the materials at the top of the test panels dried out during the first days of the run. The moisture could escape readily from the panels without a vapor retarder, and in the panels with the solid polyethylene vapor retarder, the water gathered on the polyethylene. In the panels having polyethylene with holes or with a water-permeable vapor retarder, some water gathered on the vapor retarder, but some also migrated through it, leaving these roof panels drier than the panel with solid polyethylene. The amount of moisture that took part in the diurnal cycles in this run was governed by the forces that drove it up in the night.

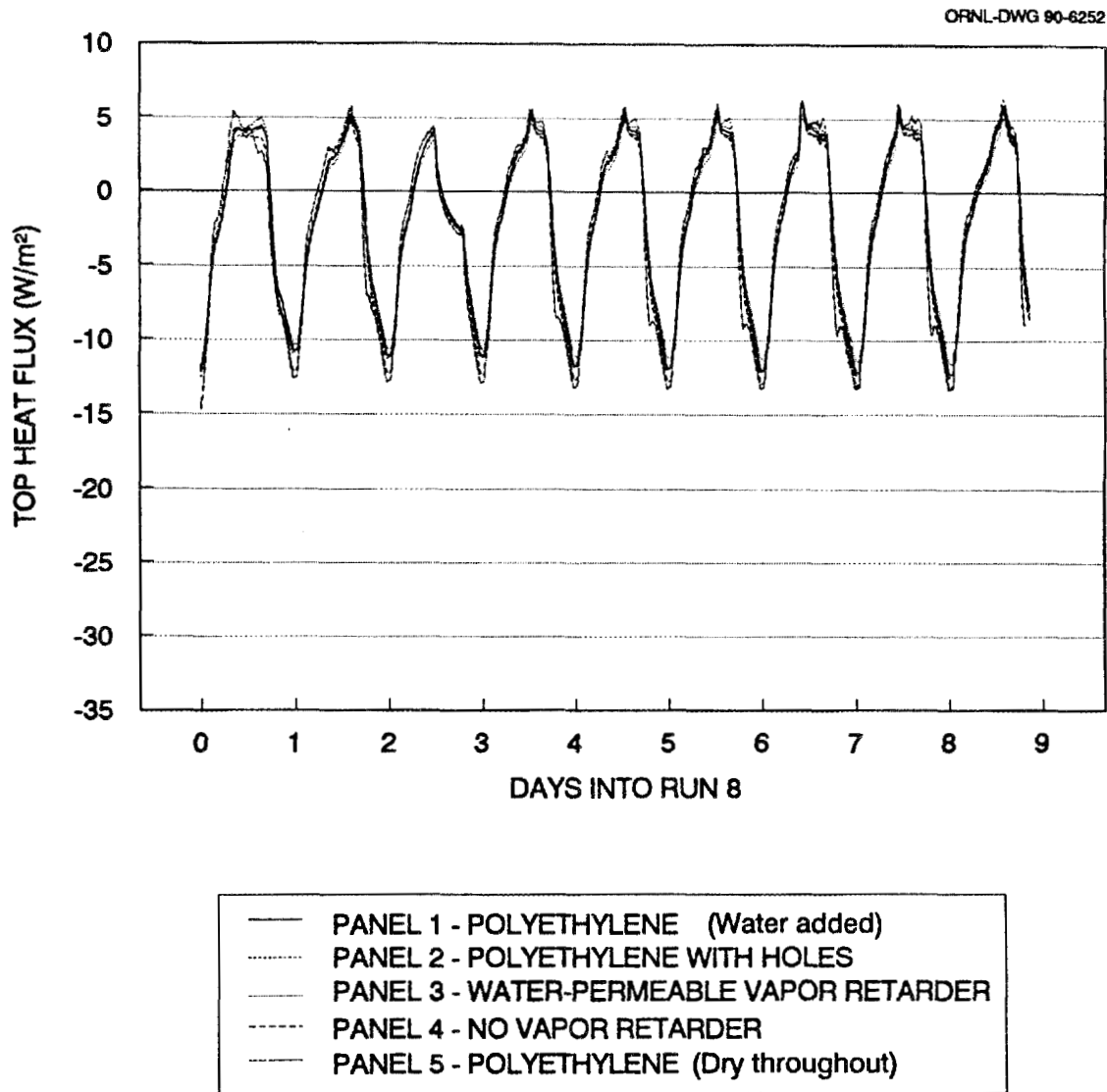
Figure 4.13 shows heat fluxes measured throughout this run at the top of the wet panels 1-4 with fibrous-glass insulation, and presents the results for panel 5 with only trapped hygroscopic moisture for comparison. The data from panel to panel are quite



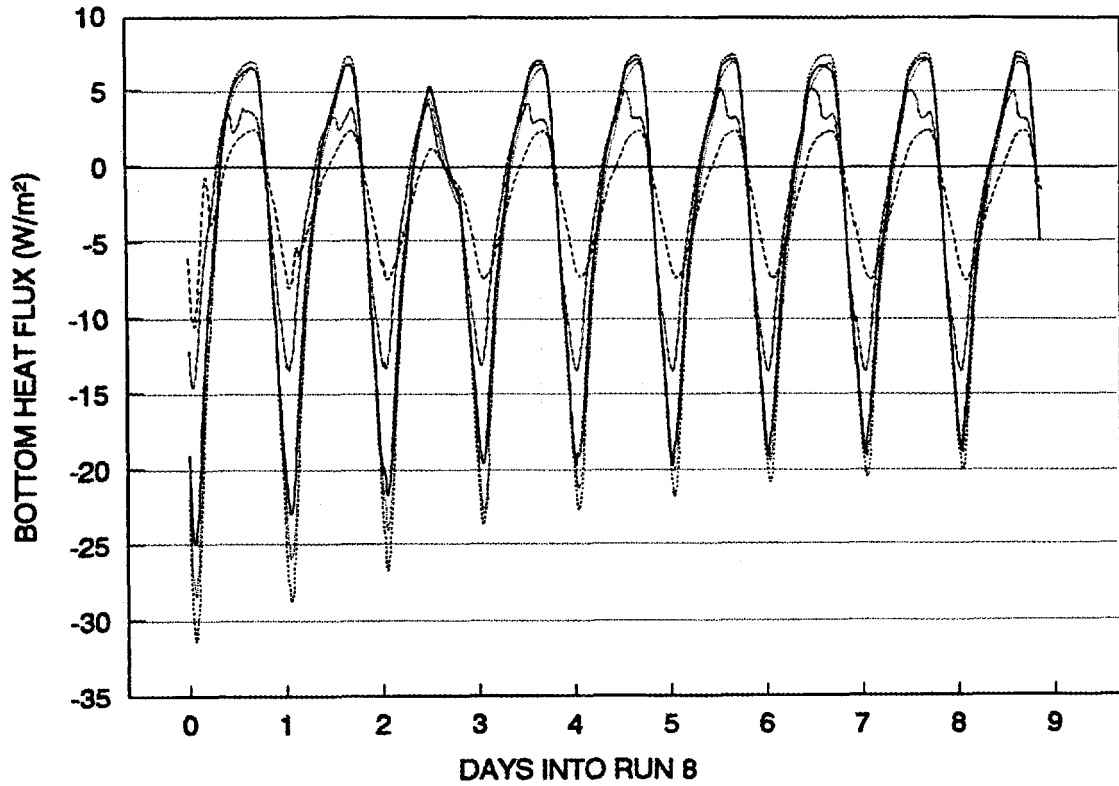
**Fig. 4.12. Measured heat fluxes in the middle of the expanded polystyrene in panels 6, 7, 8, and 9 during wet, dynamic run 7.**

similar. From day 2 to day 3, a problem with control of the imposed temperatures caused a slight deviation from the regular pattern and a small change in the response of all transducers. Note that this figure shows results for a panel that remained wet throughout the whole run (panel 1), panels that dried out slightly (panels 2 and 3), and a panel with significant drying (panel 4). The similarity of these data implies that there were essentially no latent heat effects on the readings from this transducer between plywood and fibrous glass during run 8. The most irregular behavior was for panel 5 with trapped hygroscopic moisture and no blotting paper at the bottom to absorb it.

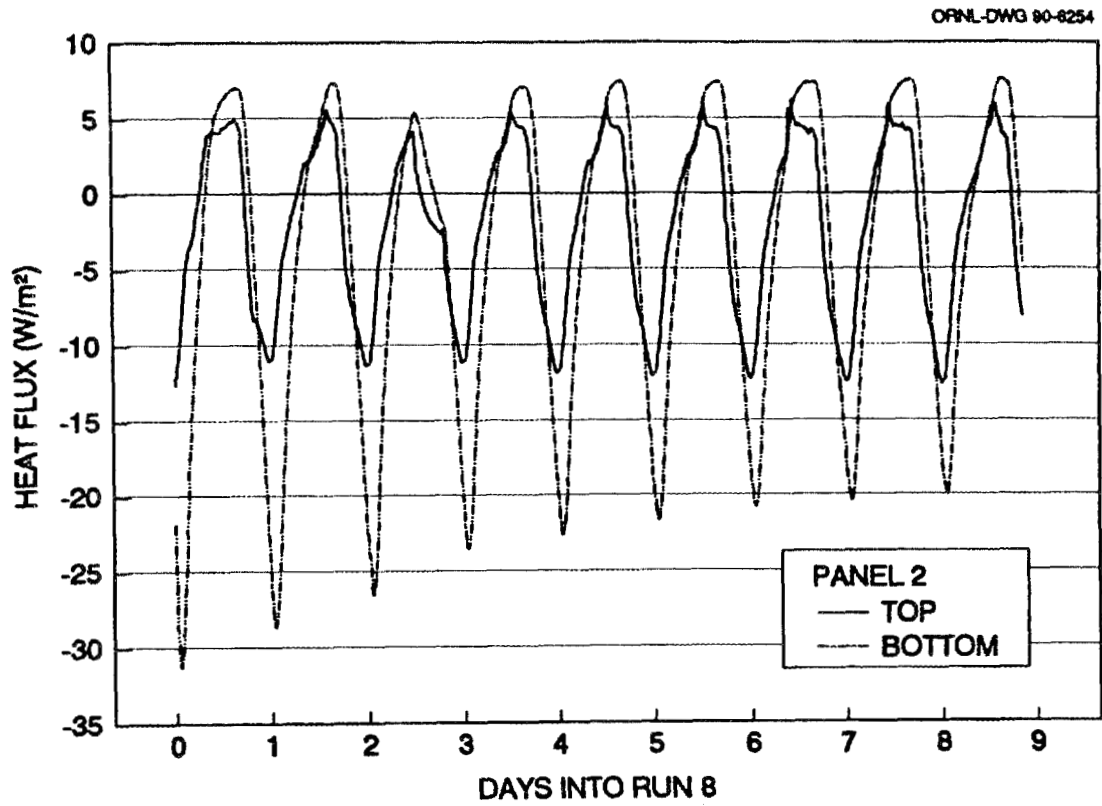
Figure 4.14 shows the measured heat fluxes at the bottom of the same panels. The peak values shown here are considerably larger in all the panels that had vapor retarders than in those measured at the top. The control problem mentioned above caused the drop off in the nighttime peak between days 2 and 3. Downward (negative) heat flows were especially large the first three days when excessive moisture from the top still migrated down in the daytime. Later, the latent heat effects were limited by the amount of moisture that migrated up in the night. Therefore, the downward moisture flow became less during the day. According to Fig. 4.14, the downward peak of heat flux from panel 1 with a solid sheet of polyethylene stabilized by the fourth day. In the other two panels with vapor retarders, the peak value became slightly less from day to day throughout the whole period. These results were consistent with these two panels continuing to dry out and, therefore, having less moisture to take part in the cycles. Again, it should be noted that the heat flux measurements in the panels with vapor retarders were more than twice those in the panel without the vapor retarder. We attribute this mainly to the fact that the latent component of the heat flux across this plane was detected only in the presence of the vapor retarder. The heat fluxes in the control panel 5 with trapped hygroscopic moisture were steady periodic throughout this run and the peaks were between those for panel 4 which dried out, and panels 1-3, which retained some of the added water. This behavior was identical to that observed in Fig. 4.10 for run 7.



**Fig. 4.13. Measured heat fluxes at the top of the fibrous glass in panels 1-5 during wet, dynamic run 8 with increased temperatures.**



**Fig. 4.14. Measured heat fluxes at the bottom of the fibrous glass in panels 1-5 during wet, dynamic run 8 with increased temperatures.**



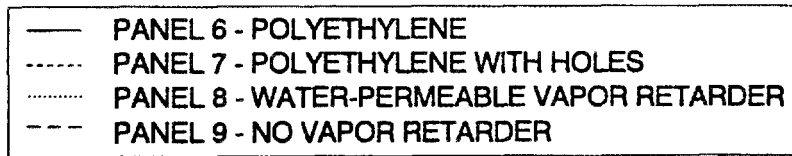
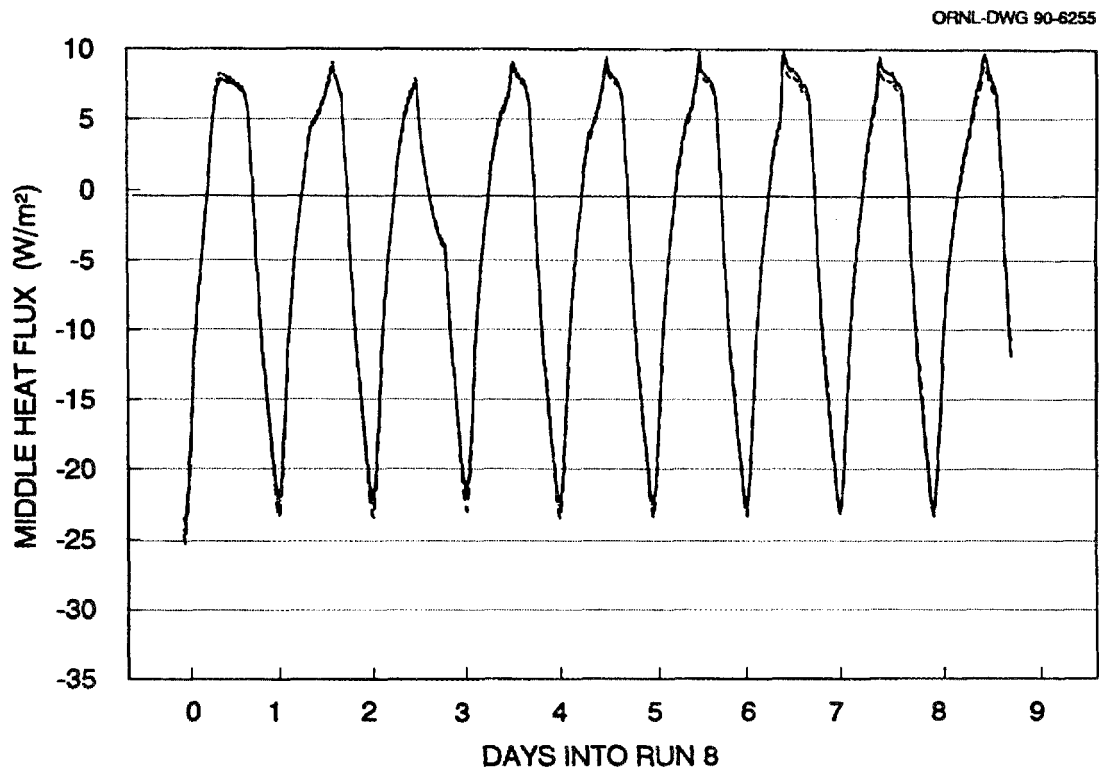
**Fig. 4.15. Measured heat fluxes at the top and bottom of panel 2 during wet, dynamic run 8 with increased temperatures.**

Figure 4.15 shows a direct comparison of results for run 8 at the top and bottom of the fibrous glass, which had polyethylene with holes as the vapor retarder. Despite the temperature variations imposed from the top, the bottom heat flux transducer clearly gave considerably larger readings. The relatively few holes in the polyethylene were not sufficient to prevent condensation on and around the heat flux transducer at the bottom of this panel.

Figure 4.16 shows the measured heat fluxes in the middle of the expanded polystyrene in the four warm-deck panels. Once again, there was no indication of latent heat effects on the readings from these transducers. Data for the panels agree, despite the fact that some panels should have dried out more than others during the course of this run.

To support the hypothesis that the top heat flux transducers indicated only the conducted heat while the bottom ones indicated the total of conduction and latent heat flow, we performed a calculation with MATCH to predict the heat fluxes for panel 2, and the results are in Fig. 4.17. The initial moisture conditions for the calculation were the hygroscopic moisture content plus the amount of water added to the blotting paper at the beginning of run 7. Boundary conditions were the measured temperatures at the upper and lower surface of the panel and the moisture concentrations in the chambers, indicated by measured dew point temperatures. We assumed the top membrane to be vapor tight, while we deduced the effective vapor resistance of the polyethylene with holes from the moisture measurements presented in Sect. 5.

Figure 4.17 shows that the calculated heat fluxes for conduction only agree with results in Fig. 4.15 measured from the top transducer. We also performed a calculation for the total heat flow, conduction plus latent, and those results are also plotted in Fig. 4.17. The results of this calculation agreed fairly well with the apparent heat flux measured by the bottom transducer (Fig. 4.15). There was a slight discrepancy between the negative peaks of the measured and calculated heat fluxes the first few days of the period shown.



**Fig. 4.16. Measured heat fluxes in the middle of the expanded polystyrene in panels 6, 7, 8, and 9 during wet, dynamic run 8 with increased temperatures.**

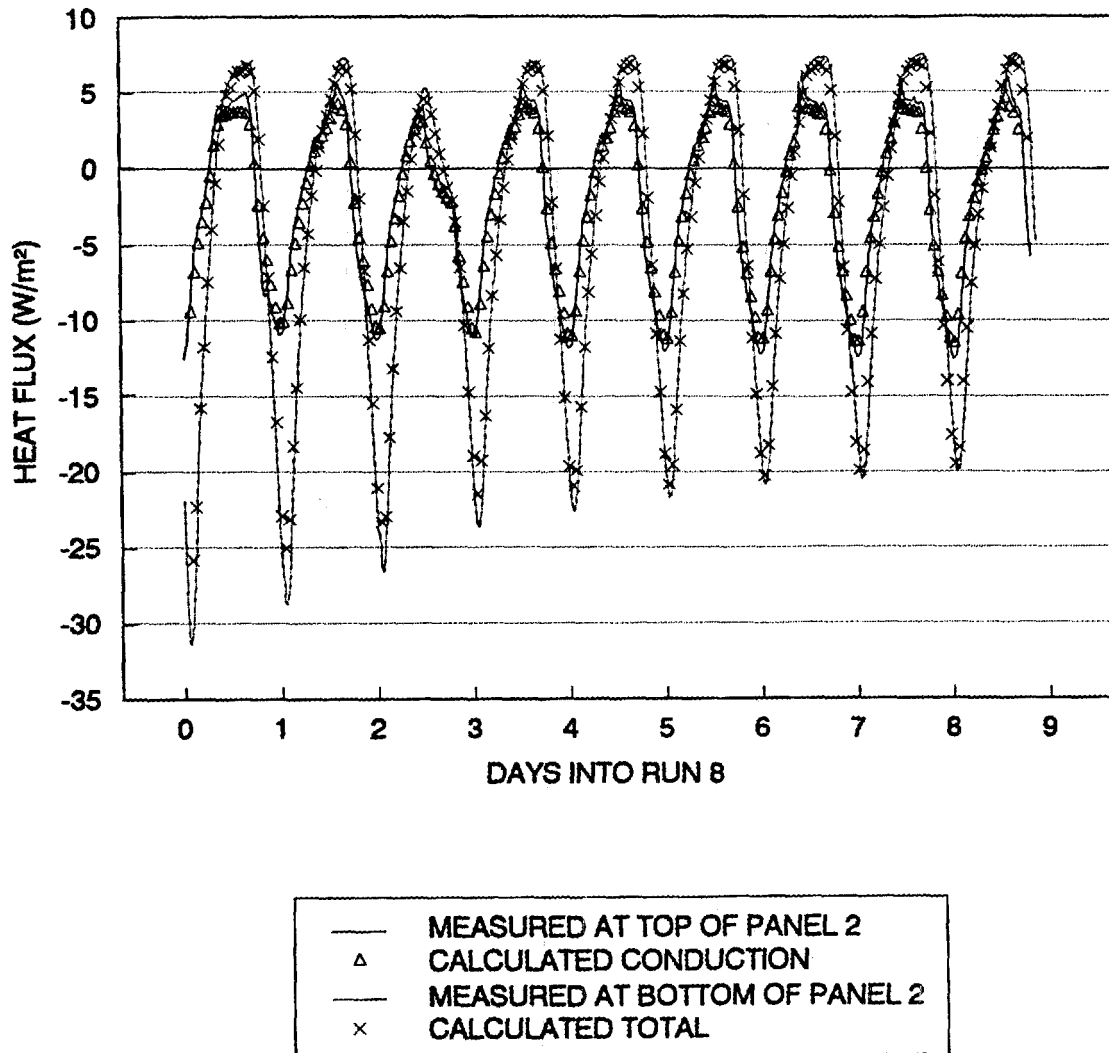


**Fig. 4.17. Results from MATCH compared to the measured heat fluxes at the top and bottom of the fibrous glass in panel 2 during wet, dynamic run 8 with increased temperatures.**

To perform these calculations, thermal as well as hygric transport and retention properties must be known for the materials in the assembly. Table 4.1 lists the thermal conductivities of the insulation. We estimated the other parameters, selecting material properties from the literature for similar materials and adjusting the properties within their uncertainties for best agreement. Because the latent heat transfer is at least half of the total heat flow, it is as important to know, for instance, the vapor permeability as it is to know the thermal conductivity. In light of the uncertainty in the vapor permeability data, the results from MATCH were remarkably close to the measurements, indicating that we made very good estimates of properties, especially for the fibrous glass.

The success of MATCH, as Fig. 4.17 indicates, encourages the effort to develop understanding of the conditions under which condensation affects heat flux readings. It appears that MATCH is capable of describing the most important physical phenomena involved in the overall transfer of heat in moist, permeable materials. The inclusion of the latent heat in calculations and measurements of heat transfer in moist materials may change the heat flux pattern very significantly in insulation materials that are highly permeable to vapor transfer. Recall, for example, the results in Fig. 4.11 at the bottom of panel 2. The amount of water added in these experiments corresponded to 0.87% by volume of the fibrous-glass insulation. This was not very much moisture and did not alter the physical appearance of the roof test sections relative to their dry condition. This amount of water could easily be present in many existing roofs.

#### **4.5 SUMMARY OF EFFECTS OF CONDENSATION AND EVAPORATION ON HEAT FLUX TRANSDUCERS**

Results shown in Figs. 4.5–4.17 indicate that the local moisture-flow pattern around the heat flux transducers installed in this experiment affected their readings when highly permeable insulation was used. We have utilized the consequences of the effects to explain the results in these figures. This section summarizes the possible effects and offers schematics of the mechanisms involved. The goal is to understand the mechanisms for latent heat effects on the transducers and to make it possible to account for the effects of condensation and evaporation in the design of experiments with moist, permeable

materials. Then, for example, certain heat flux transducers could be located to register only the conducted heat, while others would measure the total heat flow.

We used typical heat flux transducers, in the shape of small plates or discs and made of an impermeable material. They generate an electrical output due to the temperature difference across a thermopile embedded in them. They were located between or next to materials that may be permeable to the flow of vapor. Thus, the moisture flow around the transducer was inherently of a multidimensional nature. Consider Fig. 4.18, a general schematic where a transducer is in the way of moisture flow. The concentration of moisture—and therefore the vapor pressure—will increase on the upstream side (the lower surface in Fig. 4.18). The moisture may even condense on the transducer surface if the vapor pressure increases to the saturation point. If the vapor pressure is less at the same vertical position to the side of the transducer, there is potential for lateral moisture migration around it. Thus, the moisture may not condense at all, or if there is water that condensed on the upstream side from earlier conditions, it may evaporate.

In the usual case when moisture and heat flows have the same direction, condensation on the upstream side of the transducer will heat up this surface and cause an increased temperature difference across the transducer itself, which in turn is seen as an increased transducer output. If evaporation takes place from the upstream side, it will decrease the transducer reading because it cools this side. Evaporation from the downstream side (the upper surface in Fig. 4.18) may also occur if moisture condensed earlier on this side when flows were reversed. This would cool the downstream side of the transducer and the measured heat flux would increase. Combined action of effects on both sides of the transducer could lead to complicated behavior, despite smooth temperature variations in the insulation near the transducer.

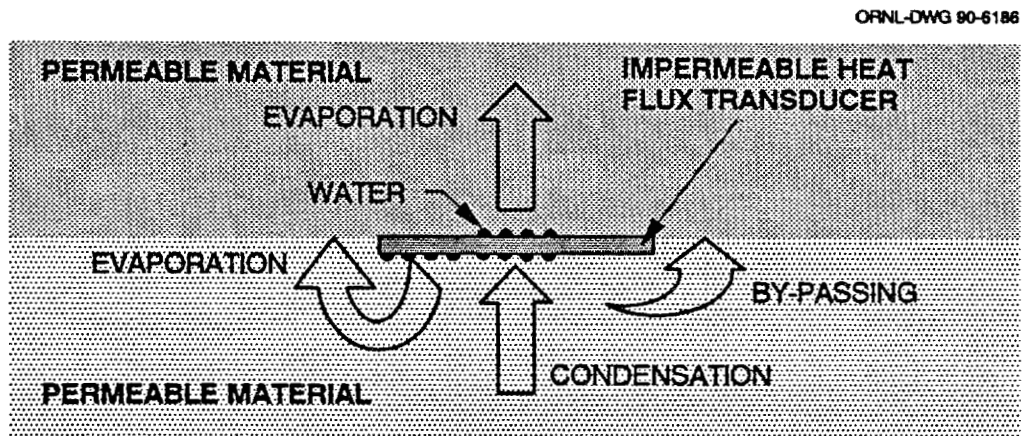


**Fig. 4.18. Local effect of condensation and evaporation of moisture on heat flux transducers in permeable materials such as fibrous glass.**

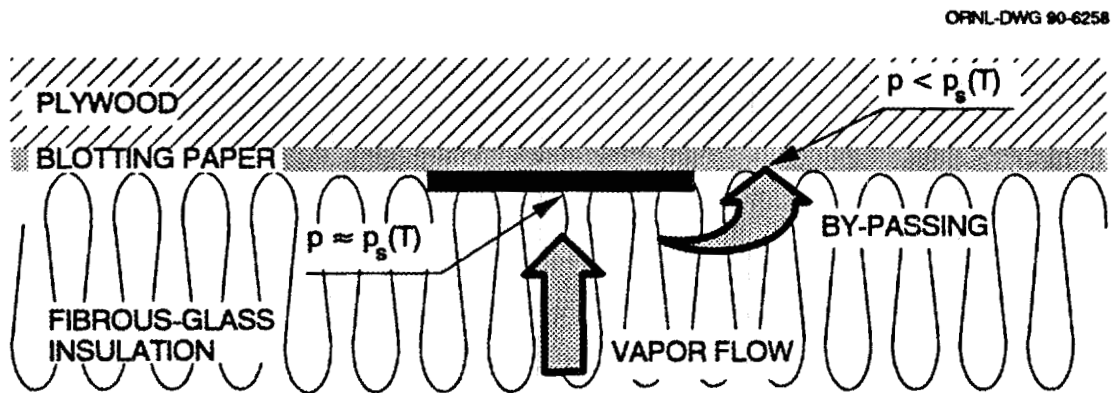


**Fig. 4.19. Local effect of a non-saturated hygroscopic material on the flow of moisture near heat flux transducers at the top of fibrous glass.**

Specific schematics can be made for the situations that we think occur around the transducers at the top and bottom of the fibrous glass in this experiment. As an approximation, we assume the temperatures are the same at all points in a horizontal plane; that is, the thermal problem is perfectly one-dimensional. Further, we assume the transducer has negligible thickness and high thermal conductivity, so that even a small temperature difference may correspond to a large heat flux.

Figure 4.19 shows the situation at the top transducer when it was located directly below the blotting paper and plywood. We assume that the blotting paper and plywood hold only hygroscopic moisture; they are not saturated with moisture. The vapor pressure at the surface of these materials will, therefore, be less than the saturation vapor pressure corresponding to the temperature of the interface between the blotting paper and the insulation.

At night, when the vapor comes from the bottom of the roof panel, vapor concentration and vapor pressure will increase below the transducer—perhaps to the condensation point. If this happens, there will be a lateral gradient of vapor pressures. Thus, some or all of the vapor coming from below the transducer will be directed sideways and become absorbed in the blotting paper and in the plywood. This may diminish or eliminate condensation on the transducer.

If the potential for sideways transport is strong enough it will result in a heat flux reading without latent heat effects. Apparently, this situation governed the top transducer throughout most of the transient runs—before and after the water addition (as Figs. 4.5, 4.9, and 4.13 indicate). Even after water is added, when heat and moisture flow reverse the next day, there will be no moisture to evaporate from the bottom of the transducer. The latent heat effect will not show up then, either. The bottom heat flux transducer when there was no vapor retarder corresponded to this situation as well.

In the first few days of run 7, just after the water was added, the blotting paper was soaking wet, as Fig. 4.20 depicts. The vapor pressure at the surface of the transducer must have been close to saturation, different from the situation in Fig. 4.19. We theorize that vapor that approaches the top heat flux transducer from below condenses on its lower surface. The vapor pressure will be equal to the saturation value at the bottom surface of the transducer and the blotting paper, so there can be no lateral migration of vapor. This moisture evaporates the following day when the gradients are reversed. In this situation, the top transducer indicates the total of conducted and latent heat both day and night.

Figure 4.21 shows the situation at the bottom heat flux transducer when it was located on top of a relatively impermeable vapor retarder or saturated blotting paper. The mechanism for the response of the heat flux transducer is the same as it is in Fig. 4.20. In the daytime, vapor comes from the top. When it reaches the vapor retarder or the heat flux transducer, its concentration rapidly increases to the saturation point, because it cannot travel any further. Condensation takes place throughout the plane of the transducer and, again, there is no potential for vapor to bypass the transducer. Some of the moisture will evaporate from the surface of the transducer at night. Thus, the bottom heat flux transducers indicate the total heat transfer both day and night when they are located on top of vapor retarders or wet blotting paper.

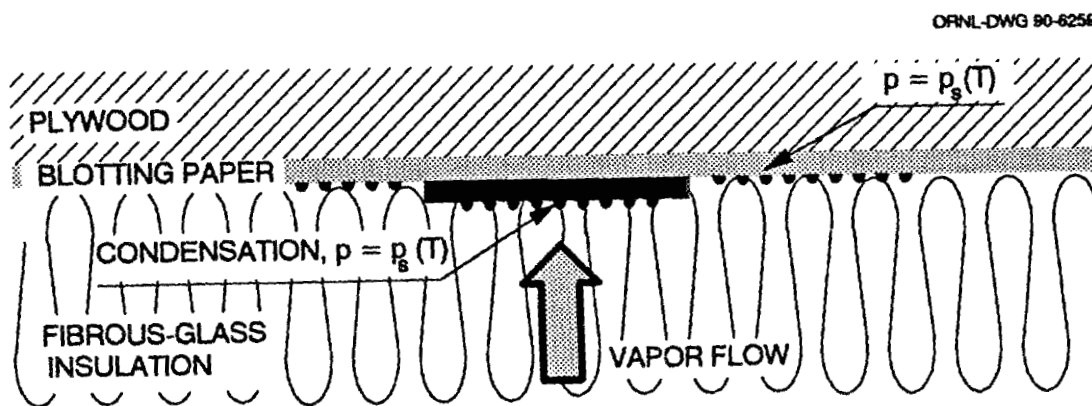


**Fig. 4.20. Local effect of over-hygroscopic moisture content on the flow of moisture near heat flux transducers at the top of fibrous glass.**

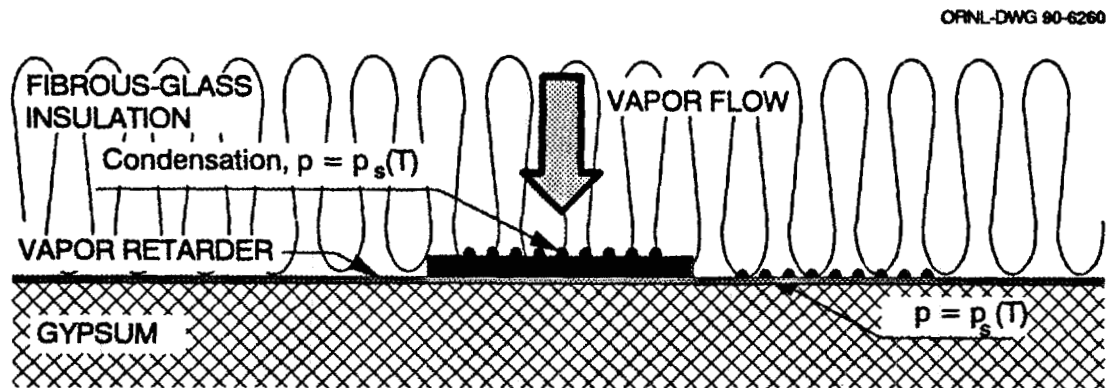


**Fig. 4.21. Local effect of a vapor retarder on the flow of moisture near heat flux transducers at the bottom of fibrous glass.**



## 5. MOISTURE MEASUREMENTS

Section 5 discusses the location and amount of moisture in the roof test panels before, and especially after, the addition of 1 kg/m<sup>2</sup> of water to eight of the nine panels. Moisture distribution was measured qualitatively by electronic probes, while the amount was quantified by weighing as much of the materials in each section as possible after each run. The results from these two kinds of measurements are discussed in Sects. 5.1 and 5.2, respectively. Section 5.3 uses the weighing results as inputs to MATCH to show predicted drying rates with the various vapor retarder systems used in the panels.

### 5.1 READINGS FROM MOISTURE PROBES

We installed moisture probes based on the electrical resistance of plywood at the top and bottom of the insulation in all panels to which water was added, and positioned pin probes based on the electrical capacitance of the material between the pins in the top and bottom of the fibrous glass in the cold-deck roof panels. The probes themselves have non-negligible size compared with the insulation thickness. We mounted the resistance probes in holes that were routed out of the insulation, while we embedded the pin probes into either the top or the bottom of the insulation boards. The pins were parallel with the top and bottom surfaces, so both types of probes registered average moisture content in a layer of material about 10–13 mm (approximately 0.5 in.) thick.

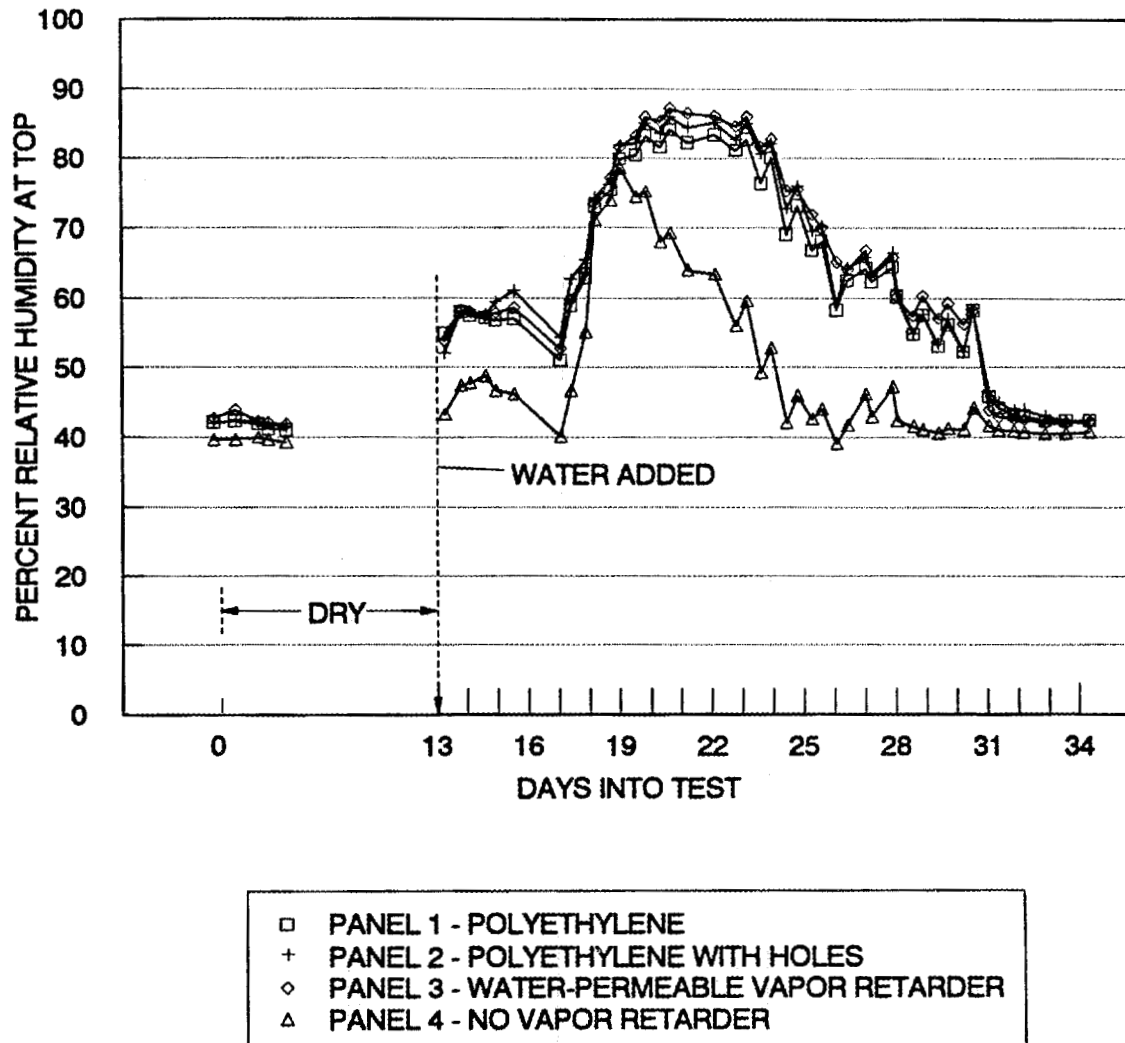
#### 5.1.1 Plywood Probes

Figures 5.1–5.5 show results from the plywood resistance probes. In all these results, diurnal variations were not seen. It takes some time for the moisture to penetrate into the plywood so that it becomes equilibrated with a higher or lower moisture content. Thus, this type of probe indicates trends over several days. Furthermore, because their calibration curve is not valid below 0°C (32°F), this report does not provide results when freezing takes place at the probe locations. In addition, the results are not reliable when the probe readings exceed certain limits, which correspond to the constraint that the plywood moisture content must be between 6 and 30% by weight. When moisture content

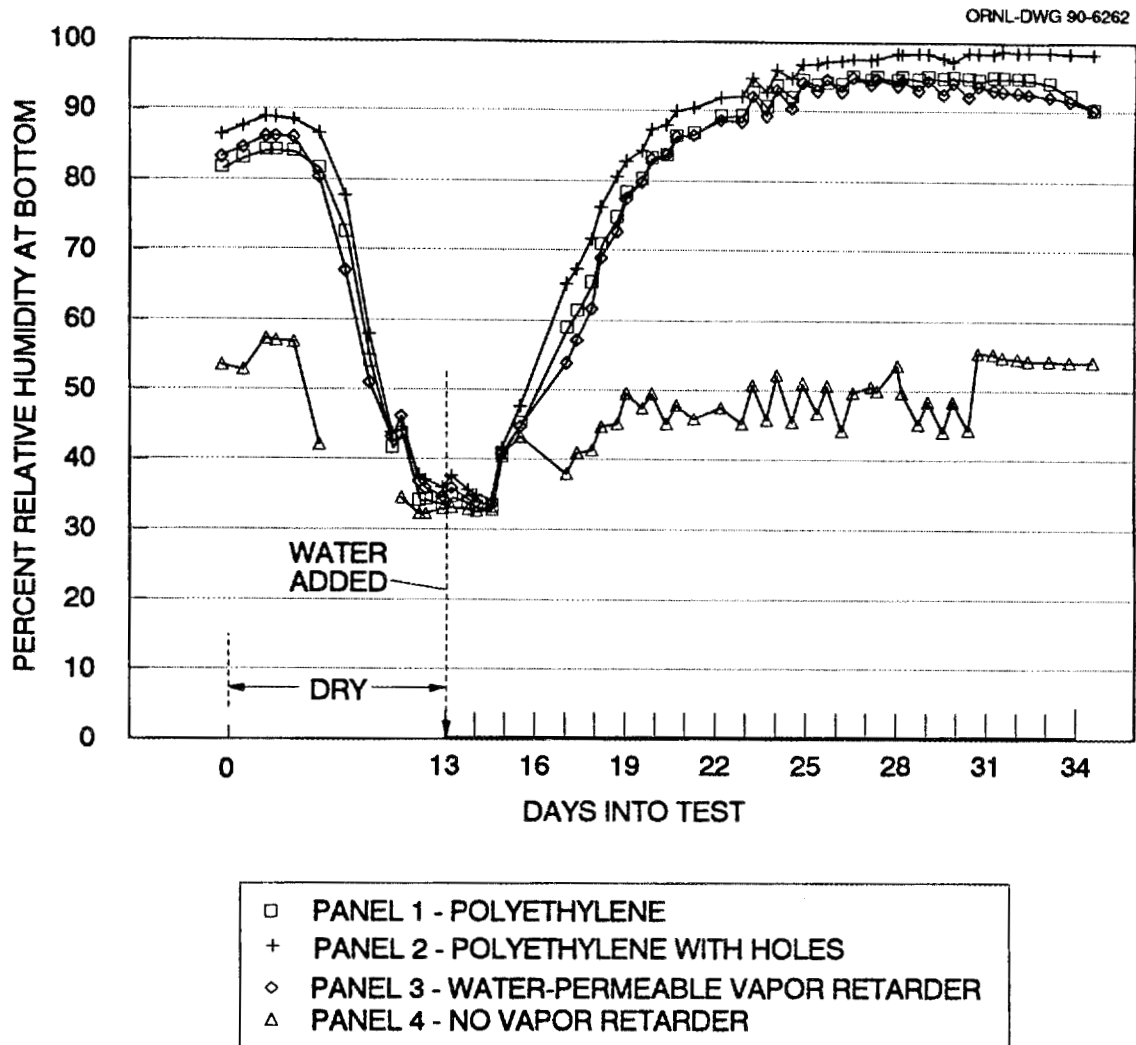
is below this range, the electrical resistance of the plywood becomes too great for the ohmmeter that we used. When the moisture content exceeds the range, resistance no longer decreases with increasing moisture content. Figures 5.1–5.5 present relative humidities that were calculated using the calibration curve for the probes and the sorption isotherms for the probe material.

Figure 5.1 shows results from the probes at the top of the cold-deck roof panels. All probes at the top gave readings in the middle of the hygroscopic range (around 50% RH) before the addition of water about 13 days into the experiment. This is reasonable because these probes were located directly under the plywood deck, which acts as a good buffer. The probes reacted slowly to the addition of water and reached maximum values 3 to 4 days later. Then they dried out again and returned to their initial values. This happened in less than 10 days for the panel without a vapor retarder (i.e., shortly after the temperature cycles with increased amplitude were imposed in the climate chamber). According to the probes, the other three panels did not become dry at the top until the start of the continuously high temperatures in the climate chamber during the last 5 days of the experiment.

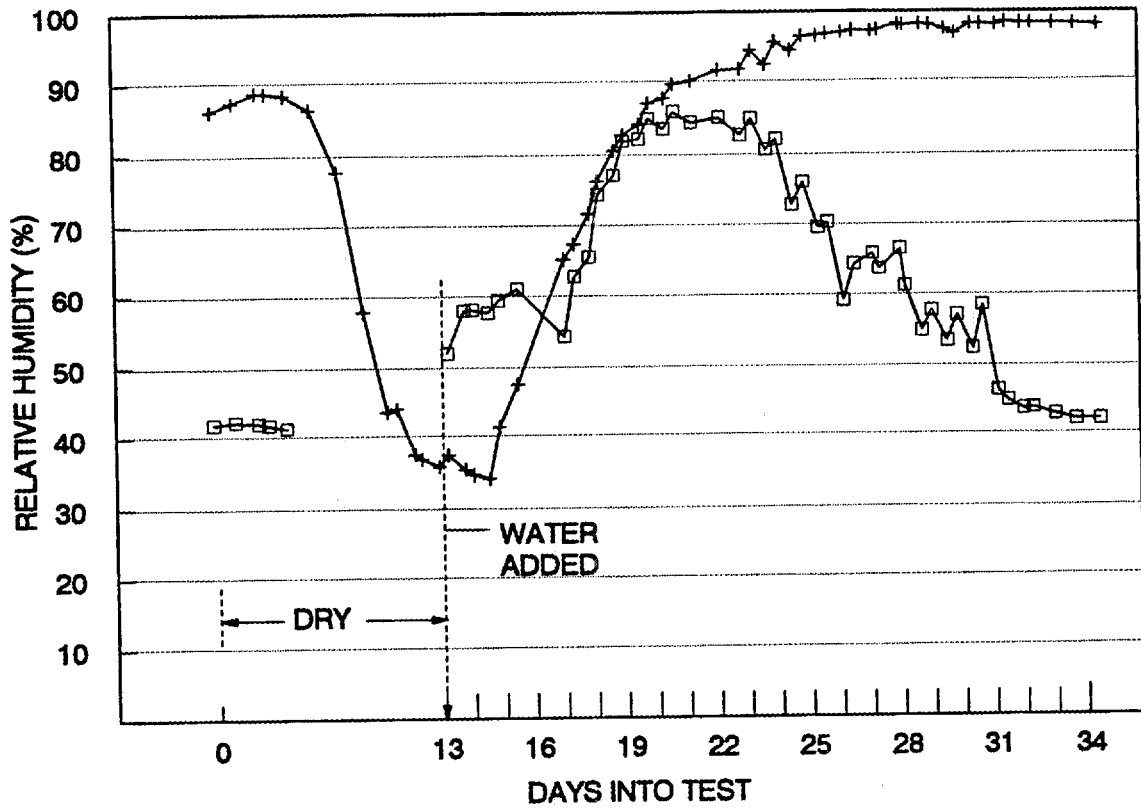
Figure 5.2 shows the output from the bottom probes in the same four panels. It appeared that even the hygroscopic moisture from the plywood was sufficient to bring the relative humidity close to saturation in the bottom of the panels with vapor retarders during the two "dry," steady-state runs early on when the thermal driving forces were directed downward. The moisture dried out quickly when the forces were reversed. The output from the bottom probes read high again after the water was added, and it was driven toward the bottom. This moisture gathered on the vapor retarder and caused the relative humidity to be close to 100%, even though some condensate could escape through some of the vapor retarders. Recall that RH is 100%, independent of the amount of moisture, when liquid water is present in a non-hygroscopic material. Panel 2 without blotting paper and a relatively water-impermeable vapor retarder seemed to hold a RH of 100% at the bottom until the end of the experiment. However, we noticed some decline the last few days in panel 3, with the water-permeable vapor retarder, and in panel 1, with a solid polyethylene vapor retarder. This may have occurred because panel 3 was about to



**Fig. 5.1. Relative humidity from the plywood probes at the top of cold-deck panels 1-4 during the entire experiment.**



**Fig. 5.2. Relative humidity from the plywood probes at the bottom of cold-deck panels 1-4 during the entire experiment.**



COLD-DECK PANEL 2  
 POLYETHYLENE WITH HOLES  
 □ TOP  
 + BOTTOM

Fig. 5.3. Relative humidity from the plywood probes at the top and bottom of panel 2 during the entire experiment.

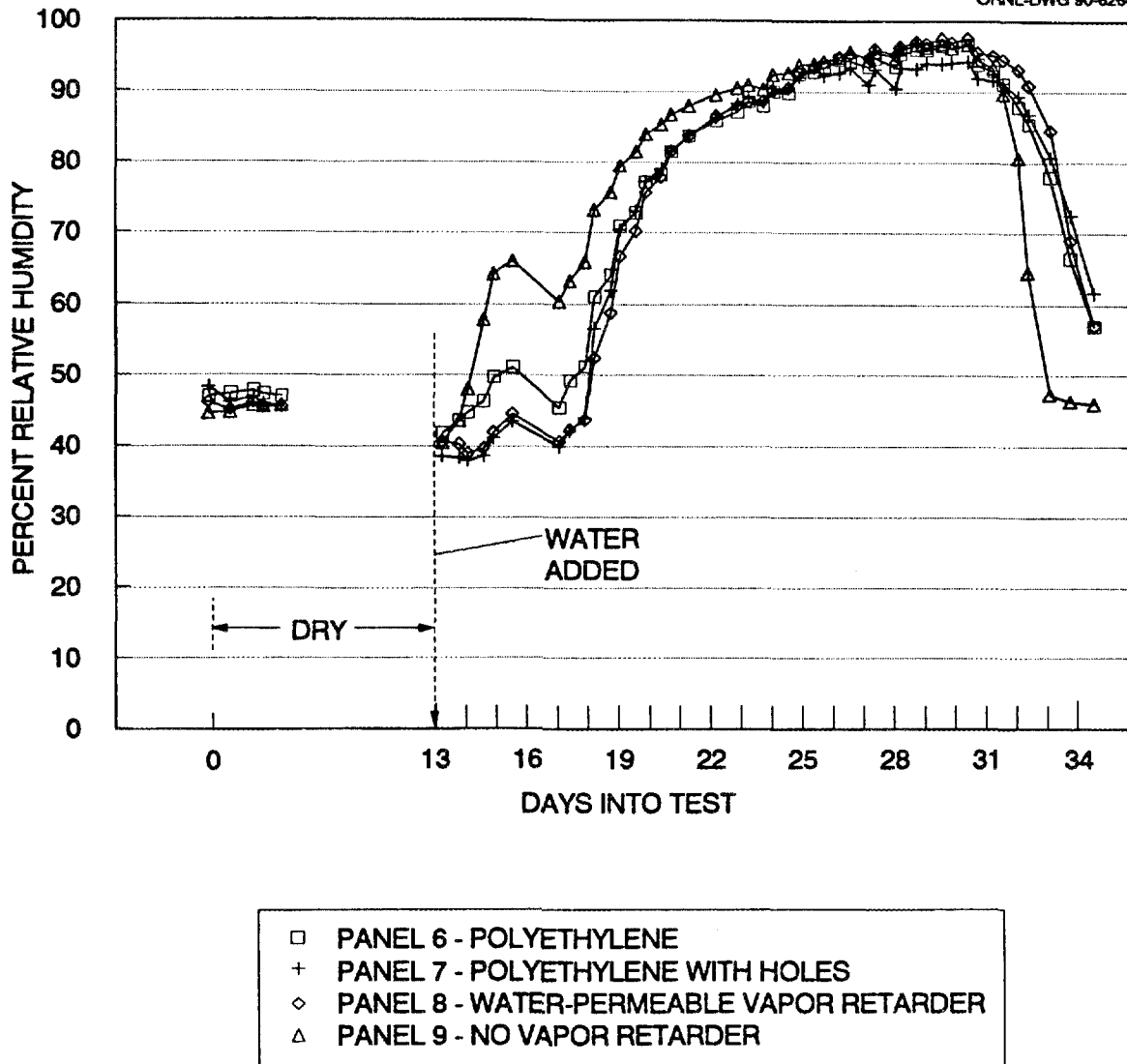


**Fig. 5.4. Relative humidity from the plywood probes at the top of warm-deck panels 6-9 during the entire experiment.**

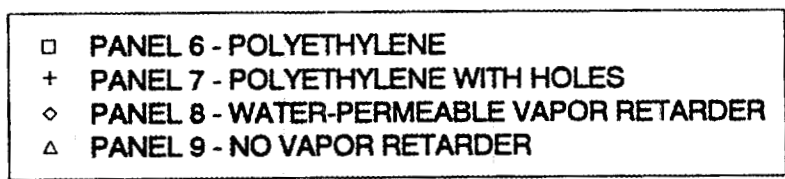
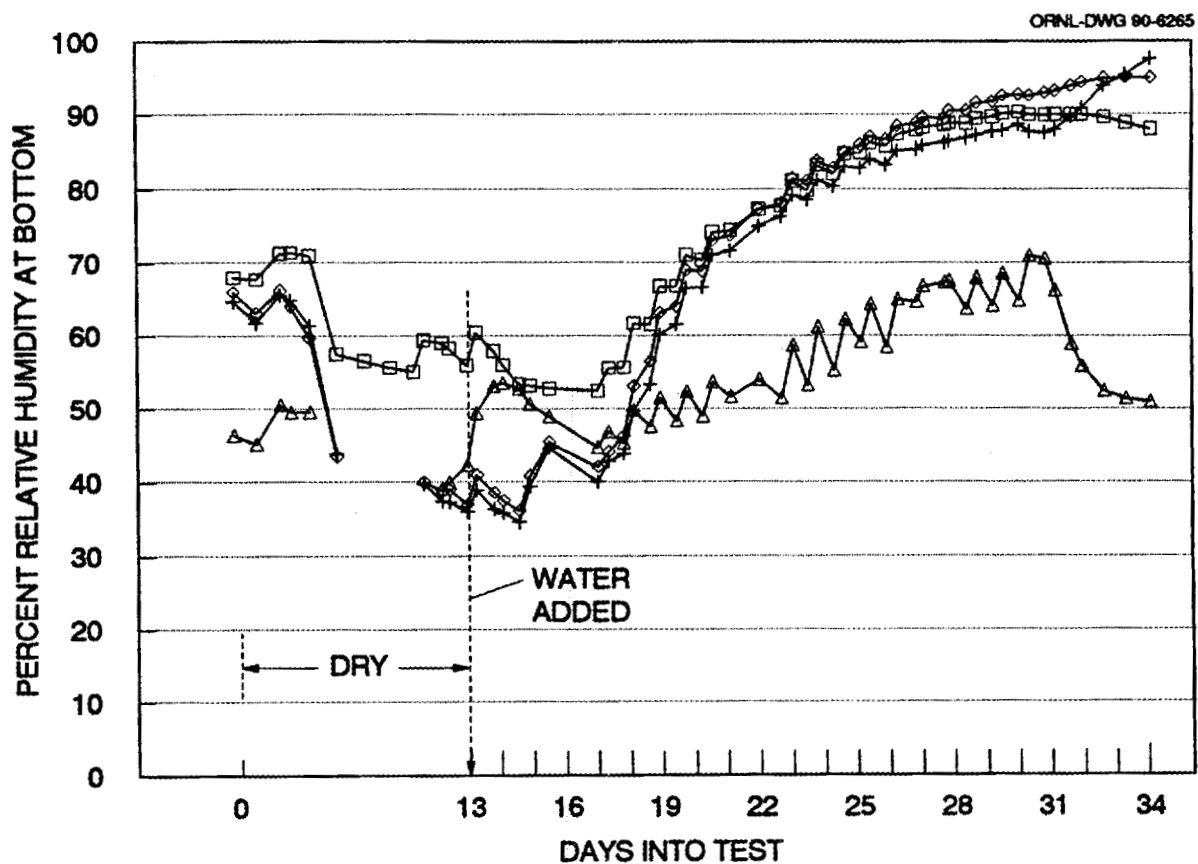


**Fig. 5.5. Relative humidity from the plywood probes at the bottom of warm-deck panels 6-9 during the entire experiment.**

become dry (no liquid water left) and because the constant high thermal driving force in the last run drove the moisture into the blotting paper in panel 1 (with the solid polyethylene vapor retarder). The bottom of panel 4, which had no vapor retarder, never got wet because all the moisture coming from the top passed unhindered through the gypsum.

Figure 5.3 focuses on the curves from Figs. 5.1 and 5.2 for panel 2, which had a polyethylene vapor retarder with holes. Notice how near the end of the experiment the probes showed the changing location of the moisture: what disappeared from the top appeared at the bottom. The moisture was driven from the part of the roof with the warmest average temperature toward the colder part, although both curves increased shortly after the water was added.

Figure 5.4 shows the results from the probes at the top of the warm-deck panels, insulated with expanded polystyrene. These curves are nearly identical. The levels of moisture content were hygroscopic before the water was added, and then the probe readings increased to values close to saturation, until the last few days when the last of the liquid at the top was driven down into the insulation. The reading from panel 9, which had no vapor retarder, increased a little more than the others immediately after we added water. Residual moisture from the concrete may have been driven upward in the panel and condensed under the membrane when steady temperatures with an upward gradient were imposed at the start, although it would take several days to sense this effect at the top. This panel was also the first to dry out. Because there was no condensation at the interface between the insulation and the concrete deck, there being no vapor retarder, the downward vapor pressure gradient was a little larger and drying from the top went faster.

Figure 5.5 shows the plywood probe results at the bottom of the warm-deck panels. Other effects overwhelmed the effect of hygroscopic moisture during the "dry" runs. There was no hygroscopic material such as plywood above the insulation, and the insulation itself was not very permeable. The probe in panel 9, which had no vapor retarder, seemed to sense moisture at the hygroscopic level in the concrete. Polystyrene's low permeability is also the reason why the bottom moisture probe's output increased

more slowly after water was added than it did in the cold-deck panels, even increasing slightly in the panel without a vapor retarder, because the concrete deck had some vapor resistance. Panel 9 without a vapor retarder dried out, however, during the last five days when top temperatures were constantly high. The blotting paper in the bottom of panel 6 with solid polyethylene appeared to have absorbed most of the moisture, as it did in the corresponding cold-deck panel 1. This may be why the curve for this panel dropped off slightly during the last few days. The drying appeared to be incomplete in the other two panels, because the probe readings were still very high.

### 5.1.2 Pin Probes

Figure 5.6 shows the pin probe results from the top of the cold-deck panels, plotted on a logarithmic scale. Such a scale should be linearly related to the moisture content in the materials (Motakef, 1989). This figure corresponds to Fig. 5.1 for the plywood probes. The pin probes in panels 3 and 4 were not connected to the data acquisition system during the dry, steady-state runs. Figure 5.6 indicates that there was lots of scatter among the results from the different probes, as well as some sudden jumps to different levels of response for particular probes. Variations in local conditions, and perhaps the local density of the fibrous glass, may require that each probe be calibrated individually at its actual position in the material. No such calibration was available, however. Therefore, results may only be used to qualitatively follow how the amount of moisture in a particular insulation board changed with time, with no significance to differences between readings for different probes at the same time even if in the same material.

Probe readings were relatively low before water was added to the panels. When water was added, all probe readings increased from their own initial levels. The decline that followed took place when moisture was driven towards the bottom over the two runs with different levels of temperature cycles.

Figure 5.7 shows the output from the pin probes at the bottom of the cold-deck panels. The probe at the bottom of panel 1 showed little change throughout the dry runs, probably because of the blotting paper there. After water was added, probe readings increased markedly for panel 2, which had polyethylene with holes, and panel 3, which had

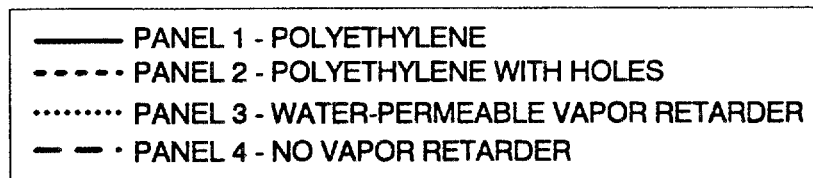
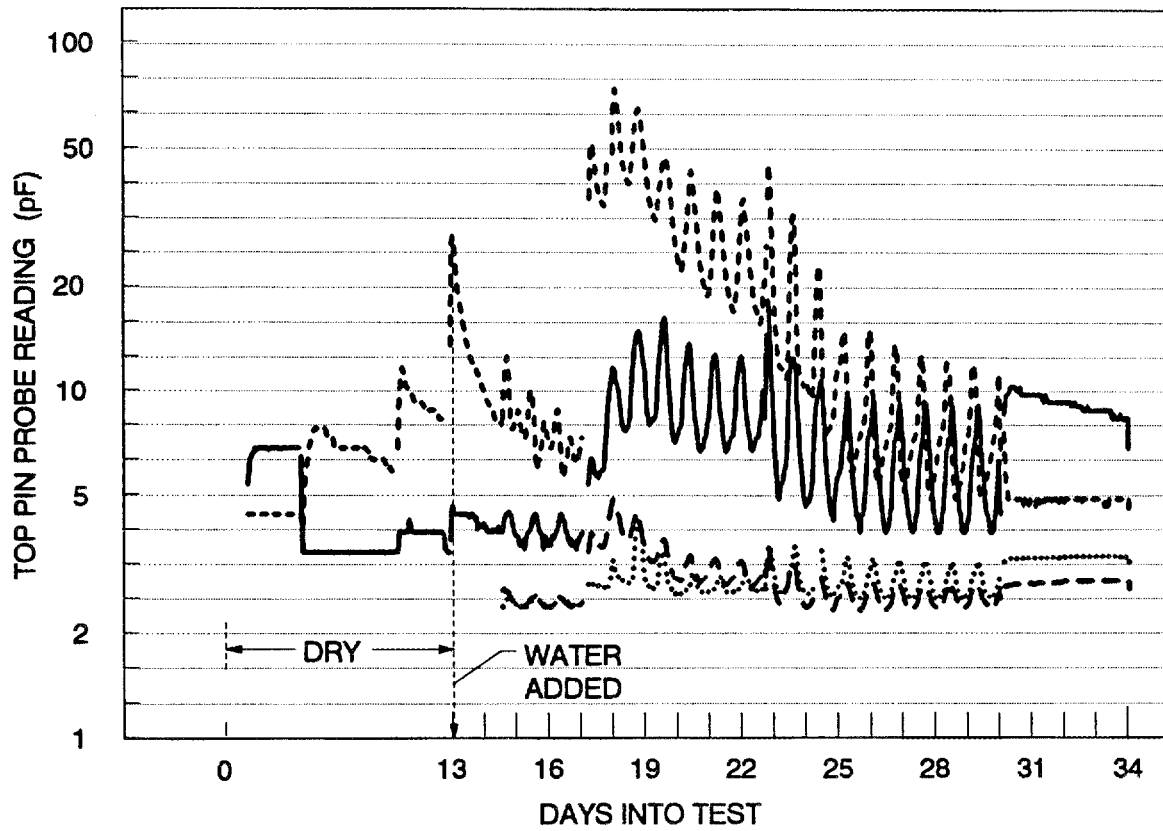


**Fig. 5.6. Uncalibrated response of the pin probes at the top of cold-deck panels 1-4 during the entire experiment.**

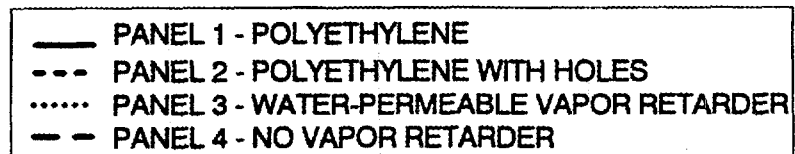
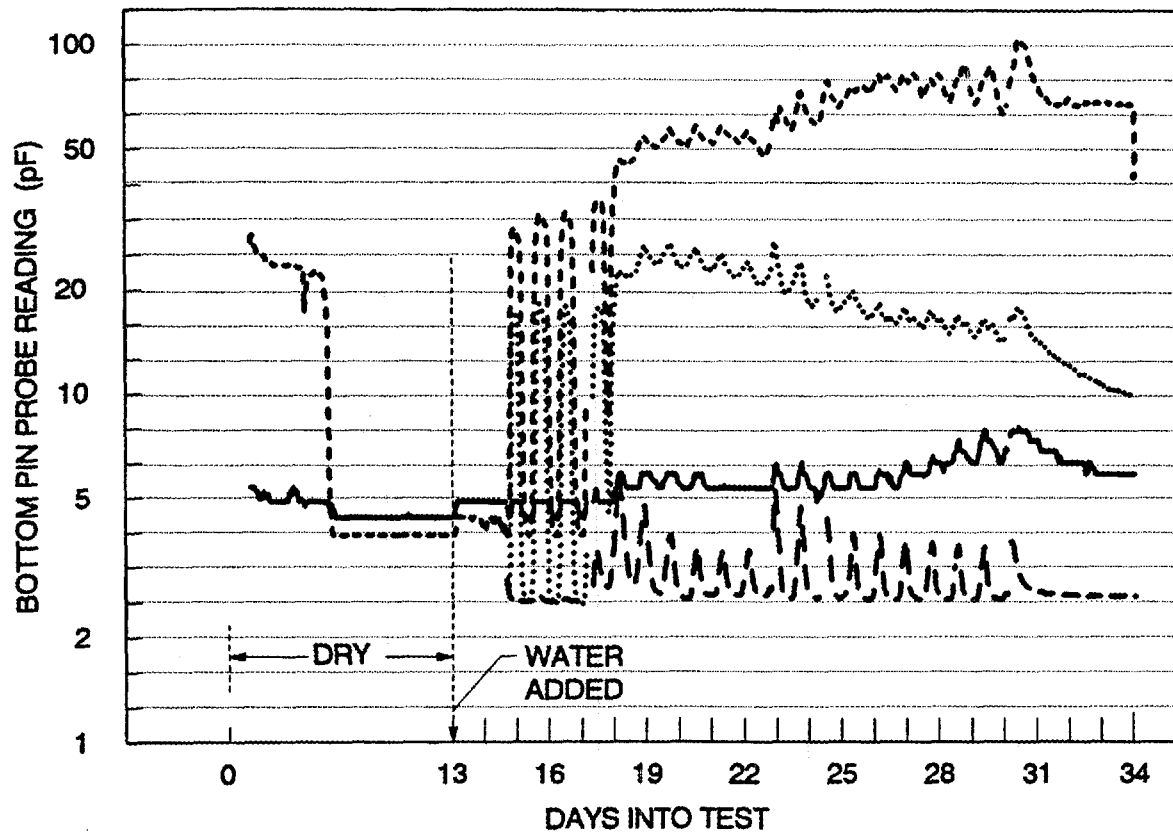


**Fig. 5.7. Uncalibrated response of the pin probes at the bottom of cold-deck panels 1-4 during the entire experiment.**

a water-permeable vapor retarder. The moisture content apparently stayed high at the bottom of panel 2 throughout the experiment, but we noticed some drying in panel 3. Probe readings were not greatly affected by the water added to panel 1 with the solid polyethylene. Apparently the moisture condensed in the sheet of blotting paper that was laid out on this vapor retarder, and was kept away from the probe in the bottom layer of the fibrous glass. Panel 4 had no vapor retarder, so the moisture could diffuse through the gypsum board at its bottom without any significant effect on the readings from the probe during the entire experiment.

Because of two independent observations, we think that the diurnal fluctuations in the probe readings were most likely caused by a temperature effect. The variations in output increased after we increased the amplitude of the temperature cycles. In addition, comparison of pin probe output from the top and bottom of the panels in Figs. 5.6 and 5.7, respectively, shows that fluctuations in output were highest at the top where temperature fluctuations were greater.

Figure 5.8 shows the data from the top and bottom pin probes in panel 2, which has the polyethylene with holes. When the moisture that moved from the top gathered at the bottom, the top probe's readings decreased, while the bottom one's increased. The diurnal variations, however, were in the same direction. This is another indicator that these fluctuations were caused by temperature effects, because the temperature rose and fell at approximately the same time on both sides of the insulation.

## **5.2 RESULTS OF GRAVIMETRIC MOISTURE MEASUREMENTS**

We weighed specimens inside the panels at the start of the experiment and removed and weighed them again before and after water was added, and then after every subsequent run until the end of the experiment. The specimens comprised most of the pieces of insulation that guarded the central area, the blotting paper at the top of all

panels and at the bottoms of panels 1 and 6 on the solid polyethylene vapor retarder, and four discs from each of the plywood decks. We removed slightly less than half the volume of the insulation and about 3% of the plywood, and assumed that moisture spread uniformly across each panel at each level.

### 5.2.1 Moisture Changes during Dry Runs

Measurements of the weights of components made as the panels were assembled at the start of the experiment and before water was deliberately added yielded different totals. They showed that some moisture apparently migrated either in or out of the test panels even during the dry runs. Panel 1, the cold-deck panel with a polyethylene vapor retarder, gained  $27 \text{ g/m}^2$ , while panel 2 with polyethylene with holes gained  $26 \text{ g/m}^2$ . Panel 3 with the water-permeable vapor retarder dried out by  $62 \text{ g/m}^2$  during these runs. Panel 4 without a vapor retarder lost  $179 \text{ g/m}^2$ . We assumed that the plywood started in equilibrium with air at 60% RH. It is possible, therefore, that it could absorb small amounts of moisture coming through the vapor retarder or, less likely, through the roof membrane with the added layer of polyethylene. During the dry diurnal cycles, however, some of the moisture in the plywood would likely have migrated downward in the roof. Part of this moisture that migrated down seemed to escape when there was no vapor retarder, and also when there was a vapor retarder permeable to liquid water.

The situation was different in the warm-deck panels, which lost small amounts of moisture during the dry runs when there was a vapor retarder:  $11 \text{ g/m}^2$  for panel 6;  $10 \text{ g/m}^2$  for panel 7; and  $8 \text{ g/m}^2$  for panel 8. Panel 9 without any vapor retarder gained  $6 \text{ g/m}^2$ , possibly due to upward diffusion from the concrete during the runs with an upward thermal driving force.

### 5.2.2 Moisture Changes after Water was Added

In the cold-deck panels, we added approximately  $500 \text{ g/m}^2$  of water to each of the two sheets of blotting paper that covered the upper and lower surfaces of the plywood. In the warm-deck panels, we added all  $1000 \text{ g/m}^2$  to a single sheet of blotting paper. Table 5.1 lists the weighing results per unit area for all the panels except panel 5. In this table, the differences in the weights of the materials between the times listed and immediately

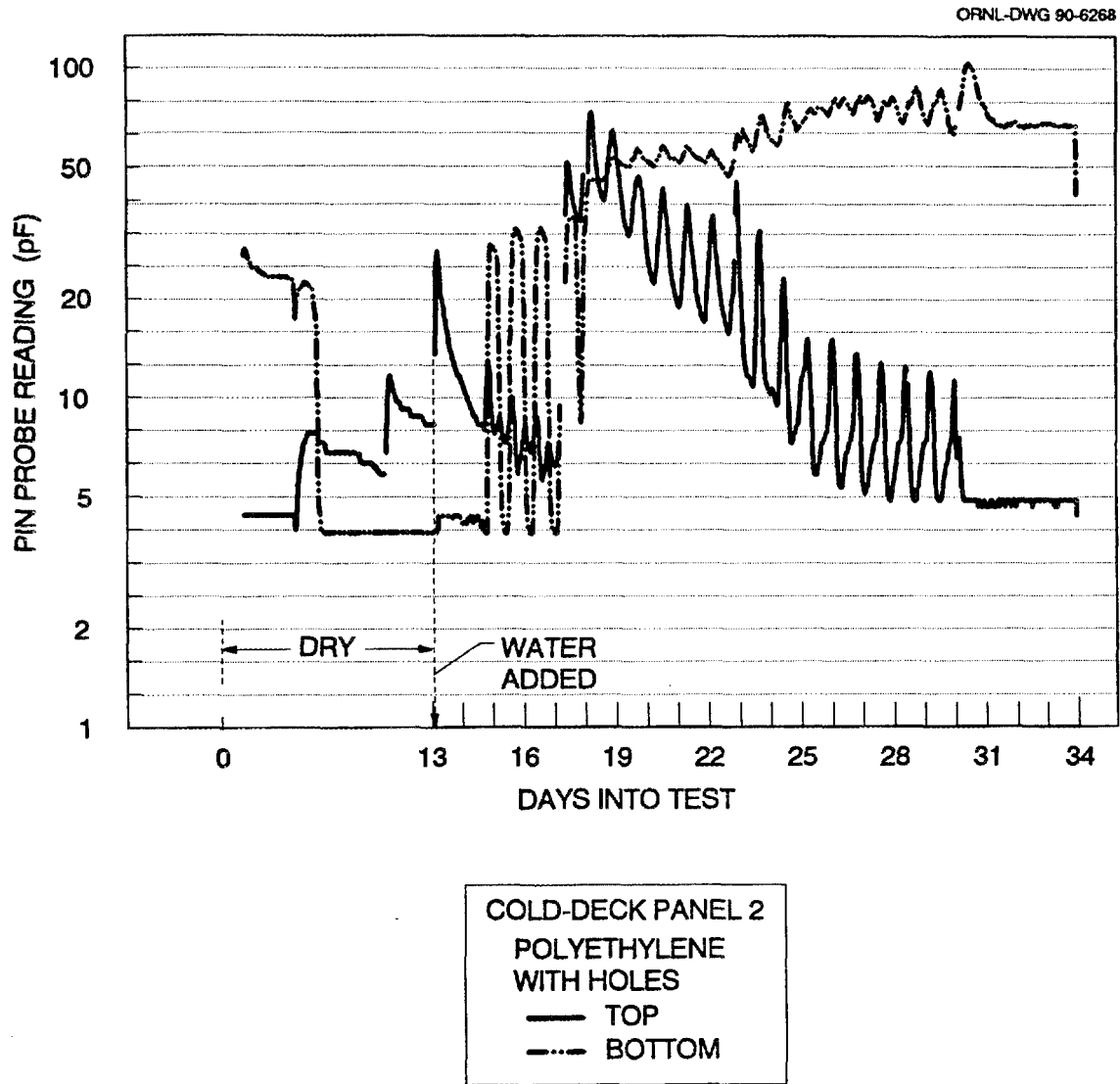


**Fig. 5.8. Uncalibrated response of the pin probes at the top and bottom of cold-deck panel 2 during the entire experiment.**

before water was added at the start of run 7 are shown after being rounded off to the nearest  $\pm 1 \text{ g/m}^2$ . Negative weights for some totals and for some components indicate drying of hygroscopic moisture that was present prior to the deliberate addition of water. Panel 5 was constructed identically to panel 1, but we added no water to it. We opened panel 5 on 16 and 21 days after we had added water to the other panels. Its weight was slightly less on those days than at the initial assembly of the panels. To the accuracy of the technique, this loss of weight represents hygroscopic moisture that dried out of the plywood.

We used paper towels to absorb the moisture that had condensed on interior surfaces of the panels in the last two runs. On day 16, we weighed the towels used for each panel, used them to absorb water, and weighed them again. Table 5.1 shows the differences in weights. We then placed the wet towels in the bottom of the panels. On day 21, we used the paper towels again to absorb the excessive moisture. We could perform this operation before and after the last run when there was no concern about backflow of moisture toward the top of the constructions. The thermal driving force was downward only in the last run of the experiment.

As Table 5.1 shows for the cold-deck panels, most of the added moisture migrated into the plywood within the first week. Some of it also migrated down into the insulation, causing a gain of moisture content for the lower layer of fibrous glass. The plywood dried out after another two weeks. Most of this moisture ended up in the bottom insulation layer, or it condensed on the vapor retarder if one was present. It was visibly noticeable that the moisture in the bottom fibrous-glass layer was confined to within only a few millimeters of the bottom. Depending on the vapor retarder system, some of the water migrated out through the bottom of the panel.

**Table 5.1. Distribution of deliberately added moisture ( $\text{g/m}^2$ ) in the roof test panels  
(FG = Fibrous glass, EPS = Expanded polystyrene)**

Panel (with features)	Days after water added at start of run 7			
	0	7	16	21
<b>1 (Cold deck, polyethylene)</b>				
Blotting paper	502	51	6	-10
Plywood	0	685	56	-281
Blotting paper	499	39	4	-11
FG top	0	13	2	-2
FG middle	0	8	5	-1
FG bottom	0	38	43	21
Blotting paper	0	84	600	1024
Paper towels	N.A.	N.A.	36	42
<b>Total</b>	<b>1001</b>	<b>918</b>	<b>752</b>	<b>782</b>
<b>2 (Cold deck, polyethylene with holes)</b>				
Blotting paper	502	60	5	-11
Plywood	0	681	65	-284
Blotting paper	500	44	3	-12
FG top	0	14	0	-3
FG middle	0	9	4	-1
FG bottom	0	136	502	535
Paper towels	N.A.	N.A.	96	315
<b>Total</b>	<b>1002</b>	<b>944</b>	<b>675</b>	<b>539</b>
<b>3 (Cold deck, water-permeable vapor retarder)</b>				
Blotting paper	501	56	8	-8
Plywood	0	689	103	-225
Blotting paper	500	44	6	-9
FG top	0	12	3	-1
FG middle	0	12	7	0
FG bottom	0	139	293	255
Paper towels	N.A.	N.A.	8	10
<b>Total</b>	<b>1001</b>	<b>952</b>	<b>428</b>	<b>22</b>
<b>4 (Cold deck, no vapor retarder)</b>				
Blotting paper	501	38	5	-6
Plywood	0	365	-3	-204
Blotting paper	500	11	-1	-5
FG top	0	4	-1	-4
FG middle	0	2	-1	-5
FG bottom	0	2	0	-4
<b>Total</b>	<b>1001</b>	<b>422</b>	<b>-1</b>	<b>-228</b>

Table 5.1 (continued)

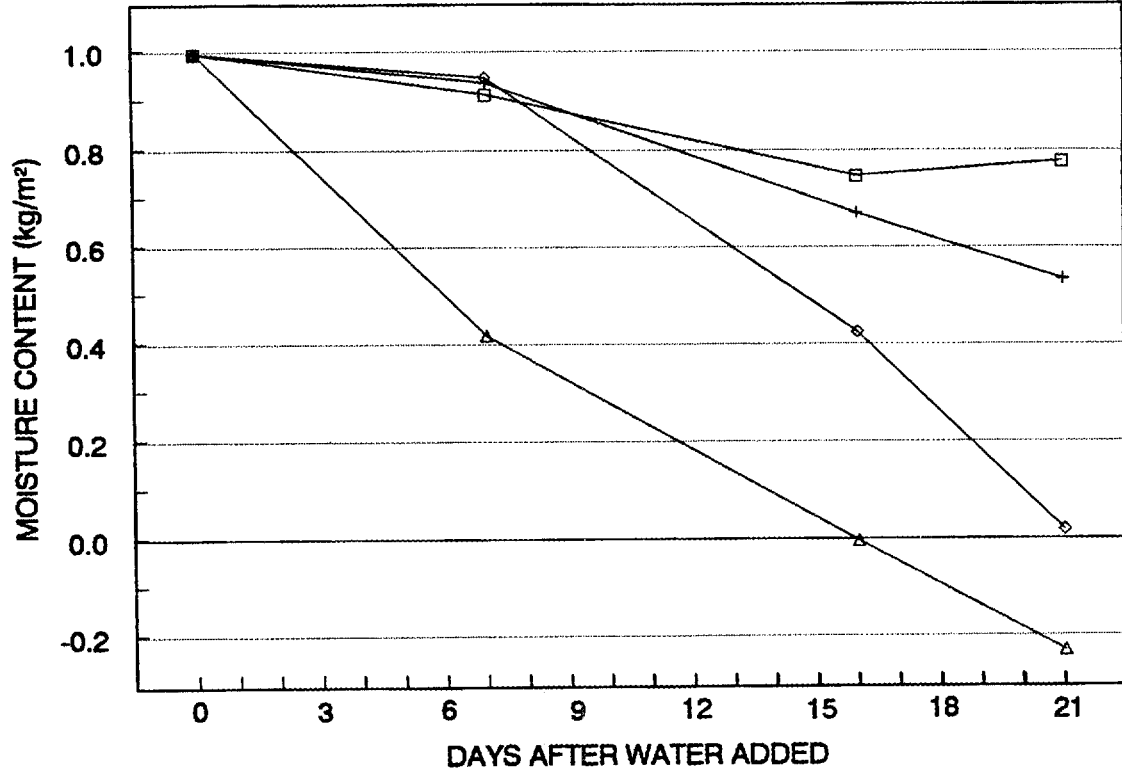
<b>6 (Warm deck, polyethylene)</b>				
Blotting paper	1002	745	161	9
EPS top	0	81	200	0
EPS bottom	0	2	110	32
Blotting paper	0	70	216	610
Paper towels	N.A.	N.A.	76	108
<b>Total</b>	<b>1002</b>	<b>898</b>	<b>763</b>	<b>759</b>
<b>7 (Warm deck, polyethylene with holes)</b>				
Blotting paper	1001	765	194	14
EPS top	0	92	217	-1
EPS bottom	0	24	212	101
Paper towels	N.A.	N.A.	98	376
<b>Total</b>	<b>1001</b>	<b>881</b>	<b>721</b>	<b>490</b>
<b>8 (Warm deck, water-permeable vapor retarder)</b>				
Blotting paper	1003	739	179	13
EPS top	0	90	219	0
EPS bottom	0	24	177	48
Paper towels	N.A.	N.A.	84	330
<b>Total</b>	<b>1003</b>	<b>853</b>	<b>659</b>	<b>391</b>
<b>9 (Warm deck, no vapor retarder)</b>				
Blotting paper	1000	663	246	-20
EPS top	0	36	47	0
EPS bottom	0	0	1	1
<b>Total</b>	<b>1000</b>	<b>699</b>	<b>294</b>	<b>-19</b>

The moisture in the warm-deck panels redistributed more slowly because of the lower permeability of the insulation. It took all three weeks for the blotting paper at the top to dry out. At first some moisture was deposited in the top layer of insulation, but it later migrated to the bottom layer or to the vapor retarder where it condensed. Some moisture also migrated all the way out of some of these panels.

Figures 5.9 and 5.10 show the changes of moisture content after water was deliberately added. Here, the totals in Table 5.1 are plotted and normalized to  $1 \text{ kg/m}^2$ , the nominal amount of water that we added to each panel. As in Table 5.1, this normalization ignored the hygroscopic moisture in the panels, so negative moisture contents were possible by the end of the experiment. Straight lines join the points to emphasize the trends, but the lines do not imply that the progress of drying between the weighings was linear. The trends from the moisture probes in Figs. 5.1–5.8 better describe how conditions changed between weighings. In the next section, the program MATCH is used to predict this information.

Figure 5.9 shows that cold-deck panel 4 without a vapor retarder dried out very rapidly. The water was gone within the first two runs after it was added, and some of the hygroscopic moisture escaped during the last run. The three cold-deck panels with vapor retarders did not dry out much, if at all, in the first week after the water was added. The apparent drying may indicate some real drying, but it also may show only that the moisture was moving away from the plywood and the blotting paper where it was easy to capture and measure. If it dispersed preferentially as condensate on some of the non-removable interior surfaces, it would escape detection. Apparently there was not enough condensate formed on the water-permeable vapor retarder under these conditions to initiate wicking action.

Later, the trends were closer to expectations. Panel 1 with the solid polyethylene at first dried out a little more, but apparently gained moisture during the last run. A possible explanation is that the procedures used to absorb the condensate and weigh it were done more thoroughly at the end of the test. Panel 2, which used the polyethylene with holes,



- PANEL 1 - POLYETHYLENE
- + PANEL 2 - POLYETHYLENE WITH HOLES
- ◇ PANEL 3 - WATER-PERMEABLE VAPOR RETARDER
- △ PANEL 4 - NO VAPOR RETARDER

**Fig. 5.9. Gravimetrically determined moisture content in cold-deck panels 1-4 (with significant hygroscopic moisture) after each wet run.**

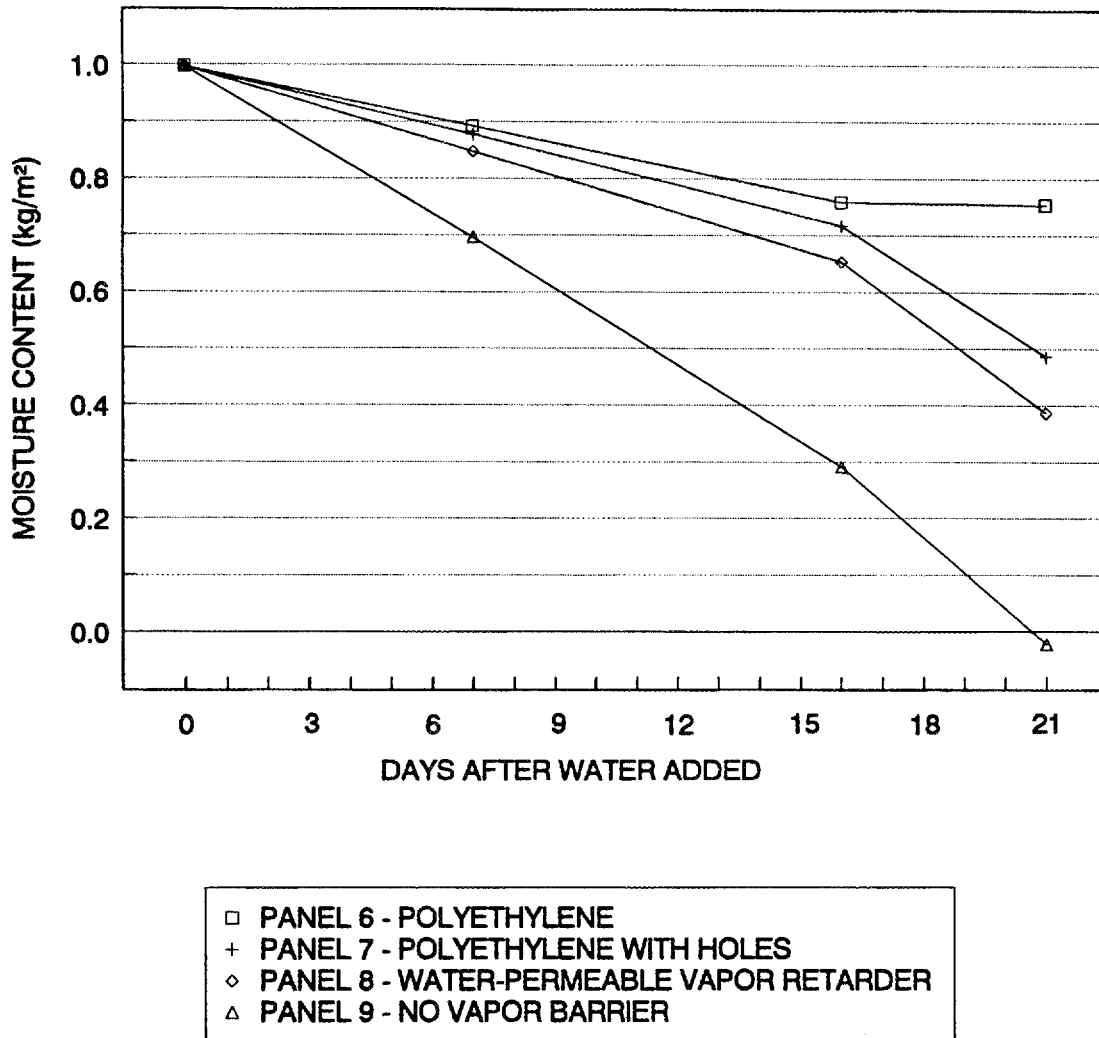


**Fig. 5.10. Gravimetrically determined moisture content in warm-deck panels 6-9 (with little hygroscopic moisture) after each wet run.**

dried out slightly more in these later runs than it had in the earlier runs. Almost half of the added water appeared to be gone after three weeks. Panel 3 with the water-permeable vapor retarder dried out quite well during the last two runs, at least as fast as panel 4 without a vapor retarder. All the water that was added had escaped from panel 3 by the end of the test.

Figure 5.10 shows data for drying in the warm-deck panels. Panel 9 without a vapor retarder dried out by the end of the experiment. Large negative values relative to the added water were not possible here, because these panels did not contain much hygroscopic moisture at the beginning. The panels that had polyethylene vapor retarders with or without holes dried out approximately the same amount as the corresponding cold-deck panels. Again, some of this drying may not have been real, because some moisture may have condensed on inaccessible surfaces. Panel 8 with a water-permeable vapor retarder dried out a little more than panel 7, which had polyethylene with holes, but it still contained 40% of the added water by the end of the experiment.

Apparently the conditions under which the water-permeable vapor retarder is able to dry out are different from those for the polyethylene with or without holes. With the use of a solid polyethylene vapor retarder, the escaping moisture flux is determined by the vapor pressure difference across it. This vapor pressure difference may be much the same no matter what type of insulation is used, because all vapor pressures within the cavity will be close to saturation most of the time. The few holes punched in the polyethylene to form the alternative vapor retarder did not provide much opportunity for liquid to escape directly until the last run.

The water-permeable vapor retarder system requires a layer of condensate to be formed on it before appreciable amounts of water can migrate through it. This happens easily in the daytime when fibrous glass is used as insulation. Expanded polystyrene insulation decreases the peaks of downward vapor flux in the daytime, so less condensate is formed. Some of the moisture is absorbed in the insulation layers instead. The use of the water-permeable vapor retarder appears to make downward drying both possible and faster than through a sheet of polyethylene. The conditions under which it works are

clearly improved, however, when the insulation is permeable and does not have a high hygroscopic capacity. Conversely, the results from the panels without a vapor retarder, where all the added water escaped both the cold- and warm-deck types, as well as some hygroscopic moisture from the cold-deck type, show that the water-permeable vapor retarder and the polyethylene with holes do present enough resistance to prevent complete drying in the time allowed in this experiment.

The gravimetric method of determining the moisture content in the panels was not as accurate as we had hoped. The problem with condensed moisture escaping detection in the non-removable materials inside the panels has already been mentioned. A more general list of possible sources of error includes:

- Some moisture may have migrated upward through the roofing membrane or through the sealing around the perimeter of the membrane.
- Taking out about half of the insulation materials in each panel was not enough to represent the whole panel if non-uniform lateral distributions occurred at any level in the construction.
- The moisture content in the plywood was determined for discs that represented about 3% of the total area of plywood. Uncertainties in the determination of the disk area and moisture content have relatively large effects on the moisture content per unit roof area.
- The insulation and wood frame around the perimeter of the panels may not have been perfectly isolated from the specimens, so lateral moisture migration took place.

The dilemma remains—on one hand, probes do not give quantitative measures of moisture content; on the other, weighing of specimens has to be intrusive and thorough if the moisture distribution is to be found. The ideal situation would be to weigh panels without opening them to give changes in the total moisture content. This would require a balance which is able to weigh heavy specimens with a very fine resolution. Quantitative moisture probes would complement the total moisture change by providing the distribution throughout the panels, not just the relative changes at one location. We plan to pursue this approach using panels supported by load cells.

### 5.3 PREDICTED DRYING RATES WITH THE VARIOUS VAPOR RETARDER SYSTEMS

The MATCH computer program was a valuable tool in interpreting heat fluxes in permeable systems where water is evaporating and condensing. As an exercise to show the information available from MATCH regarding moisture distributions, we applied it to the drying process indicated by the gravimetric results in Sect. 5.2. We used the temperatures measured at the top and bottom of the panels and the dew point temperatures measured in the upper climate chamber and lower guard chamber as boundary conditions for the calculations. Simulated time began when water was added at the start of run 7 and continued through the subsequent three wet runs of the experiment. The initial amount of moisture in each panel was the water added at the start of run 7, plus an estimate of the hygroscopic moisture in each panel at that time. The latter moisture content consisted of the hygroscopic moisture content of the materials at 60% RH, corrected for the measured weight changes during the dry runs. The hygroscopic moisture content is particularly important for the plywood layer in the cold-deck panels. As we estimated in Sect. 4.3, the weight of the hygroscopic moisture is about 75% of the weight of water that was deliberately added to the panels.

Moisture and thermal parameters were required for all materials in the constructions. The dry thermal conductivities were those determined in the early runs of this experiment and listed in Table 4.1. We estimated the dry densities from the weighing results. Most other parameters, such as the specific heat, water-vapor permeability, and sorption isotherms, were taken for similar materials from MATCH's materials library. Because of the extra polyethylene layer added under all membranes, the membranes were simulated as vapor-tight barriers. The permeability of the lightweight concrete was determined from wet-cup measurements in the laboratory at the Technical University of Denmark after the experiment was finished. We inferred the permeability of the expanded polystyrene from the weighing results for panel 9, the warm-deck panel without a vapor retarder. In order to get the same rate of loss of moisture as found in the experiments, the polystyrene needs

to have a permeability of  $9 \cdot 10^{-12}$  kg/(Pa·s·m) (6 Perm in.). This is toward the upper end of the range given for expanded polystyrene (ASHRAE, 1989):  $4\text{--}12 \cdot 10^{-12}$  kg/(Pa·s·m) (3–9 Perm in.). The permeability for expanded polystyrene was assumed to be independent of the level of moisture content.

An additional parameter is needed by MATCH in order to produce the same apparent drying as shown by the gravimetric measurements. This parameter is the value of the vapor resistance of the vapor-retarder systems. We performed a few iterations for each panel in order to refine the vapor resistance of the vapor-retarder systems until the calculated and measured losses of moisture content over the last three weeks of the experiment agreed with each other. Any inaccuracy in the gravimetric results appears, therefore, in the apparent water vapor resistances. The resistance required for the solid sheet of polyethylene was about  $15 \cdot 10^9$  Pa·m<sup>2</sup>·s/kg (1 Rep). This vapor retarder has resistances from  $105\text{--}575 \cdot 10^9$  Pa·m<sup>2</sup>·s/kg (6–33 Rep) depending on weight per unit area (ASHRAE, 1989) when measured with traditional methods. This would have produced negligible weight losses for these panels throughout this experiment. With the low value of vapor resistance for polyethylene, MATCH showed little drying in the first few weeks after water was added, but enough drying in the last few days of the experiment so that the overall weight loss agreed with the measurements.

Figures 5.11–5.18 show the calculated distributions of moisture in the eight panels to which water was added. We plotted the amount of moisture in the layers inside the roof cavities additively for each layer, starting with the bottom layer. Thus, the top line shows the total moisture predicted to be within the cavities at any time. The graphs show both the hygroscopic moisture and the added water, so the values are not directly comparable to data in Table 5.1.

For the cold-deck panels, the water added to the layers of blotting paper directly above and below the plywood dried out of the paper within a few days and migrated into the plywood. This was the effect that we strived for, because the experiments were supposed to reflect conditions when a deck has absorbed moisture over some time—all winter, for instance. The weighing results confirmed that the moisture moved quickly from the

blotting paper into the plywood. In addition to migration into the plywood, moisture begins its downward transport through the blotting paper directly below the plywood. This moisture will gather in the bottom layers of the roof system if the resistance of the vapor retarder is high, or it will escape from the roof cavity when there is no vapor retarder. The panels with a solid polyethylene vapor retarder also had a layer of blotting paper below the insulation, which would absorb most of this moisture in panel 1. The bottom insulation layer absorbed a little and the other layers remained dry. The panels having polyethylene with holes had no blotting paper at the bottom, and the lower insulation layer in panel 2 absorbed all the moisture instead. We simulated the water-permeable vapor retarder as a hygroscopic layer with a grid point on the upstream side of the vapor resistance that represents it in MATCH. Figure 5.13 shows how the water-permeable vapor retarder, when at first it was dry, absorbed most of the moisture that came down. Later, when it was wet, it passed the water through and its water content decreased toward the end of the experiment.

The warm-deck panels differed from the cold-deck panels in that they did not have any plywood to add hygroscopic moisture or to absorb the water that we added to the blotting paper. Thus, the most the moisture content could be was about  $1 \text{ kg/m}^2$ . The expanded polystyrene insulation was able to absorb some of the moisture. However, it had a low permeability, so the blotting paper at the top held the moisture for a long time. This dominated the predicted fate of the moisture until late in the experiment. The bottom blotting paper in Fig. 5.15 for panel 6 shows less moisture absorption than the bottom blotting paper in Fig. 5.11 for panel 1. The lower layer of insulation in Fig. 5.16 for panel 7 also has less moisture than the lower layer in Fig. 5.12 for panel 2. Figure 5.17 for panel 8, like Fig. 5.13 for panel 3, shows the ability of the water-permeable vapor retarder to absorb, then pass through, moisture, although the effect is not as pronounced. The water-permeable vapor retarder never seems to get completely wet in Fig. 5.17 due to the impermeable materials above it. A little water escaped from panel 8, but relatively more water escaped from panel 3 because of its permeable insulation. Figures 5.14 and 5.18, for the panels without a vapor retarder, show that all the moisture that reaches the bottom of the insulation escapes from the system. Not all of the hygroscopic moisture is able to dry out of plywood, as Sect. 4.3 points out, and Fig. 5.14 reflects.

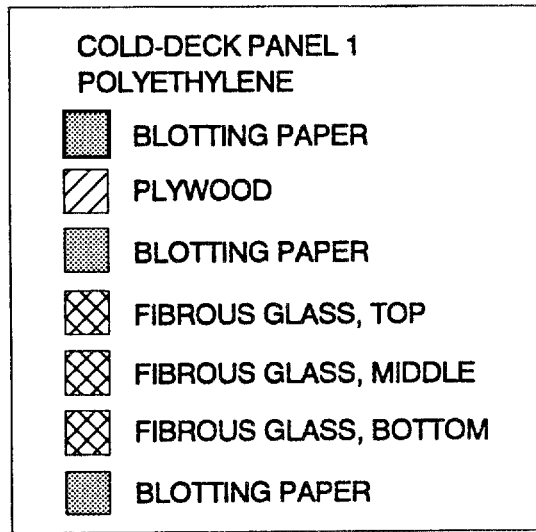
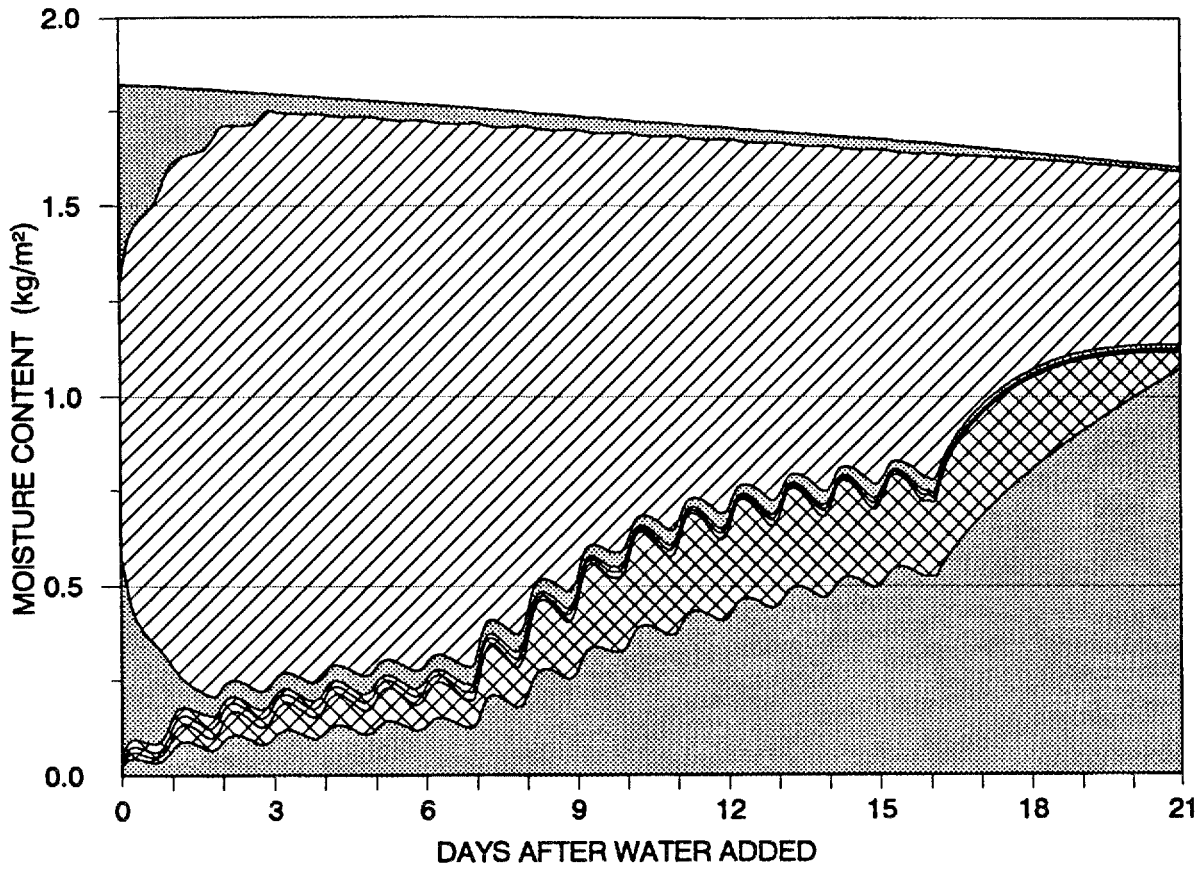


**Fig. 5.11. Moisture content in the layers of cold-deck panel 1, calculated by MATCH after water was added.**

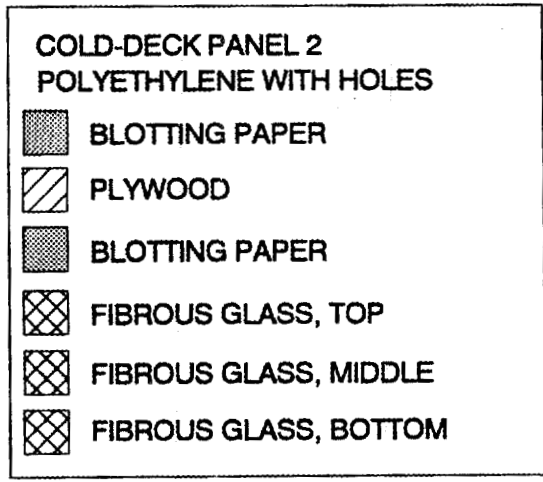
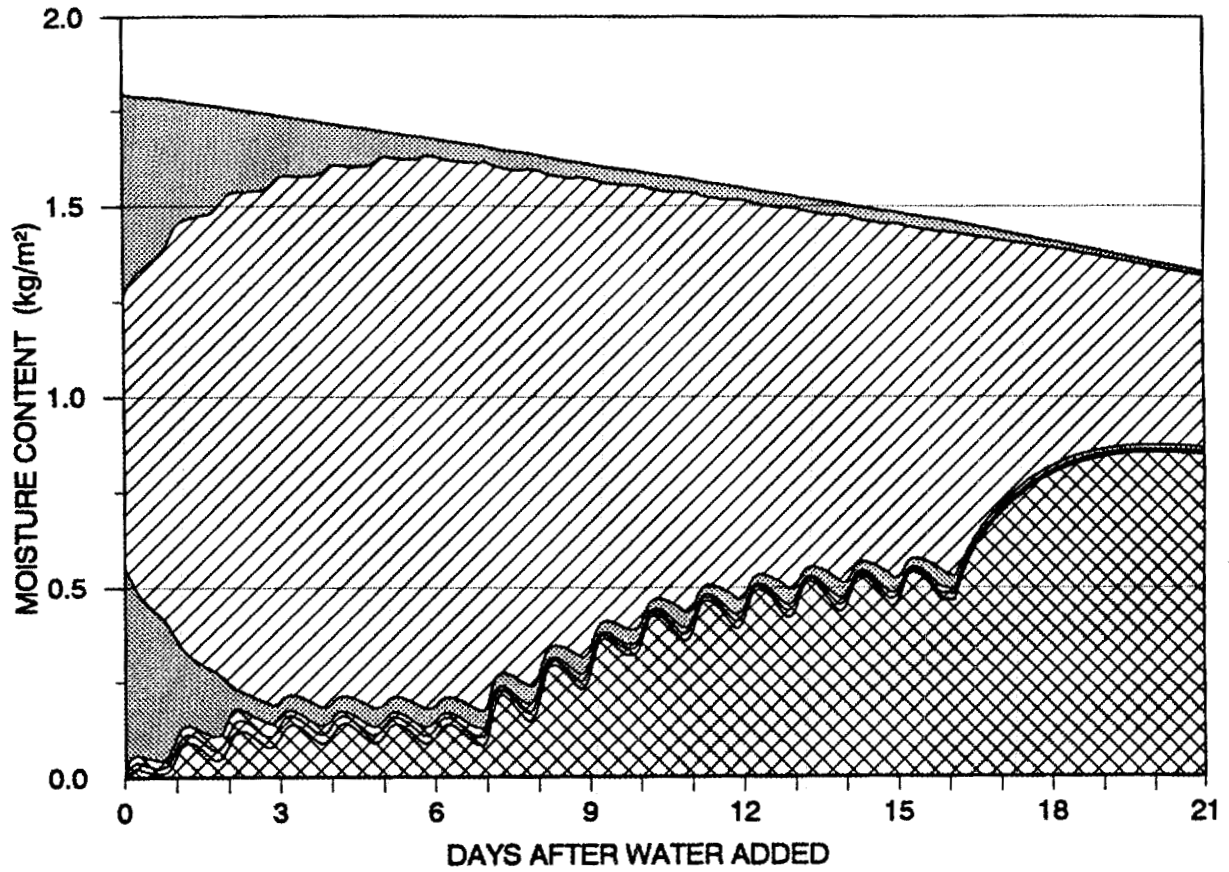


**Fig. 5.12. Moisture content in the layers of cold-deck panel 2, calculated by MATCH after water was added.**

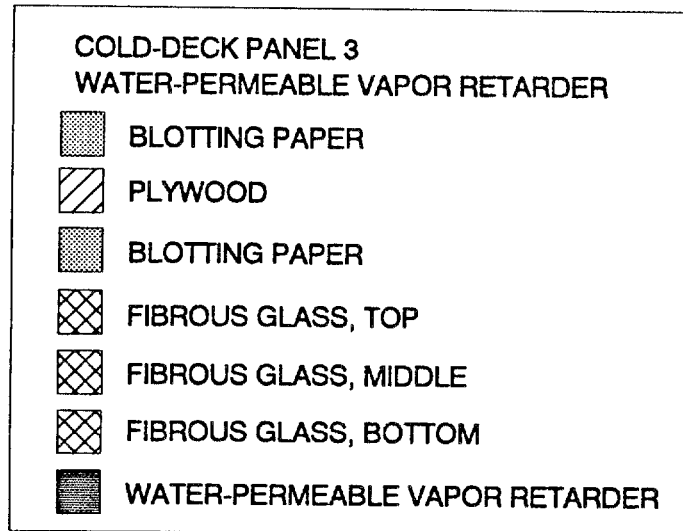
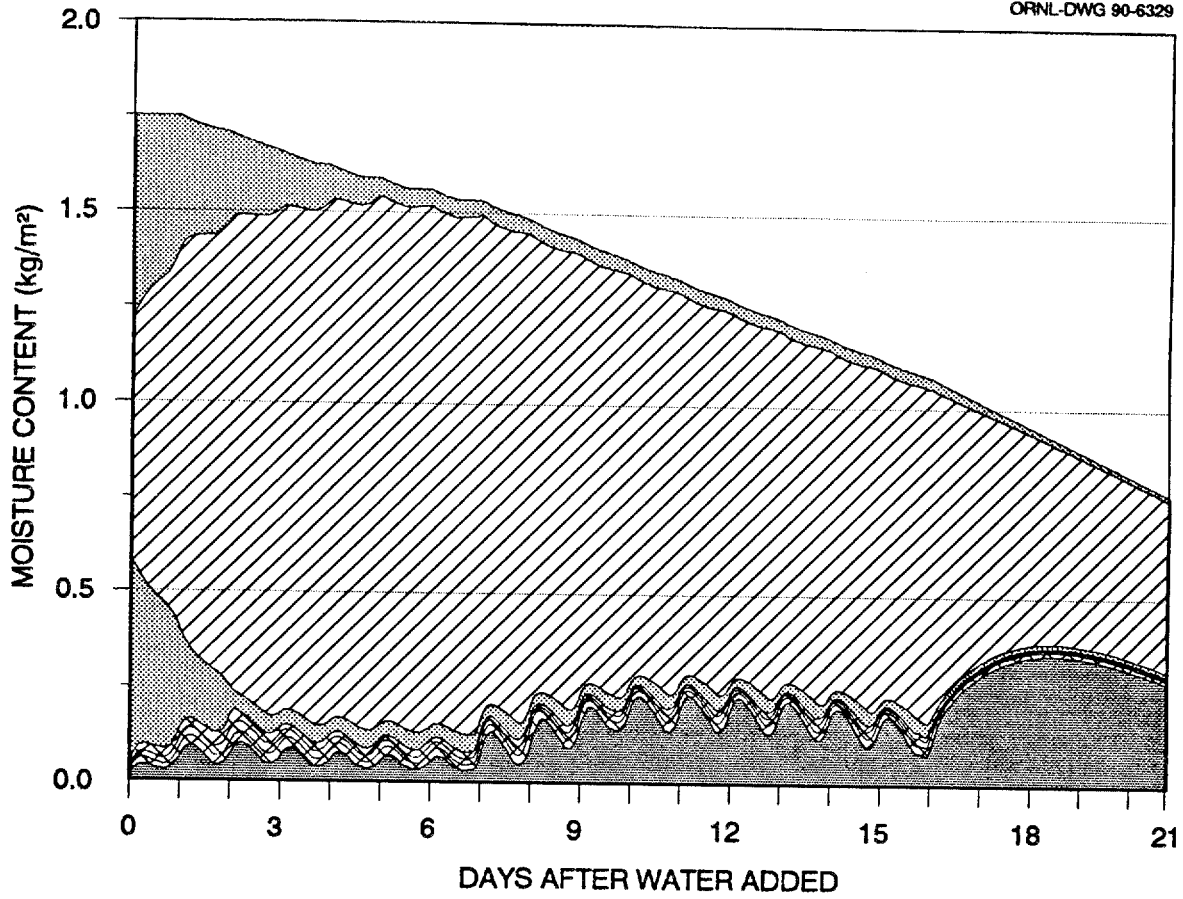


**Fig. 5.13. Moisture content in the layers of cold-deck panel 3, calculated by MATCH after water was added.**

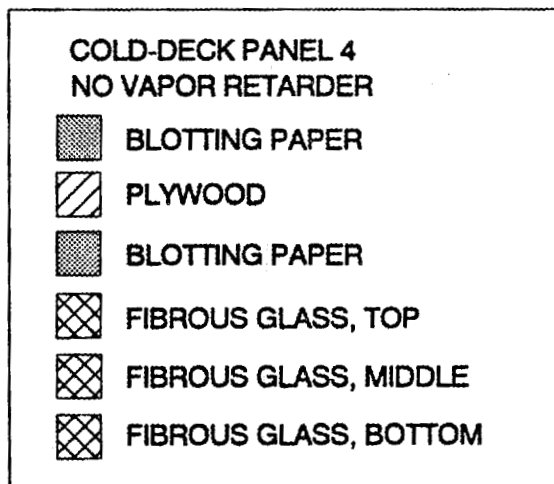
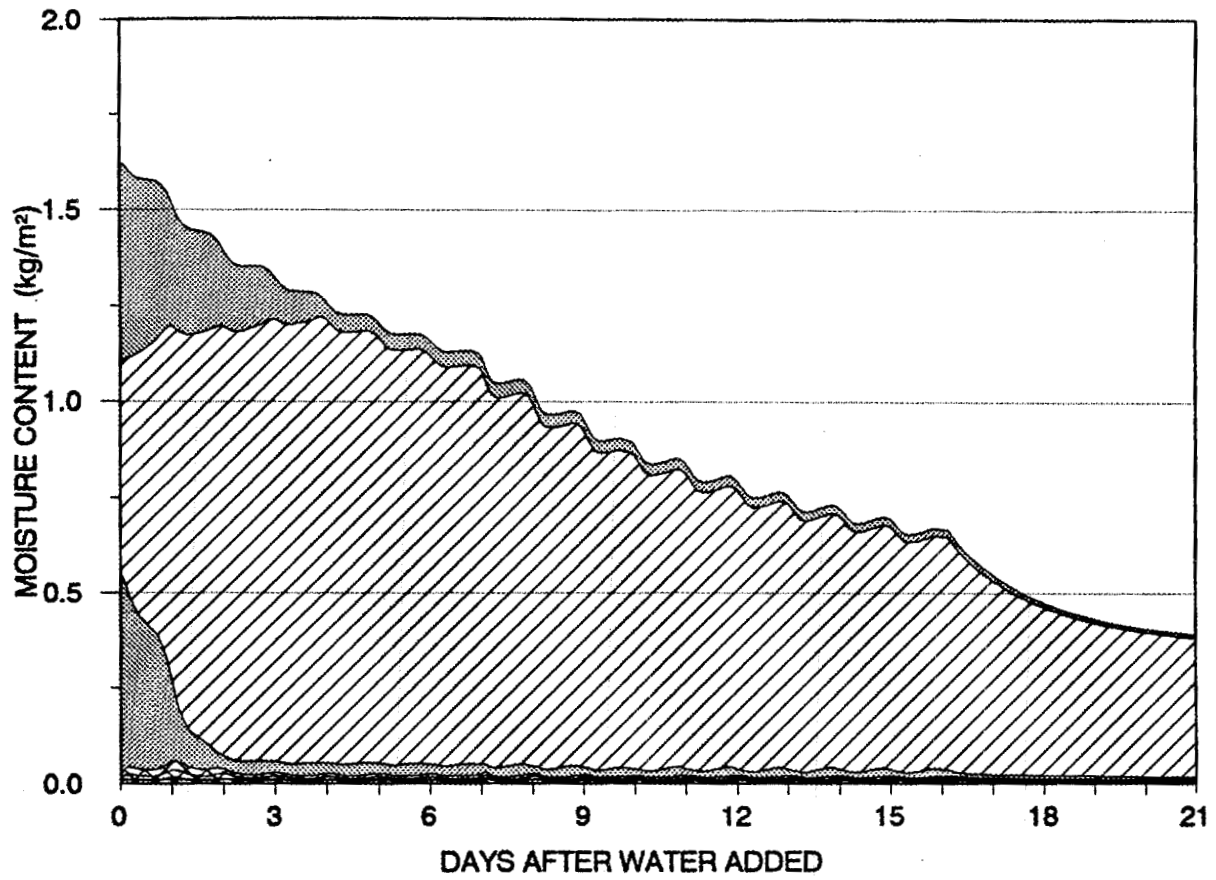


**Fig. 5.14. Moisture content in the layers of cold-deck panel 4, calculated by MATCH after water was added.**

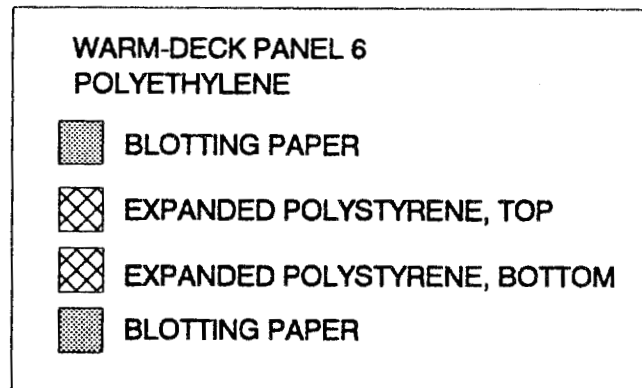
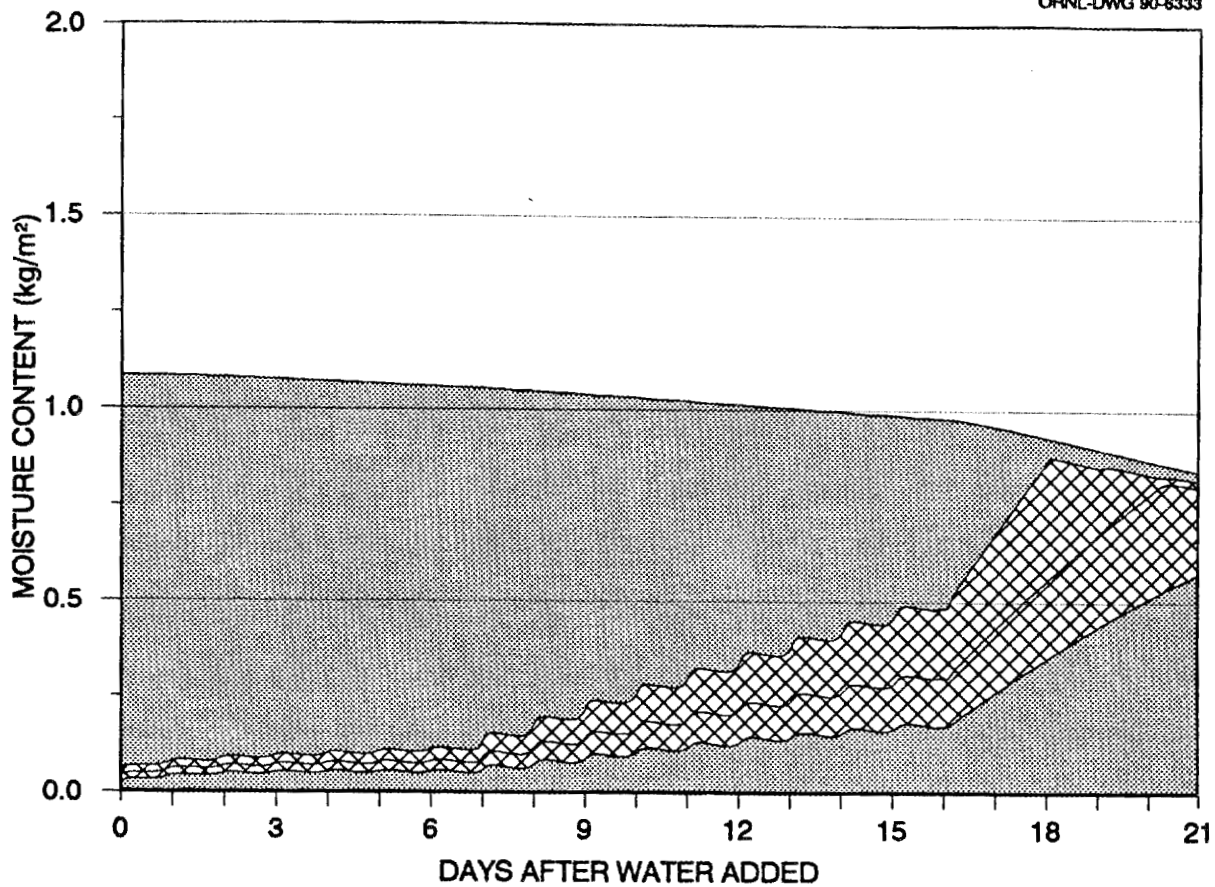


**Fig. 5.15. Moisture content in the layers of warm-deck panel 6, calculated by MATCH after water was added.**

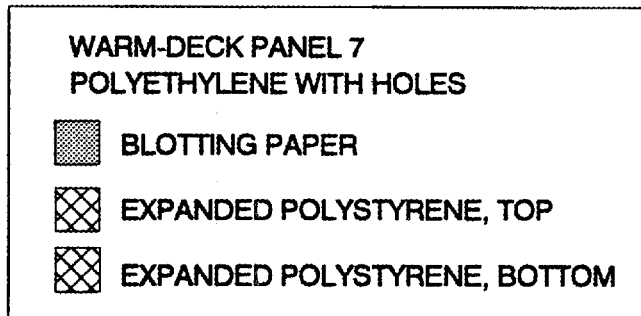
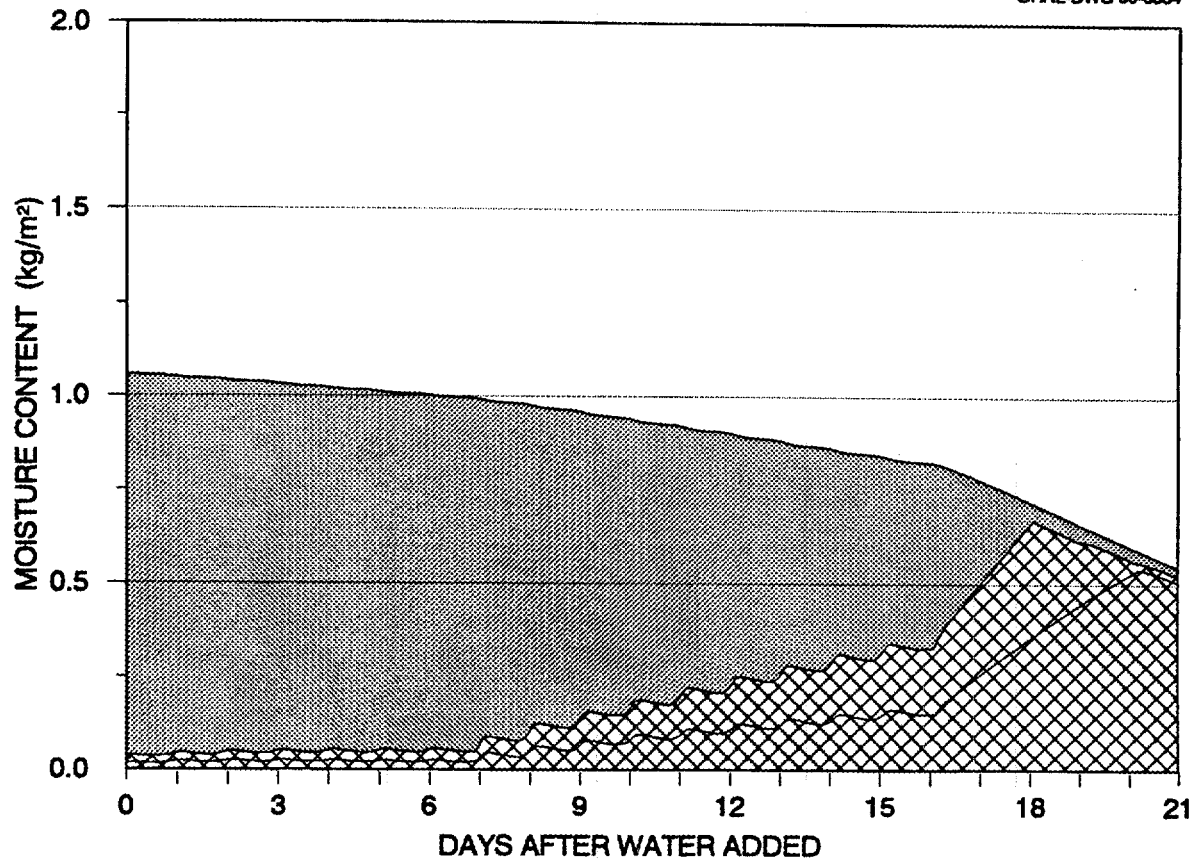


**Fig. 5.16. Moisture content in the layers of warm-deck panel 7, calculated by MATCH after water was added.**

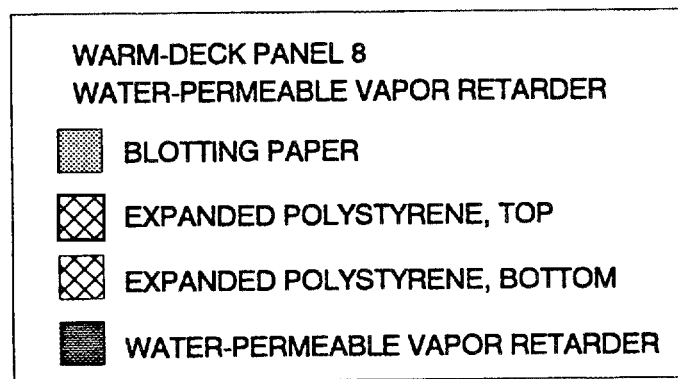
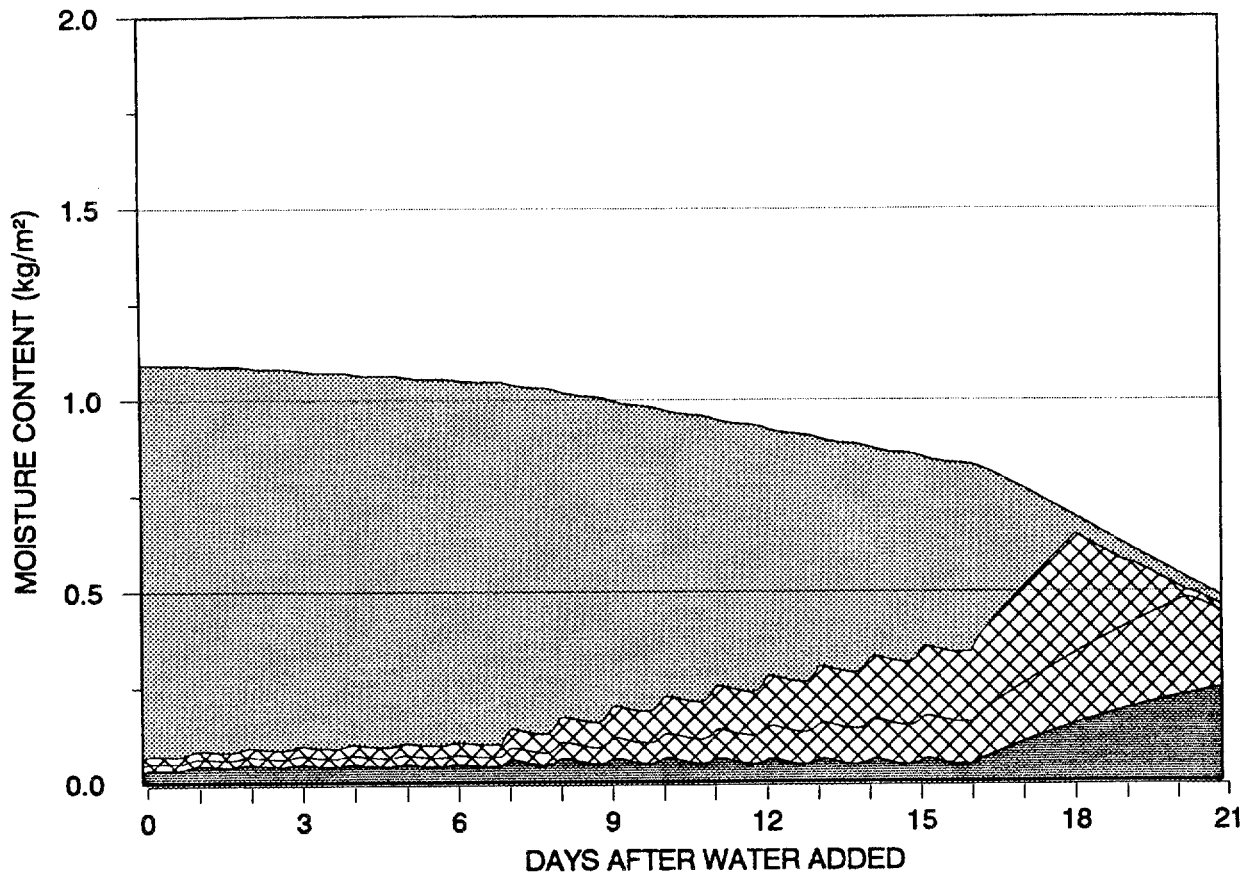


**Fig. 5.17. Moisture content in the layers of warm-deck panel 8, calculated by MATCH after water was added.**

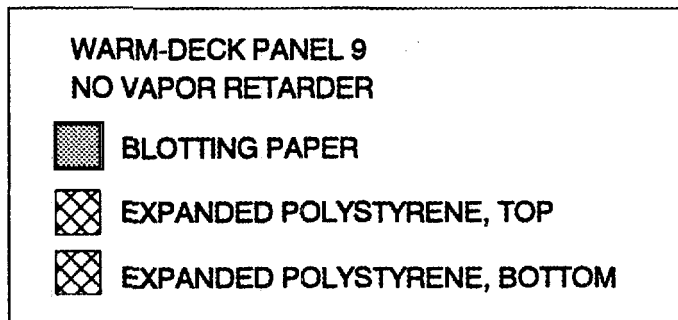
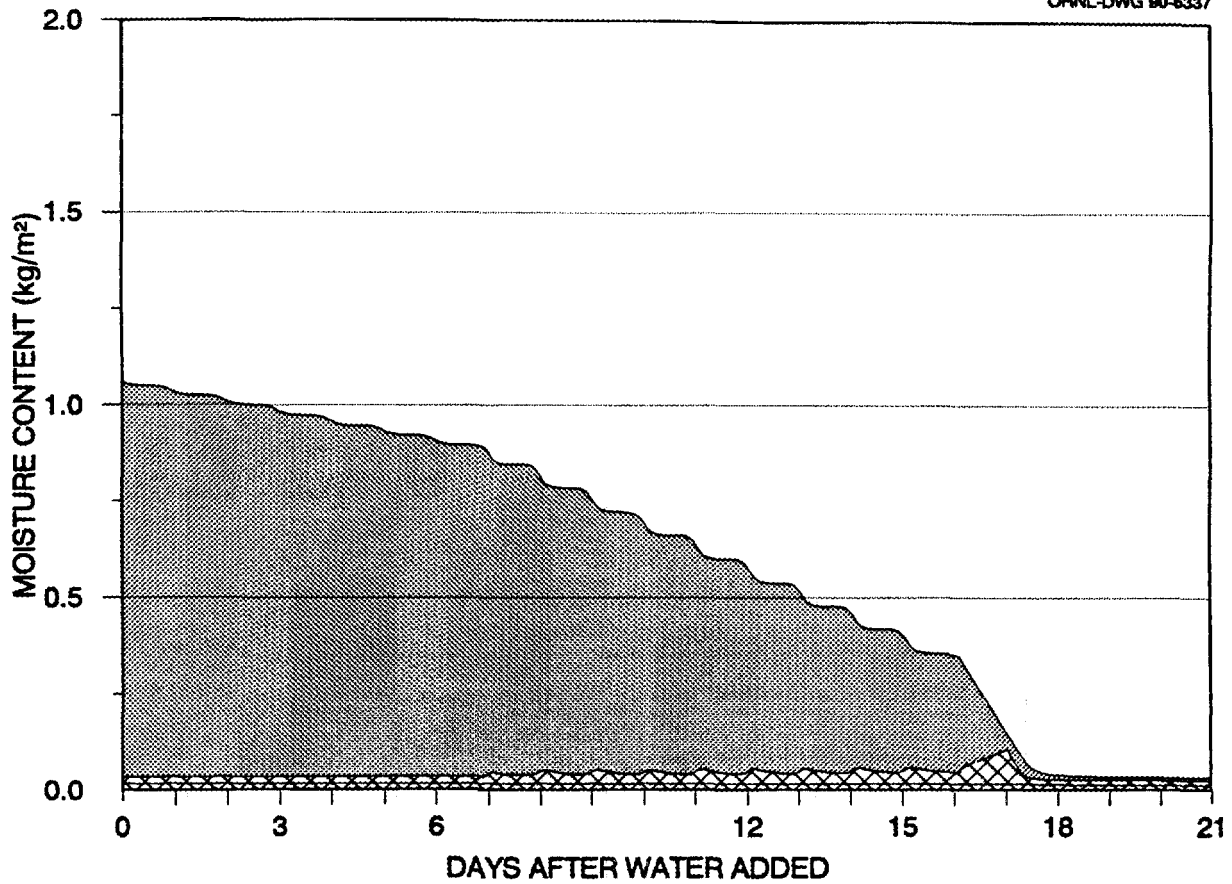


**Fig. 5.18. Moisture content in the layers of warm-deck panel 9, calculated by MATCH after water was added.**

The moisture that the paper towels absorbed was, for the most part, assigned to the interface between the vapor retarder and the bottom of the insulation. In MATCH, this moisture was simulated as if it were absorbed in the lowest hygroscopic layer next to this interface (i.e., blotting paper in panels 1 and 6, the bottom insulation layer in panels 2 and 7, or the synthetic fabric of the water-permeable vapor retarder in panels 3 and 8).

The general trends in Figs. 5.11–5.18 corresponded with observations from the data in Table 5.1, and MATCH provided valuable insight to relative drying rates in the various systems. Accurate in-service values of moisture and thermal properties are needed for absolute predictions by MATCH. This section presents results that show that the water-vapor resistance is especially critical. We are continuing work at the Building Envelope Research Center to devise a method to measure the water-vapor resistance of vapor retarders in place in roof systems.

## 6. SUMMARY AND CONCLUSIONS

We simultaneously tested two types of roof systems, examples of cold- and warm-deck types in the LSCS of the DOE Building Envelope Research Center at the ORNL. The cold-deck type had vapor-permeable insulation, while the warm-deck type did not. There were four panels of each roof type to accommodate three different vapor-retarder systems and no vapor retarder. The main purpose was to investigate the potential for downward drying without venting under summer-like conditions after the deliberate addition of 1 kg/m<sup>2</sup> of water to each panel. For comparison, a ninth panel that was of the cold-deck type had no water added during the experiment. Hygroscopic levels of water remained trapped in it throughout the whole test. In addition to monitoring the moisture content, we measured the heat fluxes through the roof specimens at different locations within the panels before and after water was added. This served the secondary purposes of the experiment: to understand how to control the latent heat effects on impermeable heat flux transducers, and to make it possible to account for the effects in the design of experiments with moist, permeable materials.

During the first runs of the test, before water was added, and again in runs after the experiment with solid vapor retarders below all the fibrous-glass insulation, we determined the apparent thermal conductivities and their reciprocals, the apparent R-values, of the materials in the roof panels as functions of temperature. The temperatures in the climate chamber above and the guard chamber below the specimens were held steady at various levels. It took approximately two days in the first runs for the measured heat fluxes to stabilize after imposition of the desired steady temperatures, but the repeat runs stabilized more quickly. The thermal driving forces imposed were directed both upward and downward in the first runs, but only upward in the repeat runs. The results from the cold-deck panel appeared unreliable when the heat flux was downward. When the hygroscopic moisture in the plywood was driven down through the insulation, it seemed to disturb the heat flux measurements. Using the results from the runs with upward thermal driving

forces gave reasonable values for the apparent thermal conductivities and their temperature variations. We used the dry thermal conductivities to analyze the results from the dynamic dry and wet runs that followed.

We also performed a run with a series of diurnal cycles of the roof surface temperatures before water was added to the panels. This run allowed direct comparisons between its results and those for a run with identical temperature variation after the water addition. We discovered, however, that the hygroscopic moisture from the plywood in the cold-deck roofs with fibrous-glass insulation influenced the heat flux readings. Heat flux transducers were located at the bottom of the fibrous glass, immediately over the vapor retarder, and at the top of the insulation, immediately under the plywood deck. Heat flux peaks were largest at the bottom, even though the temperature variations were imposed from the top of the roof. We concluded that moisture driven out of the plywood condensed and evaporated on the bottom transducer and caused the increased measured heat fluxes there. The location of the top transducer next to the plywood, which is a very hygroscopic material, seemed to prevent similar effects on this transducer.

The warm-deck roofs were insulated with expanded polystyrene, which is considerably less permeable to the flow of water vapor than fibrous glass. These roof panels had only one heat flux transducer, which was located in the middle of the insulation. There were no latent heat effects apparent in the results from the transducers in these panels, either before or after water was added. The only effect of moisture in expanded polystyrene insulation was a small increase in heat flows, which may be accounted for by the slightly higher apparent thermal conductivity of this insulation when moisture accumulated in it.

The bottom heat flux transducers in the cold-deck panels appeared to be surrounded by much condensate shortly after addition of water. This condensate came from downward migration during daytime hours that was not removed by backflow during nighttime, or did not escape to the lower guard chamber. The transducers responded significantly to moisture effects. MATCH, a numerical model for the combined heat and moisture transfer that takes the latent heat effects into account, showed that these bottom transducers indicated the combined latent and sensible heat flow. Meanwhile, because of

the hygroscopic materials next to the top transducers, the readings approximated those observed in the dry run with the same temperature variation. Consistent with results from MATCH, the top transducers seemed to indicate the sensible (conducted) heat only. We approximated the latent heat component of the total heat transfer by comparing the top and the bottom heat fluxes, and we found it to be at least as large as the sensible heat (i.e., the total heat flux more than doubled due to the effects of moisture).

In conclusion, the evaporation of small amounts of moisture from one location, migration as vapor, and condensation at a colder location carries very significant amounts of heat through permeable insulation materials such as fibrous glass. Less than 1% moisture by volume is sufficient to provide important contributions from the latent heat. The vapor flux through less permeable insulation materials such as expanded polystyrene appears to be small enough that the latent heat effects are negligible. The only effect of moisture in these materials is its slight impact on apparent thermal conductivity.

We obtained the distribution and amount of moisture versus time in the panels to which water was added. An electrical resistance probe consisted of a 50 mm (2 in.) disc of 12.7 mm (0.5-in.) plywood. The probe produced signals that could be converted to moisture content in the plywood using its calibration curve, and subsequently into relative humidities in the environment of the probe using the sorption isotherm for the plywood. This probe gave reliable readings in a rather narrow range, but did not pick up diurnal changes due to its slow response time. The range was restricted, in that the probe could not be used below the freezing point of water or when moisture content in the plywood was either very low or above fiber saturation. The probe was used to signal trends over several days in its range of response.

Another moisture probe measured the electrical capacitance between two parallel rows of needle-size pins. We knew that the capacitance would change with the moisture content of the material into which the pin probe was embedded, but no calibration curve was available for the actual probes in the materials and at the temperatures used in this experiment. The probe appeared to respond clearly and quickly to the migration of moisture in the panels, and appeared to give a measurable response over a large range of

moisture levels, so its use looks promising provided calibration problems can be overcome. Such a calibration should consider the effect of the temperature on the probe readings. We used the probes in this experiment to qualitatively follow the moisture movement.

Specimens were taken out of the test panels and weighed before and after the water addition and after every subsequent wet run of about a week's duration. This should have been a quantitative way to determine the moisture content in the panels, but there were major uncertainties. The most important uncertainty was that it was impossible to pick up all the condensed moisture from interior surfaces in the panels. Thus, even the two panels, one of each type, which had a solid sheet of polyethylene as vapor retarder appeared to have lost about 25% of the water that was added, but likely did not lose any. Two panels had polyethylene vapor retarders with holes punched in them to simulate in a regular manner conditions when the vapor retarder is not installed correctly, with tight overlaps and sealed penetrations. About half the added water escaped from these panels. We expected the same inaccuracy in apparent drying as in the panels with a solid vapor retarder.

A novel vapor retarder, a water-permeable system, was used in two other panels. It consists of a layer of synthetic fabric with strips of polyethylene on each side and exposed fabric between them. The top and bottom strips are staggered so that the system has a good vapor resistance and works well as a vapor retarder. When moisture condenses on the water-permeable vapor retarder, which occurs in this experiment when the moisture is driven down in the construction by hotter roof surface temperatures, it flows through by capillary action. The effect is to dry out the roof. The water-permeable vapor retarder in the permeable cold-deck panel allowed all the added water to escape within three weeks, while the cold-deck panel with polyethylene with holes showed that 45% of the added water escaped. In the warm-deck panel insulated with expanded polystyrene, approximately 60% of the added water appeared to have dried out through the water permeable vapor retarder, compared to 50% for the polyethylene with holes. Thus, the drying effect with a water-permeable vapor retarder is at least as good as when the

polyethylene has holes punched in it. Drying with the water-permeable vapor retarder is better, however, when the insulation is permeable and non-hygroscopic, giving optimal conditions for condensate to gather on this vapor retarder and wick through the synthetic fabric which forms its core.

A fourth pair of panels had no vapor retarder at all. In the cold-deck panel all the water added, plus a substantial amount of the hygroscopic moisture from the plywood, escaped within the three weeks of the wet tests. All the added water in the warm-deck panel also dried out. Thus, both the water-permeable vapor retarder and the polyethylene with holes present enough resistance to prevent complete drying in the time allowed in this experiment.

The experiment showed that downward drying without venting is possible using the high temperatures imposed on a roof during summer days, if vapor retarders are installed that allow some moisture to migrate through them. However, some climates still require roofs to have a good vapor retarder in order to minimize the accumulation of moisture during cold periods. The water-permeable vapor retarder appears to meet both criteria when building new roofs. How the principles the water-permeable vapor retarder embodies should be implemented when reroofing over wet roofs so as to obtain drying in the summer and avoid further moisture penetration in the winter is still uncertain, and we recommend further study.



## 7. REFERENCES

- ASHRAE 1989. *ASHRAE Handbook: 1989 Fundamentals*, American Society of Heating, Refrigeration and Air Conditioning Engineers, Atlanta.
- ASTM 1987. *Standard Test Method for Steady-State Thermal Performance of Building Assemblies by Means of a Guarded Hot Box*, Designation: C 236-87, American Society for Testing and Materials, Philadelphia.
- Courville, G. E., et al. 1987. *Electric Field Probes for Quantitative Moisture Measurements in Building Materials*, ORNL/CONF-871271, Oak Ridge National Laboratory, Oak Ridge, TN.
- Hansen, K. K. 1986. *Sorption Isotherms, A Catalogue*, Building Materials Laboratory Report 162/86, Technical University of Denmark.
- Huntley, W. R. 1989. *Design Description of the Large Scale Climate Simulator*, ORNL/TM-10675, Oak Ridge National Laboratory, Oak Ridge, TN.
- Korsgaard, V. 1985. "Hygro Diode Membrane: A New Vapor Barrier," *Proceedings, ASHRAE/DOE/BTECC Thermal Performance of the Exterior Envelopes of Buildings III*, December 2-5, 1985, Clearwater Beach, Florida, 985-991.
- Motakef, S. and Glicksman, L. R. 1989. *A Capacitance Probe for Measurement of Moisture Content in Open Pore Thermal Insulations*, ORNL/Sub/85-27486/1, Oak Ridge National Laboratory, Oak Ridge, TN.
- Pedersen, C. Rode. 1990. *Combined Heat and Moisture Transfer in Building Constructions*, Ph.D. Thesis, Technical University of Denmark, Thermal Insulation Laboratory.
- Richards, R. F., Burch, D. M. and Thomas, W. C. 1992. "Water Vapor Sorption Measurements of Common Building Materials," *ASHRAE Transactions, Part II*, 98, Paper BA-92-6-1.



## INTERNAL DISTRIBUTION

- |        |                  |        |                            |
|--------|------------------|--------|----------------------------|
| 1-10.  | P. W. Childs     | 48.    | M. A. Kuliasha             |
| 11-20. | G. E. Courville  | 49.    | P. M. Love                 |
| 21-30. | A. O. Desjarlais | 50.    | G. M. Mackiewicz-Ludtka    |
| 31-40. | K. E. Wilkes     | 51.    | H. A. McLain               |
| 41.    | J. E. Christian  | 52.    | V. C. Mei                  |
| 42.    | R. B. Shelton    | 53.    | ORNL Patent Office         |
| 43.    | C. L. Brown      | 54.    | Central Research Library   |
| 44.    | R. S. Carlsmith  | 55.    | Document Reference Section |
| 45.    | P. D. Fairchild  | 56-58. | Laboratory Records         |
| 46.    | R. S. Graves     | 59.    | Laboratory Records - RC    |
| 47.    | J. O. Kolb       |        |                            |

## EXTERNAL DISTRIBUTION

60. Robert L. Alumbaugh, Naval Civil Engineering Laboratory, Port Hueneme, CA 93043-5003
61. James L. Andersen, Foam Enterprises, Inc., 13630 Watertower Circle, Minneapolis, MN 55441
62. Aaron Applegate, Box 292, Okemos, MI 48864
63. Dave Bailey, U.S. Army, CERL, Attn: Bailey/FMS, P.O. Box 9005, Champaign, IL 61826-9005
64. Erv Bales, University Heights, New Jersey Institute of Technology, Newark, NJ 07102
65. Mark Bomberg, National Research Council Canada, Ottawa, Ontario, Canada K1A 0R6
66. Jean Boulin, Dept. of Energy, CE-43, FORSTL, 1000 Independence Ave., S.W., Washington, D.C. 20585
67. Jeff Brisley, Knauf Fiber Glass, 240 Elizabeth Street, Shelbyville, IN 46176
68. Donald E. Brotherson, One E. Saint Mary's Road, Champaign, IL 61820
69. Bruce G. Buchanan, Computer Science Dept., University of Pittsburgh, 206 Mineral Industries Building, Pittsburgh, PA 15260
70. CAREIRS Librarian, 2000 N. 15th Street, Suite 407, Arlington, VA 22201-2627
71. Walker C. Carll, Steelo Systems, P.O. Box 8181, Mason, OH 45040
72. John Carmody, Underground Space Center, 500 Pillsbury Drive, S.E., Minneapolis, MN 55455
73. Kraig S. Clawson, 2225 E. Murray-Holladay Road, #104, Salt Lake City, UT 84117
74. John L. Clinton, NRG Barriers, 15 Lund Road, Saco, ME 04072-1859
75. David M. Crouse, Stepan, 22 W. Frontage Road, Northfield, IL 60093
76. Clayton DeKorne, Journal of Light Construction, RR2, Box 146, Richmond, VT 05477

77. Kevin P. Dostaler, JPS Elastomerics Corp., 395 Pleasant Street, Northampton, MA 01060
78. Hubert T. Dudley, W. R. Grace & Co., 62 Whittemore Avenue, Cambridge, MA 02140
79. Rene M. Dupuis, Structural Research, Inc., 3213 Laura Lane, Middleton, WI 53562
80. Floyd England, England & Associates, P.O. Box 154578, Waco, TX 76715
81. Helen English, Passive Solar Industries Council, 1511 K Street, N.,W., Suite 600, Washington, D.C. 20005
82. P. R. Fiset, Room 126, Holdsworth Hall, University of Massachusetts, Amherst, MA 01003
83. Warren R. French, French Engineering, Inc., 15531 Kuykendahl, Suite 275, Houston, TX 77090
84. Smith A. Funk, Celotex Roofing Products, 4010 Boy Scout Blvd., Tampa, FL 33607-5750
85. Geof Garabedian, U.S. Intec, Inc., 1250 Fourteen Mile Road, Clawson, MI 48017
86. Leon R. Glicksman, M.I.T., 4-209, 77 Massachusetts Avenue, Cambridge, MA 02139
87. Frank C. Gorman, Roofing Services, Inc., 6106 Roxbury Avenue, Springfield, VA 22152-1621
88. William Goss, Mechanical Engineering Dept., University of Massachusetts, Amherst, MA 01003
89. Joseph Hagan, Center for Applied Engineering, 10301 Ninth Street, North, St. Petersburg, FL 33716
90. David Harris, National Institute of Building Sciences, 1201 L Street, N.W., Suite 400, Washington, D.C. 20005
91. Donna Hawkins, Dept. of Energy, CE-40, FORSTL, 1000 Independence Ave., S.W., Washington, D.C. 20585
92. Ron E. Haynes, Southnavfac, 2155 Eagle Drive, Charleston, SC 29411
93. Phil Hendrickson, Dow Chemical, USA, P.O. Box 515, Granville, OH 43023
94. Bion Howard, 14513 Kent Drive, Upper Marlboro, MD 20772
95. Helen M. Ingram, Udall Center for Studies in Public Policy, The University of Arizona, 803/811 East First Street, Tucson, AZ 85719
96. Julian L. Ius, HQ AFCESA/ENC, 139 Barnes Drive, Tyndall AFB, FL 32404
97. Richard Karney, Dept. of Energy, CE-421, FORSTL, 1000 Independence Ave., S.W., Washington, D.C. 20585
98. Mark Kelley, Building Science Engineering, 85 Depot Road, Harvard, MA 01451
99. William A. Kirn, Rohm and Haas Co., 727 Norristown Road, Spring House, PA 19477
100. Gene Leger, Leger Designs, 256 Middle Branch Road, New Boston, NH 03070
101. John J. Leimanis, Dept. of State, FBO/BDE/ESB, P.O. Box 12248, Rosslyn Station, Arlington, VA 22219
102. Calvin D. MacCracken, Calmac Manufacturing Corporation, 101 West Sheffield Avenue, P.O. Box 710, Englewood, NJ 07631
103. Robert F. Martin, Roof Maintenance Systems, P.O. Box 67, Farmingoak, NJ 07727
104. William F. Martin, Roof Design Works, Inc., 5516 Renford Drive, Knoxville, TN 37919
105. Merle F. McBride, Owens-Corning Fiberglas, 2790 Columbus Road, Granville, OH 43023-1200
106. R. Gerry Miller, Center for Applied Engineering, Inc., 10301 9th Street, N., St. Petersburg, FL 33716
107. Thomas J. Miller, Box 435, Delphos, OH 45833

108. NCAT Library, National Center for Appropriate Technology, P.O. Box 3838, Butte, MT 59702
109. Ned Nisson, Energy Design Update, P.O. Box 1709, Ansonia Station, New York, NY 10023
110. David G. Ober, 25 Wiggins Avenue, Bedford, MA 01730
- 111-120. Tom Petrie, Marquette University, Dept. of Mechanical Engineering, Milwaukee, WI 53233
121. R. W. Phillips, ADSS, P.O. Box 261, Goldsboro, NC 27533-0261
122. Donald C. Portfolio, Tremco, Inc., 10701 Shaker Blvd., Cleveland, OH 44139
123. Frank J. Powell, 12218 Cattail Lane, Jacksonville, FL 32223
124. Donald Prowler, 2302 Locust Street, Philadelphia, PA 19103
125. Stephen L. Quarles, University of California, Forest Products Laboratory, 1301 S. 46th Street, Richmond, CA 94804
126. Harold J. Roberts, Jr., RMAX, Inc., 13524 Welch Road, Dallas, TX 75244
127. David Roodvoets, Dow Chemical U.S.A., 3825 Columbus Road, S.W., F Bldg., Granville, OH 43023
128. W. J. Rossiter, NIST, Bldg. 226, Rm. B348, Gaithersburg, MD 20899
129. R. C. Schroter, 120 Village Square, #121, Orinod, CA 94563
130. Peter Scofield, Department of Energy, CE-421, FORSTL, 1000 Independence Ave., S.W., Washington, D.C. 20585
131. Morton Sherman, Consultant, 6723 14th Avenue, N., St. Petersburg, FL 33710-5405
132. Jacqueline B. Shrago, Office of Technology Transfer, 405 Kirkland Hall, Vanderbilt University, Nashville, TN 37240
133. A. T. Skinner, Roofing Service Assoc., Inc., 6500 Papermill Road, #209, Knoxville, TN 37919
134. S. E. Smith, Physical Sciences Group, 48 Chester Street, Somerville, MA 02144
135. Tom Smith, National Roofing Contractors Assoc., O'Hare International Center, 10255 W. Higgins Road, Suite 600, Rosemont, IL 60018-5607
136. Lawrence G. Spielvogel, Lawrence G. Spielvogel, Inc., 203 Hughes Road, King of Prussia, PA 19406-3785
137. Ed Story, Insul-Tray, Inc., E. 1881 Crestview Drive, Shelton, WA 98584-9082
138. William R. Strzepek, Dow U.S.A., P.O. Box 515, Granville, OH 43023
139. Bob Swisher, Dow Corning, 1225 Northmeadow Pkwy, #104, Roswell, GA 30076
140. Anton Ten Wolde, Forest Products Laboratory, One Gifford Pinchot Drive, Madison, WI 53705-2398
141. Timothy Tong, Dept. of Mechanical & Aerospace Eng., Arizona State University, Tempe, AZ 85287
142. George Tsongas, Portland State University, Mechanical Engineering Dept., Portland, OR 97207-0751
143. Adrian Tuluca, Steven Winter Associates, Inc., 50 Washington Street, Norwalk, CT 06854
144. R. P. Tye, 292 Jerusalem Road, Cohasset, MA 02025
145. Carl R. Vander Linden, Vander Linden & Assoc., 5 Brassie Way, Littleton, CO 80123
146. Martha G. Van Geem, Construction Technology Laboratory, 5420 Old Orchard Road, Skokie, IL 60077
147. James R. Wells, Owens-Corning Fiberglas, 2790 Columbus Road, Granville, OH 43023
148. David Williams, Dow Chemical, P.O. Box 515, Granville, OH 43023

149. Martin Williams, Department of Economics, Northern Illinois University, DeKalb, IL 60115
150. David W. Yarbrough, Tennessee Technological University, Box 5013, Cookeville, TN 38505
151. James E. Young, Global Thermo Coatings, Inc., 5303 E. Evans Ave., #200, Denver, CO 80222
152. Robert R. Zarr, National Institute of Standards and Technology, Bldg. 226, B320, Gaithersburg, MD 10899
153. Office of the Assistant Manager for Energy Research and Development, DOE-ORO, P.O. Box 2001, Oak Ridge, TN 37831-8600
- 154-193. BTESM Library, Oak Ridge National Laboratory, P.O. Box 2008, Bldg. 3114, Oak Ridge, TN 37831-6070
- 194-203. OSTI, U.S. Dept. of Energy, P.O. Box 62, Oak Ridge, TN 37831